

**MECHANISMS OF POSTOPERATIVE JUNCTIONAL
ECTOPIC TACHYCARDIA:
Chronotropic and Inotropic Regulation in the Neonate Heart**

by

Xiaoye (Helen) Sheng

M.D., Shanghai Second Medical University, China, 1996

THESIS SUBMITTED IN PARTIAL FULFILLMENT OF
THE REQUIREMENTS FOR THE DEGREE OF
MASTER OF SCIENCE

In the School
of
Kinesiology

© Xiaoye Sheng 2005

SIMON FRASER UNIVERSITY

Spring 2005

All rights reserved. This work may not be
reproduced in whole or in part, by photocopy
or other means, without permission of the author.

APPROVAL

Name: Xiaoye (Helen) Sheng

Degree: Master of Science

Title of Thesis: MECHANISMS OF POSTOPERATIVE
JUNCTIONAL ECTOPIC TACHYCARDIA:
Chronotropic and Inotropic Regulation in the Neonate
Heart

Examining Committee:

Chair: Dr. Amandio Vieira
Assistant Professor

Dr. Glen Tibbits
Senior Supervisor
Professor, School of Kinesiology

Dr. Eric Accili
Supervisor
Associate Professor, School of Kinesiology

Dr. Shubhayan Sanatani
Supervisor
Assistant Professor, Department of Pediatrics
Faculty of Medicine, University British Columbia

Dr. Edwin D.W. Moore
External Examiner
Associate Professor, Department of Physiology
University British Columbia

Date Approved: 19th April 2005

SIMON FRASER UNIVERSITY



PARTIAL COPYRIGHT LICENCE

The author, whose copyright is declared on the title page of this work, has granted to Simon Fraser University the right to lend this thesis, project or extended essay to users of the Simon Fraser University Library, and to make partial or single copies only for such users or in response to a request from the library of any other university, or other educational institution, on its own behalf or for one of its users.

The author has further granted permission to Simon Fraser University to keep or make a digital copy for use in its circulating collection.

The author has further agreed that permission for multiple copying of this work for scholarly purposes may be granted by either the author or the Dean of Graduate Studies.

It is understood that copying or publication of this work for financial gain shall not be allowed without the author's written permission.\

Permission for public performance, or limited permission for private scholarly use, of any multimedia materials forming part of this work, may have been granted by the author. This information may be found on the separately catalogued multimedia material and in the signed Partial Copyright Licence.

The original Partial Copyright Licence attesting to these terms, and signed by this author, may be found in the original bound copy of this work, retained in the Simon Fraser University Archive.

W. A. C. Bennett Library
Simon Fraser University
Burnaby, BC, Canada

ABSTRACT

Junctional ectopic tachycardia (JET) is a common arrhythmia in postoperative pediatric patients after open-heart surgery for congenital heart defects. This arrhythmia is life-threatening and mechanisms of this arrhythmia are not yet clear. Isolated working hearts from neonate rabbits were administered β -adrenergic agonists alone or with antagonists under normal or ischemia-reperfusion stunned conditions. The effect of the sodium hydrogen exchanger inhibitor HOE642 on the recovery of ischemia-reperfusion stunned left ventricle was tested, the potential for β -adrenergic agonist-induced arrhythmogenesis on the stunned neonate hearts was examined as well. We found that dopamine has a positive chronotropic, and a negative inotropic effect on the isolated neonate rabbit heart. Furthermore, dopamine has an arrhythmogenic effect on the ischemia-reperfusion stunned neonate myocardium. Finally, it was shown that HOE642 has a significant protective effect on contractile function in the neonate myocardium on recovery from ischemia-reperfusion stunning, but was not robust in its antiarrhythmic effect.

献给我亲爱的父母亲及
挚爱的丈夫，阮海雄先生！

*This thesis is dedicated
to my family, especially
to my husband,
Haixiong Ruan, for
without his support this
work would have never
been completed.*

ACKNOWLEDGEMENTS

I would like to express my gratitude to those who helped me to complete this thesis. First and foremost, I am deeply indebted to my senior supervisor, Dr. Glen Tibbits, for giving me the opportunity to pursue graduate studies in the School of Kinesiology. His guidance and stimulating suggestions were appreciated. In addition, his financial support and encouragement helped me get through the most difficult period of my life. I also want to thank my committee members, Dr. Eric Accili and Dr. Shubhayan Sanatani, for their guidance, constant support and trouble shooting throughout the project. I thank Mr. Rich Wolmbot, whose advice and assistance were so helpful to me at a time when “the working heart was not working”. Many thanks go to the members of CMRL. Special thanks to Ms. Haruyo Kashihara, for teaching me the technique needed for the working heart setup and her limitless support during the project. I thank Eric Lin for solving computer problems and setting up the EP recording. Thanks also to Bo Liang for writing the program for P-V recording and his valuable advice. I especially want to thank Christian Marshall and Perveen Biln for their kindness to reading this thesis and helping me to improve my English writing. To my other colleagues in CMRL: Jingbo, Franca, Tiffany, Keith, Caly, Vivian, and Pauline; I thank you for all your help, support, interest and valuable suggestions.

TABLE OF CONTENTS

Approval.....	ii
Abstract.....	iii
Dedication.....	iv
Acknowledgements.....	v
Table of Contents.....	vi
List of Tables.....	viii
List of Figures.....	viii
List of Abbreviations.....	xi
Chapter One: Introduction.....	1
1.1 Background.....	1
1.2 Postoperative junctional ectopic tachycardia.....	3
1.3 Ischemia-reperfusion insult may trigger arrhythmias.....	5
1.4 Chronotropic and inotropic regulation in the myocardium.....	11
1.4.1 HR modulation by HCN channels.....	12
1.4.2 Chronotropic modulation.....	16
1.4.3 β -adrenergic modulation.....	17
1.5 Neonate phenotype in arrhythmogenesis.....	19
1.5.1 Developmental changes in cardiac electrophysiology.....	19
1.5.2 Developmental changes in innervation.....	20
Chapter Two: Objectives of The thesis.....	22
Chapter Three: Experimental Design and Methods.....	23
3.1 Working heart apparatus.....	23
3.2 Methods.....	24
3.2.1 Animals.....	24
3.2.2 Heart isolation and perfusion.....	24
3.2.3 Exclusion criteria.....	25
3.2.4 Perfusion fluid.....	25
3.3 Experiment protocols.....	26
3.3.1 Study 1: Normal neonate myocardium regulation.....	26
3.3.2 Study2: NHE inhibition on the ischemia/reperfusion stunned neonate myocardium.....	26
3.3.3 Study 3: Effect of myocardial stunning on arrhythmogenesis.....	27
3.4 Left ventricular hemodynamics.....	27
3.5. Statistical analysis.....	28
3.5.1 Calculation of sample size.....	28
3.5.2 Statistical significance.....	28
Chapter Four: Results.....	29
4.1 Study 1: Normal neonate myocardium regulation.....	29

4.1.1 β -adrenergic agonist and antagonist.....	29
4.1.2 I_f inhibitors.....	31
4.1.3 Cholinergic agonist and antagonist.....	31
4.2 Study 2: NHE inhibition on the ischemia/reperfusion stunned neonate myocardium	32
4.3 Study 3: Effect of myocardial stunning on arrhythmogenesis	32
Chapter Five: Discussion	34
5.1 Study 1: Normal neonate myocardium regulation	34
5.1.1 β -adrenergic agonist and antagonist.....	34
5.1.2 I_f inhibitors.....	37
5.1.3 Cholinergic agonist and antagonist.....	38
5.2 Study 2: Cardioprotective activity of NHE inhibitors.....	40
5.3 Study 3: The arrhythmogenic role of dopamine and the antiarrhythmic effect of NHE inhibitor in neonate.....	41
5.4 Summary	42
Bibliography.....	94

LIST OF TABLES

Table 1 Arrhythmogenesis of 20 μM dopamine.....	93
------------------------------------------------------------	----

LIST OF FIGURES

Figure 1 Isolated Langendorff /working heart apparatus. (Adapted from Panagiotis Galanopoulos ²⁰⁰¹ with permission).....	44
Figure 2 Pre-ischemia 2.5 μM dopamine applied every 5'30 (N=10)	45
Figure 3 Pre-ischemia 2.5 μM dopamine applied every 5'30 (N=10)	45
Figure 4 Pre-ischemia 2.5 μM dopamine applied every 5'30 (N=10)	46
Figure 5 Pre-ischemia 2.5 μM dopamine applied every 5'30 (N=10)	46
Figure 6 Pre-ischemia 2.5 μM dopamine applied every 5'30 (N=10)	47
Figure 7 Pre-ischemia 2.5 μM dopamine applied every 5'30 (N=10)	47
Figure 8 Pre-ischemia 2.5 μM dopamine applied every 5'30 (N=10)	48
Figure 9 Pre-ischemia 2.5 μM dopamine applied every 5'30 (N=10)	48
Figure 10 Pre-ischemia 10 μM esmolol followed by 2.5 μM dopamine (N=8).....	49
Figure 11 Pre-ischemia 10 μM esmolol followed by 2.5 μM dopamine (N=8).....	49
Figure 12 Pre-ischemia 10 μM esmolol followed by 2.5 μM dopamine (N=8).....	50
Figure 13 Pre-ischemia 10 μM esmolol followed by 2.5 μM dopamine (N=8).....	50
Figure 14 Pre-ischemia 10 μM esmolol followed by 2.5 μM dopamine (N=8).....	51
Figure 15 Pre-ischemia 10 μM esmolol followed by 2.5 μM dopamine (N=8).....	51
Figure 16 Pre-ischemia 10 μM esmolol followed by 2.5 μM dopamine (N=8).....	52
Figure 17 Pre-ischemia 10 μM esmolol followed by 2.5 μM dopamine (N=8).....	52
Figure 18 Pre-ischemia 10 μM propranolol followed by 20 μM dopamine (N=8).....	53
Figure 19 Pre-ischemia 10 μM propranolol followed by 20 μM dopamine (N=8).....	53
Figure 20 Pre-ischemia 10 μM propranolol followed by 20 μM dopamine (N=8).....	54
Figure 21 Pre-ischemia 10 μM propranolol followed by 20 μM dopamine (N=8).....	54
Figure 22 Pre-ischemia 10 μM propranolol followed by 20 μM dopamine (N=8).....	55
Figure 23 Pre-ischemia 10 μM propranolol followed by 20 μM dopamine (N=8).....	55
Figure 24 Pre-ischemia 10 μM propranolol followed by 20 μM dopamine (N=8).....	56
Figure 25 Pre-ischemia 10 μM propranolol followed by 20 μM dopamine (N=8).....	56
Figure 26 Pre-ischemia single dose of 40 nM isoproterenol (N=8).....	57

Figure 27 Pre-ischemia single dose of 40 nM isoproterenol (N=8).....	57
Figure 28 Pre-ischemia single dose of 40 nM isoproterenol (N=8).....	58
Figure 29 Pre-ischemia single dose of 40 nM isoproterenol (N=8).....	58
Figure 30 Pre-ischemia single dose of 40 nM isoproterenol (N=8).....	59
Figure 31 Pre-ischemia single dose of 40 nM isoproterenol (N=8).....	59
Figure 32 Pre-ischemia single dose of 40 nM isoproterenol (N=8).....	60
Figure 33 Pre-ischemia single dose of 40 nM isoproterenol (N=8).....	60
Figure 34 Pre-ischemia 10 μ M esmolol followed by 40 nM isoproterenol (N=8).....	61
Figure 35 Pre-ischemia 10 μ M esmolol followed by 40 nM isoproterenol (N=8).....	61
Figure 36 Pre-ischemia 10 μ M esmolol followed by 40 nM isoproterenol (N=8).....	62
Figure 37 Pre-ischemia 10 μ M esmolol followed by 40 nM isoproterenol (N=8).....	62
Figure 38 Pre-ischemia 10 μ M esmolol followed by 40 nM isoproterenol (N=8).....	63
Figure 39 Pre-ischemia 10 μ M esmolol followed by 40 nM isoproterenol (N=8).....	63
Figure 40 Pre-ischemia 10 μ M esmolol followed by 40 nM isoproterenol (N=8).....	64
Figure 41 Pre-ischemia 10 μ M esmolol followed by 40 nM isoproterenol (N=8).....	64
Figure 42 Post-ischemia 2.5 μ M dopamine applied every 5'30 (N=10).....	65
Figure 43 Post-ischemia 2.5 μ M dopamine applied every 5'30 (N=10).....	65
Figure 44 Post-ischemia 2.5 μ M dopamine applied every 5'30 (N=10).....	66
Figure 45 Post-ischemia 2.5 μ M dopamine applied every 5'30 (N=10).....	66
Figure 46 Post-ischemia 2.5 μ M dopamine applied every 5'30 (N=10).....	67
Figure 47 Post-ischemia 2.5 μ M dopamine applied every 5'30 (N=10).....	67
Figure 48 Post-ischemia 2.5 μ M dopamine applied every 5'30 (N=10).....	68
Figure 49 Post-ischemia 2.5 μ M dopamine applied every 5'30 (N=10).....	68
Figure 50 Pre-ischemia single dose of 5 μ M ZD7288 (N=8).....	69
Figure 51 Pre-ischemia single dose of 5 μ M ZD7288 (N=8).....	69
Figure 52 Pre-ischemia single dose of 5 μ M ZD7288 (N=8).....	70
Figure 53 Pre-ischemia single dose of 5 μ M ZD7288 (N=8).....	70
Figure 54 Pre-ischemia single dose of 5 μ M ZD7288 (N=8).....	71
Figure 55 Pre-ischemia single dose of 5 μ M ZD7288 (N=8).....	71
Figure 56 Pre-ischemia single dose of 5 μ M ZD7288 (N=8).....	72
Figure 57 Pre-ischemia single dose of 5 μ M ZD7288 (N=8).....	72
Figure 58 Pre-ischemia 5 μ M ZD7288 followed by 20 μ M dopamine (N=8).....	73
Figure 59 Pre-ischemia 5 μ M ZD7288 followed by 20 μ M dopamine (N=8).....	73
Figure 60 Pre-ischemia 5 μ M ZD7288 followed by 20 μ M dopamine (N=8).....	74
Figure 61 Pre-ischemia 5 μ M ZD7288 followed by 20 μ M dopamine (N=8).....	74
Figure 62 Pre-ischemia 5 μ M ZD7288 followed by 20 μ M dopamine (N=8).....	75
Figure 63 Pre-ischemia 5 μ M ZD7288 followed by 20 μ M dopamine (N=8).....	75
Figure 64 Pre-ischemia 5 μ M ZD7288 followed by 20 μ M dopamine (N=8).....	76

Figure 65 Pre-ischemia 5 μ M ZD7288 followed by 20 μ M dopamine (N=8)	76
Figure 66 Pre-ischemia single dose of 30 μ M atropine (N=8)	77
Figure 67 Pre-ischemia single dose of 30 μ M atropine (N=8)	77
Figure 68 Pre-ischemia single dose of 30 μ M atropine (N=8)	78
Figure 69 Pre-ischemia single dose of 30 μ M atropine (N=8)	78
Figure 70 Pre-ischemia single dose of 30 μ M atropine (N=8)	79
Figure 71 Pre-ischemia single dose of 30 μ M atropine (N=8)	79
Figure 72 Pre-ischemia single dose of 30 μ M atropine (N=8)	80
Figure 73 Pre-ischemia single dose of 30 μ M atropine (N=8)	80
Figure 74 Pre-ischemia 5 μ M ACh followed by 30 μ M atropine (N=8).....	81
Figure 75 Pre-ischemia 5 μ M ACh followed by 30 μ M atropine (N=8).....	81
Figure 76 Pre-ischemia 5 μ M ACh followed by 30 μ M atropine (N=8).....	82
Figure 77 Pre-ischemia 5 μ M ACh followed by 30 μ M atropine (N=8).....	82
Figure 78 Pre-ischemia 5 μ M ACh followed by 30 μ M atropine (N=8).....	83
Figure 79 Pre-ischemia 5 μ M ACh followed by 30 μ M atropine (N=8).....	83
Figure 80 Pre-ischemia 5 μ M ACh followed by 30 μ M atropine (N=8).....	84
Figure 81 Pre-ischemia 5 μ M ACh followed by 30 μ M atropine (N=8).....	84
Figure 82 Post-ischemia heart rate recovery (N=6).....	85
Figure 83 Post-ischemia aortic flow recovery (N=6) * P<0.05 ** P<0.01	86
Figure 84 Post-ischemia cardiac output recovery (N=6) * P<0.05 ** P<0.01	87
Figure 85 Post-ischemia stroke volume recovery (N=6) * P<0.05 **P<0.01	88
Figure 86 Post-ischemia ejection fraction recovery (N=6) * P<0.05 **P<0.01	89
Figure 87 Post-ischemia dP/dt _{max} recovery (N=6) * P<0.05 **P<0.01	90
Figure 88 Post-ischemia dP/dt _{min} recovery (N=6) * P<0.05 ** P<0.01	91
Figure 89 Dopamine-induced arrhythmogenesis in the reperfusion phase.....	92

LIST OF ABBREVIATIONS

AA	---	arachidonic acid
ACh	---	acetylcholine
AP	---	action potential
AV node	---	atrioventricular node
AVSD	---	atrioventricular septal defect
CHD	---	congenital heart disease
DD	---	diastolic depolarization
EAD	---	early afterdepolarization
E-C coupling	---	excitation-contraction coupling
E_m	---	membrane potential
FFA	---	free fatty acid
HCN channel	---	hyperpolarization-activated cyclic nucleotide-gated channel
JET	---	junctional ectopic tachycardia
LCAC	---	long-chain acylcaritines
LPG	---	lysophosphoglyceride
NBC	---	Na^+ - HCO_3^- cotransport
NCX	---	Na^+ / Ca^{2+} exchange
NE	---	norpinephrine
NHE	---	Na^+ / H^+ exchanger
PKA	---	protein kinase A
RYR	---	ryanodine receptor
SA node	---	sinoatrial node
SERCA2A	---	sarcoplasmic reticulum Ca^{2+} -ATPase
SR	---	sarcoplasmic reticulum
TOF	---	tetralogy of Fallot
T-tubule system	---	transverse tubule system
VSD	---	ventricular septal defect
β -AR	---	β -adrenergic receptor

CHAPTER ONE: INTRODUCTION

1.1 Background

Congenital heart disease (CHD) often results in gross structural abnormalities of the heart or intrathoracic great vessels, which in turn can have potentially deleterious effects on cardiopulmonary function [1]. With a prevalence rate of 0.7% to 1% of live births [2-4], CHD represents the most common severe birth defect. The most common forms of CHD are isolated ventricular septal defects (VSDs), patent ductus arteriosus, atrial septal defects of the fossa ovalis (secundum) type, atrioventricular septal defects (AVSDs), and bicuspid aortic valve defects [5]. Many children with CHD will require surgery in order to survive or to reduce long term morbidity. Despite its obvious benefits, cardiothoracic surgery is a relatively high-risk procedure in neonates. The mortality and morbidity associated with repair of a congenital heart malformation is much higher than that in adult cardiac surgery. This may be due to the immaturity of the neonate heart that renders it unable to respond effectively to the ischemia-reperfusion (I-R) injury that occurs as a consequence of cardiopulmonary bypass.

Moreover, cardiac arrhythmias are a frequent problem in the early postoperative period after open heart surgery. Many arrhythmias are transient and readily treated; while others are life-threatening or intractable to therapy. Factors that may cause or increase the risk of neonate postoperative arrhythmias are both structural and functional, including pre-existing myocardial compromise by cardiac defects; complex operative

procedure with extensive scarring and suture lines; postoperative electrolyte disturbances; increased adrenergic tone; and/or catecholamine stimulation or neonate phenotype [6].

Junctional ectopic tachycardia (JET) is the most common postoperative arrhythmia seen in the neonate. Although self-limited, JET is life-threatening and refractory to therapy. Because of its unknown etiology, strategies in the treatment of JET have had equivocal success and as a consequence this arrhythmia has been associated with an increased risk of morbidity and mortality.

1.2 Postoperative junctional ectopic tachycardia

Although a congenital or familial form of JET exists, it is rarely encountered. The reported incidence of postoperative JET varies with institute, ranging from ~2% - 10.8%[7-10]. It has been reported to occur after every type of surgical repair, but is most often observed after surgery in the region of the atrioventricular (AV) node, especially with repair or closure of a VSD such as in AV canals, Tetralogy of Fallot (TOF), and transposition of the great arteries with VSD. Although the precise cause of JET is not clearly understood, a combination of factors, including underlying heart disease, type of surgical procedure, hemodynamic instability, and electrolyte imbalance may contribute to the development of JET [8]. It has been suggested that JET results from enhanced excitability of the right atrial or ventricular portion of the conducting Bundle of His. This enhanced excitability may be attributed to various forms of irritation and minor trauma, as well as other factors [11]. However, JET also occurs in patients for whom there is either no intracardiac surgical procedure or no intervention near the atrioventricular node, such as transplantation or extracardiac Fontan operation.

In general, JET is usually a self-limiting disorder that resolves within the first few days. The lack of atrioventricular synchrony and the high ventricular rate may lead to diminished cardiac output, which in turn may lead to increased adrenergic tone. The resulting heart rate acceleration may further create a deteriorating clinical condition [11, 12]. Diagnosis of JET is made by the examination of an ECG trace which typically includes a narrowed QRS complex, with a ventricular rate of 170 to 260 bpm and AV dissociation in which the atrial rate is slower than the ventricular rate [13]. If the P wave is not visible on the rhythm-strip or 12-lead ECG, an ECG using atrial leads must be

performed. If the diagnosis of JET is still uncertain, other manoeuvres may be needed [14, 15].

As JET is difficult to determinate once established, the aim of JET therapy is to reinstate AV synchrony at physiologic heart rates, thereby obtaining adequate circulation. The factors that can initiate or increase the probability of JET should be treated first. Based on previous studies, the following treatments are currently used in different clinic centres:

- 1) Ensuring no significant hemodynamic residue;
- 2) Supportive treatment including pain therapy or sedation to reduce the endogenous catecholamine levels;
- 3) Correcting electrolytes and pH imbalances and inadequate intravascular volume status;
- 4) Surface cooling hypothermia [16-18];
- 5) The usage of medications such as magnesium, and amiodarone [19, 20];
- 6) Once the rate has been slowed, atria pacing overdrive [21].

However, many of these medical treatment strategies have morbidity associated with them. As well the impact on this particular arrhythmia is not guaranteed; therefore recovery is often prolonged with increased risk of morbidity and mortality.

1.3 Ischemia-reperfusion injury may trigger arrhythmias

The basic mechanisms of cardiac arrhythmias include automaticity inside and outside the sinoatrial (SA) node, triggered activity and/or reentry [22]. However, some risk factors are linked to cardiac arrhythmias. One factor that may cause or increase the risk of postoperative arrhythmias is cardiac I-R injury. Cardiac ischemia is defined as insufficient coronary blood flow relative to myocardial demand. It frequently causes deterioration of electrical behaviour and failure of contraction. In the process of cardiopulmonary bypass, the heart's energy supply and waste removal are dramatically reduced. Reperfusion is necessary to salvage the myocardial cells and cardiac function. However, reperfusion often initiates a cascade of events that lead to reperfusion injury, including lethal arrhythmias, no-reflow phenomenon, myocardial stunning, and cell death. During I-R, there are substantial changes in cardiac contractile and metabolic functions that normally result in reduced oxidative metabolism and a subsequent fall in the ATP/ADP ratio. Possible mechanisms for this phenomenon are discussed below.

1) Increase free radical-induced oxidant stress

Oxidative stress is caused by either the excessive generation or attenuated elimination of free radicals. Free radicals are a normal by-product of the mitochondrial electron transport chain, possess one or more unpaired electrons and are highly reactive. Oxygen radicals oxidize sulfhydryl groups of proteins, thereby forming disulfide bridges and altering protein tertiary structure. Modifications affecting the normal function of membrane proteins often result in changes in ionic currents [23]. During ischemia or reperfusion, the formation of free radicals is amplified compared to aerobic metabolism [24, 25], and the excessive radicals may cause membrane peroxidation, thereby changing

the behaviour of channels. Oxygen free radicals can have numerous effects including inhibition of the I_{CaL} , a reduction in the Ca^{2+} transient [26], and inhibition of most K^+ currents except I_{KATP} [27, 28] and Na^+-K^+ pump current [29]. However, oxygen radicals activate the sarcoplasmic reticulum (SR) Ca^{2+} release channel by disulfide bond formation [28] and the mitochondrial mega-channel [30]. Together, these conditions result in a reduction of the upstroke and conduction velocity of the action potential and a prolonged plateau and may result in early afterdepolarization (EAD) and delayed afterdepolarization (DAD). Eventually the action potential shortens; the cells become unexcitable and go into contracture.

2) Release of catecholamines

During ischemia, catecholamines are released globally, followed by a local release that is caused by blocking the reuptake mechanism (due to increased intracellular Na^+) in nerve endings. Catecholamines bind to two at least different types of adrenergic receptors (α and β). α -receptor stimulation results in enhanced I_{KATP} [31], I_{KACH} [32], and Na^+-K^+ pump activity [33], but does not affect the I_{K1} current [34]. The outcome of α -adrenergic receptor stimulation is a prolonged action potential and enhanced frequency of DAD. β -adrenergic receptor (β -AR) activation stimulates most plasma membrane currents except I_{to} , I_{KSS} and I_{K1} . As a result, pacemaker activity is increased, and in addition the plateau phase of the action potential is shortened. These excessive stimulations may induce Ca^{2+} overload and triggered activity, leading to cardiac arrhythmia.

3) Disturbances of ionic homeostasis

3a) Increased $[K^+]_o$

Under normal conditions, $[K^+]_i$ is approximately 104~180 mM [35] and $[K^+]_o$ is about 5.4 mM. Passive K^+ efflux through a variety of sarcolemmal K^+ channels is compensated by active K^+ influx through the Na^+-K^+ pump. During ischemia, increases in $[K^+]_o$ may be the result of either a decrease in active K^+ influx through a reduction in Na^+-K^+ pump activity, or may be due to an increase in K^+ efflux as a result of changes in I_{Na} , I_{NSC} and I_{Cl} concomitant with activation of I_{KATP} [36] and I_{KAA} [37]. This results in stabilization of E_m and cell inexcitability. Eventually, cells depolarize and the action potentials are reduced in amplitude, rate, and duration. These changes may increase the susceptibility of the heart to arrhythmias.

3b) Increased $[H^+]_o$, and $[H^+]_i$

Under aerobic perfusion, pH_i is slightly more acidic than pH_o . Under normal conditions, H^+ -equivalent elimination via Na^+/H^+ exchanger (NHE) and $Na^+-HCO_3^-$ cotransport (NBC) compensates for the production of protons that occur during metabolism. During ischemia, O_2 availability is decreased forcing ATP to be produced through anaerobic glycolysis instead of the aerobic mitochondrial system, thereby increasing proton production. This along with the potential inhibition of the acid removal system, due to the increase in $[Na^+]_i$, eventually leads to a fall in pH_i and pH_o . With both extracellular and intracellular acidosis, most membrane channels and ion transporters (except for K_{ATP} and K_{AA}), such as gap junction channels, the SR Ca^{2+} release channel and Na^+/Ca^{2+} exchanger (NCX) [38], are inhibited. The overall effect of acidosis is a fall in resting membrane potential, a prolongation of the action potential, with eventual

oscillations at the plateau level of depolarization and occurrence of EAD. All of these acidosis-induced changes are potentially arrhythmogenic.

3c) Increased $[\text{Na}^+]_i$

Under normal perfusion, extracellular $[\text{Na}^+]_o$ is roughly 10 times greater than the cytosolic $[\text{Na}^+]_i$. During ischemia, $[\text{Na}^+]_i$ may increase two- to five-fold [39, 40] and is due, at least in part, to the partial inhibition of the Na^+-K^+ pump and Na^+ influx via NHE and I_{Na} . Na^+-K^+ pump inhibition may be due to the fall in free energy of ATP hydrolysis under anaerobic conditions, a reduction of enzymatic activity under the influence of long-chain acylcaritines (LCAC) and/or oxidative stress. Ischemia is normally accompanied by intracellular acidosis which activates NHE activity, leading to Na^+ influx. An increase in $[\text{Na}^+]_i$ will reduce the driving force for normal mode NCX and may actually result in reverse mode NCX activity. This will result in Ca^{2+} influx, which can cause Ca^{2+} overload and can be arrhythmogenic.

3d) Increased $[\text{Ca}^{2+}]_i$

Ca^{2+} plays a critical role in myocardial excitation-contraction (E-C) coupling. Cytosolic $[\text{Ca}^{2+}]$ is a crucial signalling factor and regulates many vital processes by binding to a variety of different proteins. Under normal conditions, the concentration of Ca^{2+} varies between the cytosol, the SR, the mitochondria and the nucleus, as it plays different roles in the different intracellular compartments. Cytosolic $[\text{Ca}^{2+}]$ modulates the activity of myofilaments and the ionic channels in the plasma membrane. It has been shown that the cytosolic $[\text{Ca}^{2+}]$ is ~50-200 nM during diastole and ~500-2000 nM during systole. Calculations indicate that free Ca^{2+} at rest is <0.03% of total Ca^{2+} , and increases to 0.1% during activity with most binding cytoplasmic proteins and lipids. NCX removes

about 90% of the Ca^{2+} that is brought in by the L-type Ca^{2+} channel [41, 42] during excitation. During ischemia, cytosolic $[\text{Ca}^{2+}]$ rises since Ca^{2+} influx exceeds Ca^{2+} efflux. Ca^{2+} sequestration into the SR is also decreased most likely due to the reduced activity of SERCA2A [43], further promoting Ca^{2+} overload. With Ca^{2+} overload, EAD and DAD may develop by the reactivation of L-type Ca^{2+} current [44], Ca^{2+} release from SR [45], and activation of transient inward current which is caused by normal mode NCX activity [46]. Ca^{2+} overload also increases the tendency in Purkinje fibres to become spontaneously active and shifts the activation curve of I_f current into a positive direction which can increase the rate of diastolic depolarization [47]. In the final stages, mitochondrial mega-channel uncouple oxidative phosphorylation, promoting hydrolysis of ATP, resulting in cell contracture [48]

3e) Decreased $[\text{Mg}^{2+}]_i$

Mg^{2+} is an important regulator of cell energy metabolism, since only MgATP can serve as a substrate for ATP utilizing processes. In the cytoplasm, most of the Mg^{2+} is bound to nucleotides and proteins resulting in the free Mg^{2+} being only 10% of the total. Under ischemic conditions, free $[\text{Mg}^{2+}]$ has been found to increase [49]. Upon reperfusion, free $[\text{Mg}^{2+}]$ decreases to normal levels [50], but may remain transiently elevated at 1.5 mM [51]. This change is the result of a net hydrolysis of ATP to which Mg^{2+} is bound and a reduction in the activity of $\text{Na}^+/\text{Mg}^{2+}$ exchanger and Mg^{2+} -ATPase, which are the mechanisms by which Mg^{2+} is removed. Under physiologic conditions, Mg^{2+} is required for the activation of enzymes that phosphorylate or dephosphorylate a variety of proteins including Na^+ , Ca^{2+} , and K^+ channels. Thus ischemia-induced increases in free $[\text{Mg}^{2+}]$ can result in cellular dysfunction.

4) Disturbances in lipid metabolism

Under normal conditions, free fatty acids (FFA) are taken up by cells where they may serve as precursors in the synthesis of other compounds, as fuel for energy production, and as substrates for ketone body synthesis. Examples include phospholipids (in membranes) eicosanoids, including prostaglandins and leucotrienes, which play important roles in physiological regulation. During I-R, the concentration of FFA continues to rise due to an enhanced breakdown of membrane phospholipids, as well as the accumulation of amphiphiles LCAC and lysophosphoglycerides (LPG) in the plasma membranes, gap junctions, and intracellular membranes. These accumulated LCAC, LPG, and FFA can interact with membrane channels and transporters and may change membrane fluidity, and have the potential, therefore, to modulate cardiac excitation.

5) Increased release of extracellular ATP

ATP is the major energy currency molecule of the cell. It is necessary for many cell functions including active transport and mechanical work, supplying the energy for myosin ATPase activity required for muscle contraction. A major role of ATP is in chemical work, supplying the energy required to synthesize myriad macromolecules required for normal cell function. In the normoxic heart, extracellular ATP is generated from sympathetic nerve ending secretion. ATP is also released as a metabolite from cardiac muscle that has been made hypoxic. In ischemic conditions, cells partly depleted of [ATP] [52], adenylate cyclase stimulated by [ATP]_o may further deplete subsarcolemmal [ATP] leading to shortening of the action potential because ATP is rapidly broken down to adenosine.

6) Mechanical trauma and stretch

An increase in cell volume caused by increases in the osmotic forces can lead to cell stretch. During ischemia, stretch is usually characterized by an increase in the longitudinal dimension concomitant with a decrease in the transversal direction. Stretch results in activation of enzymes and stretch-sensitive channels, thereby increasing the vulnerability to arrhythmia generation.

In summary, all of these ischemia-induced changes are potentially arrhythmogenic in nature. Some of the changes which make arrhythmias more probable include: I-R induced changes in pacemaker activity, Ca^{2+} overload and catecholamine secretion.

1.4 Chronotropic and inotropic regulation in the myocardium

Corrective cardiac surgery in infants and neonates may induce acute circulatory and autonomic changes, which, together with the myocardial ischemia of cardiopulmonary bypass, can result in impaired cardiac function. Low cardiac output syndrome is a significant complication after open-heart surgery, and often requires both pharmacological inotropic and chronotropic treatment until recovery.

Chronotropy is altered by parasympathetic (vagal) activation, which releases acetylcholine (ACh) onto the SA node to decrease diastolic depolarization pacemaker rate. This is accomplished by ACh increasing conductance of I_{KACH} and decreasing conductance of $I_{\text{Ca,T}}$ and I_{Na} as well as shifting I_f activation curve to negative direction. Sympathetic activation results in norepinephrine (NE) release which has the opposite effect. Hormones also alter pacemaker activity. For example, hyperthyroidism results in

tachycardia. Circulating epinephrine causes tachycardia similar to norepinephrine released by sympathetic nerves.

Sympathetic nerves play a prominent role in ventricular and atrial inotropic regulation, while parasympathetic nerves have a significant negative inotropic effect in the atria but only a small effect in the ventricles. In the mammalian heart, an increase in heart rate can modulate inotropy due to the force-frequency relationship. Changes in beat frequency can modulate the kinetics of whole cell $I_{Ca,L}$, alter $[Ca^{2+}]_i$ due to changes in Ca^{2+} influx and less time between contractions for Ca^{2+} extrusion, and alter SR Ca^{2+} load available for release. Higher beating frequencies may also raise $[Na^+]_i$ [53], making E_{NCX} more negative which shifts the NCX balance further toward less Ca^{2+} extrusion and more Ca^{2+} influx. Eventually this results in more Ca^{2+} in the subsarcolemma space and in the SR.

1.4.1 HR modulation by HCN channels

In the mammalian heart, it is generally accepted that the normal spontaneous heartbeat is initiated in the SA node as the cells in this region have the highest pacemaker rate [54]. The membrane potential (E_m) in the SA node is characterized by the existence of diastolic depolarization which allows the cell to spontaneously achieve threshold for activation, thereby triggering an action potential [55]. There are several currents which have been implicated in these processes including: I_{K1} , $I_{Na/Ca}$, $I_{Ca,T}$, I_f , I_{Na} , $I_{Ca,L}$ [56]. I_{K1} , the inward rectifier K^+ channel, is responsible for stabilizing the resting E_m near E_K . Its density has been shown to be low in pacemaker cells [54], decreasing the magnitude of the outward current that must be overcome by I_{Na} or I_{Ca} , to cause a regenerative action

potential. $I_{Na/Ca}$ may also be an important component as it contributes to early pacemaking since E_m declines faster than $[Ca^{2+}]_i$. It is also thought to participate in the latter part of diastolic depolarization because of $I_{Ca,T}$ and spontaneously triggered local SR Ca release through sparks [57]. The purported high density of $I_{Ca,T}$ in nodal cells as well as the fact that they are activated in the pacemaker E_m range, may allow them to contribute to depolarization [58]. In nodal cells, most I_{Na} channels are inactivated, thus only a few Na^+ channels can contribute to the inward current associated with diastolic depolarization [59]. $I_{Ca,L}$ may also participate in the latter part of pacemaker activity because of its relatively positive E_m for activation. Probably the most important of the pacemaker currents, I_f , is activated by hyperpolarization and is often referred to as the funny current. It has unusual characteristics, including activation upon hyperpolarization, permeability to K^+ and Na^+ , modulation by internal cAMP, and a relatively small, single-channel conductance[60].

HCN Channels

It is generally accepted that I_f is a critical component of the pacemaker current. This current has been described primarily in SA node, AV node, and Purkinje cells, but is also present in atrial and ventricular cells as well as in other tissues including brain. The channels responsible for I_f have been cloned and are known as hyperpolarization-activated cyclic nucleotide-gated (HCN) channels. So far, four mammalian HCN genes have been cloned with HCN2 being the predominant type found in the heart. The molecular structure of HCN channels is similar to voltage-gated K^+ channels with six transmembrane segments, a positively charged S4 segment, and the GYG pore sequence which is found in most known K^+ -selective channels. HCN channels also exhibit a high

similarity to cyclic nucleotide-gated channels in the cyclic nucleotide-binding domain located in the COOH terminus.

In the SA node, Difrancesco et al [61] have suggested that I_f may be exclusively responsible for the pacemaker potential. This is supported by the following evidence:

- 1) I_f is a mixed cation current with a relative permeability ratio $P_{Na^+}/P_{K^+} \sim 0.2 - 0.4$ [61], activated on hyperpolarization normally below about -40 mV with properties specifically designed for generating a slow depolarization following hyperpolarization [62];
- 2) I_f is highly expressed, specifically, in pacing tissue but poorly expressed in non-pacing tissues;
- 3) I_f block by Cs^+ slows diastolic rate and spontaneous activity [63];
- 4) cAMP accelerates I_f activation kinetics and shifts its voltage dependence of activation to more positive voltages. This cAMP-mediated enhancement of channel activity accounts for the positive chronotropic effect of β -adrenergic agonists in the heart [64];
- 5) ACh lowers the cellular cAMP level, thereby inhibiting the rate and extent to which I_f channels open after action potential and reduces the firing frequency of pacemaker potential [37];
- 6) Mice with cardiomyocyte-specific deletion of HCN2 displayed cardiac sinus dysrhythmia, a reduction of the sinoatrial HCN current and a shift of the maximum diastolic potential to hyperpolarized values, which strongly

suggests that the HCN2 subunit is a major determinant of membrane resting potential and is required for regular cardiac rhythmicity [65].

However, the critical importance of I_f in the pacemaker activity has been challenged by several groups, based on the following evidence:

- 1) In dominant pacemaker cells, the diastolic depolarization (DD) range is -35 to -50/-60 mV, which only slightly overlaps the I_f activation range of -50/-60mV to -100/-120mV. This restricts the role of I_f in SA node pacemaking;
- 2) I_f activates with a time constant of 1-2 seconds while I_K deactivates with a time constant of 300ms, thus only I_K decay can account for DD rate in the pacemaking cells;
- 3) Cs^+ blocks DD in subsidiary pacemaker cells but not in dominant ones [66].

Furthermore, Lakatta et al [67] argued that cyclic variation of submembrane $[Ca^{2+}]$ and activation of normal mode NCX during DD act in concert with ion channels to confer on SA node cells their status of dominance with respect to pacemaker function, based on the following facts:

- 1) Bogdanov et al [68] demonstrated that local Ca^{2+} release during the later part of DD via RyRs in SA nodal cells activates NCX. This resultant inward current enhances the rate of DD, leading to an increase in the beating rate.
- 2) β -AR stimulation by isoproterenol recruits additional RyRs to release Ca^{2+} during DD; this activates NCX current and increases the rate of DD. Partial inhibition of normal RyR function by ryanodine, which results in SR Ca^{2+}

depletion, blunts the dose response of isoproterenol to increase the beating rate [69].

1.4.2 Chronotropic modulation

Cholinergic modulation

Acetylcholine (ACh) is released from parasympathetic vagal nerves. In the heart, ACh shortens the atrial action potential, slows SA node depolarization and conduction through AV node, and causes a minor decrease in ventricular contractility by binding to the M_2 muscarinic receptor. However, a mechanistic explanation surrounding ACh action is unclear. In the rabbit SA node, ACh release can activate an ACh-activated K^+ current, $I_{K_{ACh}}$, resulting in a hyperpolarizing shift in the I_f activation curve [37]. However, ACh at nanomolar concentrations inhibits I_f and slows spontaneous rate, whereas 20-fold higher concentrations are required to activate the acetylcholine-dependent potassium current ($I_{K_{ACh}}$). Thus, DiFrancesco et al [61] suggested that modulation of I_f , rather than $I_{K_{ACh}}$, is the mechanism underlying the muscarinic control of cardiac pacing at nanomolar acetylcholine concentrations. However, Boyette et al [70] showed that block of I_f by Cs^+ or ZD7288 does not abolish the effect of ACh on the rabbit SA node, therefore, arguing that slowing of heart rate by ACh is primarily the result of the activation of $I_{K_{ACh}}$. However, the non-specific blocker of $I_{K_{ACh}}$, Ba^{2+} substantially reduced the effect of ACh.

In general, ACh can also induce both positive and negative inotropic responses in the heart. The positive inotropic effect is thought to be mediated through prostaglandin release from the endocardial endothelium [71, 72]. The inotropic effect of ACh on the

heart is both dose dependent and species specific. Korth et al [73] reported that in guinea pig papillary muscle carbachol produced concentration-dependent increases in force by stimulating NCX. Furthermore, Tsuji et al [74] found that ACh caused a positive inotropic effect in embryonic chick ventricle, and. Du et al [75] have suggested that the positive inotropic response is mediated by M_1 receptors. Wang et al [76] found that ACh elicits a rebound positive inotropic stimulation of $I_{Ca,L}$, which is mediated via cAMP-dependent protein kinase A (PKA) enhanced by ACh-induced inhibition of phosphodiesterase. In conclusion, the mechanisms of positive inotropic effect of ACh remain unclear.

1.4.3 β -adrenergic modulation

β -adrenergic receptor (β -AR) activation is particularly important for both inotropic and chronotropic regulation of the heart. β -agonists stimulate adenylyl cyclase, elevating cAMP, which activates cAMP-dependent PKA and leads to phosphorylation of several downstream proteins including the L-type Ca^{2+} channel, troponin I, phospholamban and RyR. The well-documented positive inotropic effect of β -AR stimulation is the result of enhanced amplitude of the intracellular Ca^{2+} transient via two different pathways. The classic pathway is through adenylyl cyclase, as previously discussed. Another putative pathway is the direct effect of the activated α subunit of G_s on the $I_{Ca,L}$ [77], so called “membrane delimited” activation. Phosphorylation of phospholamban, in response to increases in cAMP levels during β -agonist administration, is accompanied by an increase in the activity of the cardiac SR Ca^{2+} transporter or SERCA2A, and therefore a faster rate of cardiac relaxation [78, 79]. The increased rates

of Ca^{2+} uptake lead to increased cardiac SR Ca^{2+} sequestration levels. This allows a greater amount of Ca^{2+} to be available for release on subsequent contractions, and results in increased contractile force. PKA-dependent phosphorylation of the cardiac RyR can also increase SR Ca^{2+} release during the twitch in response to isoproterenol. RyR is phosphorylated by PKA during β -AR stimulation [80]. Phosphorylation results in an increase in the open probability of RyR, promoting Ca^{2+} release from the SR [81, 82]. β -AR stimulation also decreases myofilament Ca^{2+} sensitivity, due to a cAMP-dependent phosphorylation of troponin I [83, 84], resulting in an increased off-rate of Ca^{2+} from TnC promoting increased mechanical relaxation. However the dramatic increase in the magnitude of the Ca^{2+} transient, for reasons cited above, more than compensates for this, so cardiac contractility is enhanced substantially in response to β -AR activation.

β -agonists also have a well documented positive chronotropic effect in the heart.

The effects include the following:

- 1) β -AR stimulation shifts the E_m -dependence of I_f activation to more depolarized potentials, leading to a more rapid DD [85, 86] by a direct effect of cAMP on HCN channels;
- 2) β -agonists accelerate the decline in gK [87] which may contribute to pacemaker activity especially in SA nodal cells, with more positive diastolic potentials [88];
- 3) Local Ca^{2+} transients during pacemaker depolarization occurs via Ca^{2+} release from RyRs, and that Ca^{2+} release is amplified, in part at least, by recruitment of additional RyR Ca^{2+} releases after β -AR stimulation [69]. This resultant amplification has a pivotal role in β -AR induced chronotropy by promoting

forward mode NCX activation and enhancing the rate of diastolic depolarization.

1.5 Neonate phenotype in arrhythmogenesis

During the first weeks of life in humans, the average sinus rate ranges from 120~150 beats per minute (bpm), and falls to below 100 bpm by 5 years of age [89]. Thus, this age-dependent change in heart rate together with the developmental changes that occur in cardiac electrophysiology alter the susceptibility of the neonate heart to arrhythmogenic stimuli to a greater degree in comparison to adult.

1.5.1 Developmental changes in cardiac electrophysiology

The characterization of developmental changes in cardiac ionic channel activity can provide insight into the mechanisms of age-related differences in E-C coupling and chronotropic regulation. Adult cardiomyocytes utilize transsarcolemmal Ca^{2+} flux through L-type voltage-gated Ca^{2+} channels to trigger SR Ca^{2+} release in a process known as Ca^{2+} -induced Ca^{2+} release (CICR). L-type Ca^{2+} channel expression in rabbit heart increases with development, with a concurrent 5-fold increase in I_{Ca} density between gestational day 21 and adult [90, 91]. The α_1 subunit of the L-type Ca^{2+} channel ($\text{Ca}_v1.2$) mRNA transcript levels increase by 2-3 fold between the perinatal period and adulthood [92]. Developmental changes in the kinetics of I_{Ca} also favour Ca^{2+} influx through L-type Ca^{2+} channels in the adult heart. The increased prevalence of L-type Ca^{2+} channels in the adult heart compared to that in the neonate [93] suggest that I_{Ca} contributes relatively little to Ca^{2+} influx in immature rabbit heart. For SR function, Fisher et al [94] demonstrated that in the rabbit heart, mRNA transcript levels of SR Ca^{2+} pump protein

were 52-63% lower in the fetus than in the adult. These results indicate the slower Ca^{2+} uptake and ATPase rates in the fetal rabbit heart can be largely related to lower SERCA2A mRNA and protein levels. However, there is evidence that despite these *in vitro* assessments, SR Ca^{2+} uptake in the neonate cardiomyocyte is not compromised [95]. Developmental changes in sarcolemmal NCX density also contributes to the age difference in E-C coupling. Artman [96] found fetal and newborn sarcolemmal vesicles had greater NCX activity and protein compared to the adult. Artman et al [97] also found that NCX current density is highest in newborn rabbits and declines by ~75% in adults relative to neonate levels. Further, Chen et al. [98] found that in the five day old rabbit heart, NCX is localized to the periphery of the cell, while in adult myocytes the NCX is more evenly distributed in the sarcolemma and T-tubule system.

These unique characteristics and expression patterns of Ca^{2+} channel and ion carriers contribute to the specific phenotype of neonate E-C coupling.

1.5.2 Developmental changes in innervation

Myocardial contractility and heart rate are controlled, in part, by cardiac sympathetic and parasympathetic innervation. In the rabbit heart innervation fully develops over the first weeks after birth [99]. Because cardiac function and autonomic innervation mature during fetal and perinatal development, it is difficult to separate intrinsic from innervation-induced changes. However, Pappano [100] demonstrated that inotropic and chronotropic effects in cardiac tissue can be elicited by agonist and antagonists before innervation is fully developed. In their study, they found that canine parasympathetic control developed faster than sympathetic control. This might suggest

important age-dependent changes in the interaction between the adrenergic and cholinergic systems. Hageman et al [101] showed that the baroreceptor reflex control in the puppy is less well developed than in the adult dog and this was attributed to developmental differences in neural regulation of the heart at or beyond the efferent nerve terminals.

CHAPTER TWO: OBJECTIVES OF THE THESIS

Based on the literature discussed in the previous chapter, the factors determining the predilection for the development of JET are likely to include the following:

- 1) Metabolic and excitation changes that are induced by myocardial stunning or injury;
- 2) β -adrenergic agonists administered during recovery from I-R injury;
- 3) Specific attributes of the neonate heart, such as differences in Ca^{2+} handling in the SA and AV nodal cells, differences in densities in HCN, NCX, NHE, and receptors that regulate intrinsic frequencies in SA and AV nodal cells, as well as the smaller cell size and attendant higher input resistances.

Since in the clinical setting JET is a postoperative phenomenon, we tested the effects of a variety of drugs which are used during or after open heart surgery on the pre-ischemic and post-ischemic neonatal rabbit heart. We hypothesized that NHE inhibition has additional protection to the neonatal heart in hypothermic cardioplegic arrest relative to hypothermic cardioplegic arrest alone. We also hypothesized that β -adrenergic agonists have an arrhythmogenic effect on the post-ischemic neonate rabbit heart and NHE inhibition can prevent this β -adrenergic agonist-induced arrhythmia.

CHAPTER THREE: EXPERIMENTAL DESIGN AND METHODS

3.1 Working heart apparatus

To test the chronotropic and inotropic regulation in the neonate heart, a Langendorff-working heart preparation was used. This perfused isolated heart system was originally described by Oscar Langendorff in 1895. The Langendorff-mode heart has become a commonly used technique for the examination of contractile strength, heart rate and vascular effects without the complications of an intact animal model. Using this technique the isolated heart can be functionally maintained for many hours by having the perfusate retrogradely forced through an aortic cannular through the coronary ostium into the coronary bed. Since the heart contracts without an afterload in this system, the technique does not permit the left ventricle to generate the pressure-volume work that is representative of typical cardiac function. A modification that allows the heart to pump fluid via the normal left ventricular circulatory pathway is called the “working” heart model and was developed by Neely and colleagues [102]. In this preparation, the perfusate enters the heart via the cannulated left atrium, passes through to the left ventricle, and is ejected out the aorta. In this case, the preload is determined by the end diastolic volume, while the afterload (pressure the heart must overcome to eject perfusate into the aorta) is controlled by the height of the column emanating from the aortic outflow. Figure 1 is a schematic representation of the perfusion system.

3.2 Methods

3.2.1 Animals

10-day old white New Zealand rabbits (either sex) were supplied from a local breeder. The animal welfare committees of Simon Fraser University and the University of British Columbia have approved the use of animals and the experimental protocol. Rabbits were anesthetized by intraperitoneal sodium pentobarbital (40 mg/kg body weight) and heparin (50 units/kg body weight).

3.2.2 Heart isolation and perfusion

Immediately following anesthetization, a tracheotomy was performed and the rabbit was connected to a Harvard rodent ventilator (Harvard Apparatus Co.). The diaphragm was accessed by a transabdominal incision and cut carefully to expose the thoracic cavity. The thorax was opened and the heart was exposed. The heart was rapidly removed and immersed in ice-cold Krebs-Henseleit buffer, the composition of which is described below. The aorta was then clamped to the cannula with a small blunt artery clip, while a ligation was rapidly tied around the aorta. Full flow perfusion was initiated as soon as the heart was mounted on the cannula. To facilitate adequate drainage, a small incision was made in the base of the pulmonary artery. Any surplus tissue, such as bits of thymus or lung, was trimmed away as well. During Langendorff mode, the left atrium was cannulated via one of the pulmonary veins in the preparation for the working heart mode. After an equilibration period of 10 minutes of aerobic perfusion in the Langendorff mode, the heart was switched into working mode by clamping the aortic inflow line and opening up the left atrial inflow line. The perfusate

was delivered to the left atria from the multi-bulb oxygenator at a preload pressure of 10 mmHg and was ejected spontaneously from the working heart into a compliance chamber and then into the outflow line. The hydrostatic overload was set at a column height equivalent to 40 mmHg pressure.

3.2.3 Exclusion criteria

The pre-assigned exclusionary criteria were: a) hearts exhibiting coronary to aortic flow ratios greater than 60%; b) an aortic flow of less than 10 ml/min and c) the existence of an arrhythmia at the end of pre-ischemia working mode. Any heart exhibiting any of these three exclusionary criteria was excluded from the study.

3.2.4 Perfusion fluid

The Langendorff mode perfusion buffer was based on a bicarbonate fluid as defined by Krebs and Henseleit in 1923, which mimics the key ionic content of blood or plasma and was maintained at a pH of 7.4 at 37°C. It had the following composition (in mM): NaCl 118.5, KCl 4.7, MgSO₄ 1.1, KH₂PO₄ 1.2, NaHCO₃ 25.0, CaCl₂ 2.0, ascorbic acid 5×10^{-5} , and glucose 11.0 and two units of insulin. The perfusate was filtered (5 μm) before use to remove any particulate impurities. The perfusion buffer for the working mode was same as the Langendorff buffer except for the addition of 0.4 mM palmitate bound to 3% bovine serum albumin. The reason for the use of free fatty acid in this mode was to keep the perfusate as similar to the in vivo condition as possible. Although β-oxidation of FFA plays a minor role in the production of metabolic energy immediately

post-partum, its role steadily increases until, by the seventh day after birth, the heart is oxidizing free fatty acids as its major metabolite and source of energy [103, 104].

3.3 Experiment protocols

3.3.1 Study 1: Normal neonate myocardium regulation

After the 10 minute Langendorff stabilization period, the heart was switched into working mode, where it continued to work for 15 minutes. After 15 minutes in the working mode, the aortic flow was measured by timed collection from the aortic ejection line. Coronary flow was determined by the collection of the effluent underneath the heart simultaneously. Once the stabilized heart function was assessed, one dose or multiple doses of a variety of pharmacological agents were added to the perfusion solution. Data were recorded every 5 minutes up for the entire one hour period of being in working heart mode.

3.3.2 Study2: NHE inhibition on the ischemia/reperfusion stunned neonate myocardium

Immediately after the stabilized heart function was assessed, the heart was arrested with a single dose of modified St. Thomas' Hospital cardioplegia solution. The solution was adjusted to pH of 7.8, maintained at 10°C and contained (in mM): NaCl 110, MgCl₂ 16.0, NaHCO₃ 10.0, KCl 16.0, and CaCl₂ 0.4 and in some experiments it also contained either 5 μM or 10 μM HOE642. The cardioplegia was delivered for three minutes at 10°C from a height of 55 cm via a side arm of the aortic ejection line and then the heart was placed in a cold water bath at 10°C for 2 hours. Following this period of

ischemia, the heart was then retrogradely reperfused at 38° C for 10 minutes in Langendorff mode followed by 60 minutes in working mode. The heart function was recorded every 15 minutes during the recovery in working mode.

3.3.3 Study 3: Effect of myocardial stunning on arrhythmogenesis

In a manner similar to that described in Study Two (see above), the heart was arrested with cold cardioplegia either with or without 10 μM HOE642 for two hours. After the stabilized heart function was assessed, a single dose of 20 μM dopamine was administered and the heart was kept working for one hour. During this period, any indications of abnormal rhythm patterns were recorded.

3.4 Left ventricular hemodynamics

Within the first 5 minutes of the heart functioning in working mode, a pre-calibrated four-electrode pressure- volume conductance sensor catheter (2F, SPR-838, Millar instruments Inc, Houston, USA) was introduced into the left ventricle. The signals from the catheter were continuously recorded at a sampling rate of 1000 s^{-1} using an ARIA pressure-volume conductance system (Millar instruments Inc.), coupled to a DAQ converter (National instruments Inc. Austin, TX), and then stored and displayed on a computer. All pressure-volume loop data were analysed with a cardiac pressure-volume analysis program (PVAN 3.2, Millar instruments Inc.). From the output of this device, the following parameters were routinely determined: heart rate, left ventricle stroke volume, cardiac output, ejection fraction, end diastolic volume, dP/dt_{max} , and dP/dt_{min} .

3.5 Statistical analysis

3.5.1 Calculation of sample size

The power of the experiments was set as 0.8. The sample size calculation was based on the following formula:

$$d = \frac{(\mu_1 - \mu_2)}{\sigma \sqrt{(1 - r)}} = 2.24$$

Where d = effect size, $(\mu_1 - \mu_2)$ = the difference of the two means which was set as 15%, γ = correlation which was set as 0.8. With $\alpha = 0.05$, G*Power which is a general power analysis program [105], predicted that our sample size should be eight per group.

3.5.2 Statistical significance

Data were expressed as mean \pm SE, and analyzed statistically using a two-way analysis of variance (ANOVA) followed by Bonferroni post hoc tests using the statistical software package SPSS (SPSS Inc, Chicago, IL, USA). A value of $p < 0.05$ was considered statistically significant.

CHAPTER FOUR: RESULTS

4.1 Study 1: Normal neonate myocardium regulation

4.1.1 β -adrenergic agonist and antagonist

It is generally recognized that dopamine has both positive chronotropic and inotropic effects on the myocardium [106]. In our isolated neonatal working heart model, 2.5 μ M dopamine applied every 5 minutes and 30 seconds during the pre-ischemia period, increased heart rate by about 42% over baseline by the fifth dose and then reached an asymptotic level of around 139% of baseline by the eighth dose. However, aortic flow was enhanced to 140% by the fourth dose and gradually decreased to 89% at the end of one-hour working mode. Cardiac output increased up to 133.9% then decreased to 87.3%. Stroke volume was enhanced to 108.4% at the first dose, and then decreased all the way down to 62.7% at the last dose, an effect which mirrored the response of the ejection fraction. However, end diastolic volume consistently exhibited a value of 105%. Furthermore, the dP/dt_{max} was increased up to 114.5%, then decreased and ended up at 91.6%, similar as dP/dt_{min} (Figures 2-9).

Esmolol is a specific β_1 -adrenergic antagonist [107]. When 10 μ M esmolol was administered prior to 2.5 μ M dopamine, it decreased heart rate by about 9.5% and eliminated the positive chronotropic effect of dopamine (Figures 10-17).

Propranolol is a nonselective β -adrenergic receptor-blocking agent [108]. When the heart received 10 μ M propranolol prior to the addition of 20 μ M dopamine, it decreased the pre-ischemia heart rate by 25% as well as abolishing the positive chronotropic and inotropic effects of 20 μ M dopamine (Figures 18-25).

We also tested another potent non-selective β -adrenergic agonist, isoproterenol [109]. A single dose of 40 nM isoproterenol increased heart rate by 51.5% and then HR gradually decreased to 118.8% at the end of one-hour working mode. With the administration of 40 nM isoproterenol, aortic flow increased up to 212.7%, then decreased to 65.8% by the end of the one-hour period. Cardiac output increased to 166.0%, then decreased to 88.3%, similar as ejection fraction, dP/dt_{max} and dP/dt_{min} . End diastolic volume decreased to 89.9% and slowly increased up to 105.6% by the end of one hour (Figures 26-33).

When 10 μ M esmolol was added prior to the administration of 40 nM isoproterenol, it partly eliminated the positive chronotropic effect on the neonatal heart, and it completely eliminated the positive inotropic effect of isoproterenol (Figures 34-41).

After the heart underwent two hours of ischemia, we applied 2.5 μ M dopamine every 5 minutes and 30 seconds during the working heart mode of the reperfusion phase. Dopamine administered under these conditions resulted in similar effects on heart rate as it did in the pre-ischemic condition (Figures 42-49).

4.1.2 I_f inhibitors

ZD7288 is considered to be a reasonably specific HCN channel blocker [110]. One dose of 5 μ M of ZD7288 decreased heart rate slowly and consistently such that heart rate was reduced to 71.6% of its original value at the end of one-hour working mode. With the administration of 5 μ M ZD7288, aortic flow was maintained at baseline levels for the first 5 minutes, and then was gradually reduced to 29.6% of its original value by 60 minutes. Stroke volume increased to 112.3% after the first 5 minutes, maintained at baseline levels for 10 minutes and then decreased to 59.8% by the end of working mode. End diastolic volume, dP/dt_{max} , and dP/dt_{min} showed a similar pattern to stroke volume (Figures 50-57).

With the administration of 5 μ M ZD7288 followed by 20 μ M dopamine, heart rate was maintained at baseline levels. However, other parameters decreased slightly with the administration of ZD7288, and increased briefly with the application of dopamine and then decreased gradually again (Figures 58-65).

4.1.3 Cholinergic agonist and antagonist

Atropine is termed an anti-muscarinic drug due to its antagonistic effect on the muscarinic actions of acetylcholine [111]. In our neonate rabbit working heart model, atropine administered over the range of 100 nM up to 30 μ M exhibited no positive chronotropic effects. In fact, 30 μ M atropine decreased heart rate in a consistent manner so that by the end of the 60 min period of working mode, HR was decreased to 65.9% of its original level. Atropine also dramatically reduced aortic flow to 3.8% of its original value at the end of one hour of working mode. In a similar fashion, cardiac output was

reduced to 16.9%, stroke volume to 32.2% and ejection fraction to 21.8% of control values in the same timeframe. End diastolic volume was maintained at baseline levels, while dP/dt_{\max} and dP/dt_{\min} decreased gradually to 38.1% and 43.9%, respectively (Figures 66-73).

With the administration of 5 μM ACh prior to 30 μM atropine, heart rate was reduced to 85.2% of its control value. With the addition of atropine, heart rate increased transiently to 90.1% and then decreased to 69.6%, while other parameters were not significantly affected (Figures 74-81).

4.2 Study 2: NHE inhibition on the ischemia/reperfusion stunned neonate myocardium

We examined the effects of NHE inhibition on the functional recovery of the post-ischemic neonatal working heart in which the preparation was arrested with a single dose of St. Thomas' Hospital cardioplegia (using a $[\text{Ca}^{2+}]_o$ of 0.4 mM) at 10°C. NHE inhibition was implemented with the addition of 5 μM or 10 μM HOE642 to the cardioplegic solution. We found that hearts exposed to HOE642 had improved recoveries of aortic flow, stroke volume, ejection fraction, and dP/dt_{\max} during one-hour reperfusion period relative to the controls (Figures 83, 85-87).

4.3 Study 3: Effect of myocardial stunning on arrhythmogenesis

Post-ischemic administration of 20 μM dopamine induced an arrhythmia significantly more frequently in comparison to control (1 of 10 hearts versus 5 of 11 hearts) (Table 1). The arrhythmia was reversed by the addition of 50 μM esmolol.

The administration of HOE642 to the cardioplegic solution had only a minor effect on the frequency of the dopamine-induced arrhythmia that occurred with the post-ischemic administration of 20 μ M dopamine compared to control (3 of 11 hearts versus 5 of 11 hearts) (Table 1).

CHAPTER FIVE: DISCUSSION

5.1 Study 1: Normal neonate myocardium regulation

5.1.1 β -adrenergic agonist and antagonist

Dopamine is often used during and/or immediately following open-heart surgery in order to correct for low cardiac output syndrome which is commonly observed following open-heart surgery.

The predominant effects of dopamine are dose-related. At low rates of infusion (0.5-2 $\mu\text{g}/\text{kg}/\text{min}$) dopamine causes vasodilation that is presumed to be due to a specific agonist action on dopamine receptors (distinct from α - and β -adrenoceptors) in the renal, mesenteric, coronary, and intracerebral vascular beds. At intermediate rates of infusion (2-10 $\mu\text{g}/\text{kg}/\text{min}$), dopamine acts mainly to stimulate the β_1 -adrenoceptors, resulting in improved myocardial contractility, increased SA rate and enhanced impulse conduction in the heart. At higher rates of infusion (10-20 $\mu\text{g}/\text{kg}/\text{min}$), there is an effect on α -adrenoceptors, resulting in vasoconstriction and a rise in blood pressure.

However, Hoffman et al [8] found that dopamine use postoperatively with patients aged less than six months was highly associated with JET. In this study, all patients received dopamine dosing strategies that ranged from 3~7.5 $\mu\text{g}/\text{kg}/\text{min}$. We estimated that pediatric patients' blood volume is 80ml/kg. So we used 2.5 μM dopamine infused every 5'30 minutes, which is an intermediate dose if converted into the

equivalent clinical concentration. Our pre-ischemia data showed that dopamine had a very powerful positive chronotropic effect on the neonatal rabbit heart. Our data also showed that dopamine enhanced aortic flow and cardiac output transiently. Furthermore, the rise in cardiac output was caused mainly by tachycardia. As can be seen in Figures 5-6, neither stroke volume nor ejection fraction increased concomitantly with increased cardiac output. Furthermore, this result may be due to myocardial characteristics related to the neonate phenotype. Durandy et al [112] have suggested that in the neonate stroke volume has a limited capacity to increase because of poor compliance.

We compared the post-ischemic dopamine effect with the pre-ischemic infusion strategy which showed that both chronotropic and inotropic effects were similar. We conclude that dopamine has an obviously negative inotropic effect under our experimental conditions in the neonate rabbit heart, an effect which is consistent with the observations of others. As Kollar et al [113] demonstrated that infusion of dopamine in the dog had a long lasting flow decrease effect at high heart rates. Dugger [114] also demonstrated that dopamine administered postoperatively had many side effects including an increased the risk of extravasation, vein and tissue damage, and possible disfigurement. In corroboration with what was observed in our study, these data suggest dopamine might not be an ideal first-line drug for postoperative low cardiac output therapy.

In our study, the concomitant administration of 10 μ M propranolol eliminated the chronotropic effects of dopamine strongly suggesting that the positive chronotropic effect of dopamine is mediated by β -AR. Furthermore, 10 μ M esmolol had the same effect as propranolol demonstrating that the chronotropic effect of dopamine is mediated through

β_1 -AR. In Study 3, esmolol also converted dopamine-induced arrhythmia to sinus rhythm (Figure 89) further confirming that the arrhythmogenic effect of dopamine is mainly mediated through β_1 -AR. However, esmolol did not eliminate the negative inotropic effect of dopamine which suggests that this effect may not be mediated through β_1 -AR. Further investigations are required.

Furthermore, Gray et al [115] conducted a clinical trial and found that esmolol was effective at rapid control of heart rate in postoperative supraventricular tachyarrhythmias. Mooss et al [116] confirmed that esmolol was highly effective in converting post-operative supraventricular tachyarrhythmic patients to normal sinus rhythm. Our data showed that esmolol has a strong negative chronotropic effect and a more potent negative inotropic effect on our isolated working heart preparation. Collectively these data suggest that esmolol might be considered for the treatment of JET since it can convert supraventricular tachycardia into sinus rhythm. However one has to be concerned with the negative inotropic effects of a beta blocker which can be deleterious.

Propranolol specifically competes with β -adrenergic receptor-stimulating agents for available receptor sites [117]. When access to β -AR sites is blocked by propranolol, the chronotropic, inotropic, and vasodilator responses to β -AR stimulation are decreased proportionately. Our data show that propranolol administered by itself decreased cardiac output more than 50% within the first 5 minutes infusion. It might be a good agent for control of tachycardia and hypertension but also raises the risk of low cardiac output syndromes.

Isoproterenol is another frequently used drug for postoperative low cardiac output syndrome. Previous work done by Holloway et al [118] showed that isoproterenol had a significant effect on both heart rate and cardiac output in the period immediately after open heart surgery. However, dopamine, in comparison to isoproterenol, also enhanced cardiac output but had minimal chronotropic effects. It was concluded therefore that dopamine should be the agent of choice in patients requiring positive inotropic agents in the period immediately after cardiac surgery. Sakata et al [119] did a similar study and compared dobutamine and isoproterenol administration in children . They doubted isoproterenol had significant chronotropic effects in children after open-heart surgery. However, dobutamine, a stimulator of β_1 -adrenergic receptors, had both powerful chronotropic and inotropic effect in these patients.

Our data showed that isoproterenol has strong positive chronotropic effects and a transient positive inotropic effect on the neonate rabbit heart. Furthermore, isoproterenol is known to cause a greater increase in myocardial oxygen consumption than dopamine and is likely associated with tachyarrhythmia. Dopamine causes less increase in myocardial oxygen consumption than isoproterenol. Moreover, as mentioned in Chapter One, the catecholamine tone is normally increased after open-heart surgery which increases the risk of development of arrhythmias. Thus the use of both isoproterenol and dopamine in pediatric patients postoperatively should be reconsidered.

5.1.2 I_f inhibitors

ZD7288 (4-(N-ethyl-N-phenylamino)-1, 2-dimethyl-6-(methylamino) pyridinium chloride), a potent blocker of HCN channels, is a SA node modulating agent which

produces a selective slowing of the heart rate. BoSmith et al [110] first did a study with dissociated guinea-pig SA node cells using whole cell patch clamp. They found that ZD7288 inhibits I_f by affecting the activation characteristics of I_f current, but not the ion selectivity of the I_f channel. They also found that ZD7288 had no significant effect on I_k . Schlack et al [120] evaluated the effect of ZD7288 on infarct size in dog. They found that ZD7288 reduced heart rate without effecting on infarct size.

We evaluated the effect of ZD7288 in our isolated neonatal working heart. Our data showed that ZD7288 caused bradycardia with a slow onset and as a consequence cardiac output decreased moderately. However, stroke volume was enhanced slightly and kept around 80% of control values most of the time. This suggests that it is a potent bradycardia agent with little effect on contractility, which might be an appropriate drug for pediatric patients with postoperative supraventricular tachycardia.

We also evaluated the effect of combining ZD7288 and dopamine to see if this combination circumvented the problems with dopamine in the post-ischemic myocardium. Our data suggest that this combination can eliminate the powerful positive chronotropic of dopamine. Furthermore, it decreased neonatal myocardial contractility.. Based on the above data, we conclude that this combination of ZD7288 and dopamine may not be efficacious for the low output pediatric patients after open-heart surgery.

5.1.3 Cholinergic agonist and antagonist

Atropine is commonly classified as an anti-cholinergic or anti-parasympathetic (parasympatholytic) drug. More precisely, however, it is an anti-muscarinic (M_2) agent since it specifically antagonizes the muscarinic actions of acetylcholine and other

chlorine esters. Clinically, atropine is used both in the treatment of post-infarction bradyarrhythmias and sometimes in the presence of ventricular tachyarrhythmias in an attempt to override suppression of the abnormal rhythm.

Therefore, we tested the effect of atropine under our experimental conditions. Our data showed that atropine in doses over the range of 100 nM to 30 μ M resulted in both negative chronotropic and inotropic effects on the isolated neonatal rabbit heart, which is contrary to the positive chronotropic effects that have been observed clinically by some groups. On the other hand, other groups have also observed the negative chronotropic effects of atropine. Cushney first described atropine-induced bradycardia on anesthetized cats in 1904. For a considerable period of time after that finding, the mechanism of atropine-induced bradycardia has been thought to result from the central stimulation of the vagal nucleus. However, Kottmeier et al [121] found that atropine methylbromide, which can not diffuse across the blood-brain barrier, also decreases heart rate in humans. As a consequence, several groups have attempted to understand the mechanism of atropine-induced bradycardia in different animals, including humans. The dose of atropine required to induce bradycardia was less than 0.2 μ M. This has been confirmed both through intravenous and oral administration. The ECG pattern in response to this dose of atropine exhibited a shortened P wave and a prolongation of both the P-R and R-T intervals. These observations together with our findings strongly suggest that the atropine-induced bradycardia results from a direct action on the heart. However, the mechanisms of the negative chronotropic effects of atropine remain unknown.

Since atropine is an anti-cholinergic agent, we also tested the chronotropic and inotropic effects of atropine in the presence of ACh. Our data showed that even in the presence of 5 μM ACh; the negative chronotropic effect of atropine was not altered significantly.

5.2 Study 2: Cardioprotective activity of NHE inhibitors

The Na^+/H^+ exchanger (NHE) is expressed in many mammalian cell types. NHE is responsible for the regulation of cytosolic pH by extruding protons using the inward directed Na^+ electrochemical gradient and exhibits a tightly coupled 1:1 stoichiometry. NHE activation is exhibited primarily in the face of intracellular acidosis. During myocardial ischemia and reperfusion due to the intracellular H^+ accumulation, NHE is activated to restore physiological pH_i by H^+ extrusion. Nevertheless, an excessive stimulation of NHE results in an increase of intracellular Na^+ concentration and a subsequent activation of Na^+/K^+ ATPase, with an attendant increase in energy consumption. However, the resultant high intracellular Na^+ level may also contribute to reverse mode $\text{Na}^+/\text{Ca}^{2+}$ exchanger activity that can lead to raised cytosolic Ca^{2+} levels. In turn, the accumulation of intracellular Ca^{2+} can contribute to cellular damage resulting in arrhythmias and myocardial stunning. As NHE1 is the predominant isoform in the mammalian myocardium, NHE1 inhibitors were investigated in several models of ischemia–reperfusion.

Gumina et al [122] tested the effect of eniporide (NHE inhibitor, EMD96785) which was administrated 15 minutes prior to myocardial ischemia induced by occluding the left anterior descending coronary artery for 60 minutes followed by 3 hours of reperfusion. In the canine model, eniporide (0.75 mg kg^{-1} , iv) significantly reduced the

infarct size and the area at risk. Knight et al [123] evaluated zonisipride (NHE1 inhibitor, CP-597,396) both *in vitro* and *in vivo* using rabbit models of myocardial ischemia-reperfusion injury. They infused eniporide 30 min before ischemia until the end of reperfusion phase; it reduced the infarct size to a greater extent than either eniporide or cariporide (NHE1 inhibitor, HOE642) and did not cause any *in vivo* hemodynamic changes. In all of the aforementioned studies, the NHE1 inhibitors were administered to the systemic circulation.

To eliminate any unnecessary side effect of drug, our previous work restricted the drug application only to the cardioplegia. We used an injured isolated neonatal rabbit heart that underwent ischemia and reperfusion injury to evaluate the effect of HOE642, which was applied to the cardioplegia and found that HOE 642 resulted in improved recovery of this injured preparation [124]. In the present study, we tested this drug in perfused hearts that did not undergo any experimentally-induced injury but the ischemia reperfusion injury occurred in the presence of a buffer containing 0.4 mM palmitic acid. Under these conditions, both 5 μ M and 10 μ M HOE groups improved the recovery significantly. Based on these results, we conclude that HOE642 may be beneficially included as a component of the cardioplegia used for pediatric open-heart surgery.

5.3 Study 3: The arrhythmogenic role of dopamine and the antiarrhythmic effect of NHE inhibitor in neonate.

As mentioned earlier, Hoffman et al [8] postulated that dopamine is associated with the development of JET. Furukawa et al [125] infused 20 μ M/kg/min of dopamine iv into adult dogs and ventricular arrhythmias were detected intermittently. Our data showed that dopamine had a tendency to elicit arrhythmias on our preparation. However,

increasing the duration of ischemia did not increase the frequency of dopamine-induced arrhythmias.

One postulated mechanism by which myocardial ischemia/reperfusion injury can be arrhythmogenic is through intracellular Ca^{2+} accumulation, which is due in part to a rise in intracellular Na^+ that results from stimulation of NHE activity [126]. Na^+ and Ca^{2+} overload may lead to the generation of arrhythmias due to onset of early and delayed after depolarizations that they can induce. Dyck et al [127] showed that ischemia and acidosis can increase the amiloride-sensitive NHE1 in the mammalian myocardium. Aye et al [128] demonstrated that HOE 642, a specific blocker of NHE-1, has anti-arrhythmic effects during reperfusion in rat hearts.

However, based on our results, HOE 642 did not show itself to have a powerful antiarrhythmic effect in our experimental conditions. One reason is that other groups infused NHE inhibitor prior to ischemia or/and right before reperfusion. We administered HOE only into the cardioplegia and upon reperfusion HOE was likely washed out completely, which may not prevent stunned pacemaker cells effectively. Another possible reason for this result is that we did not have direct ECG electrodes on the rabbit hearts and arrhythmias were determined by the presence of the R wave calculated from the pressure-volume loop, which may result in arrhythmias not being detected. Therefore, a direct ECG device should be setup for further investigation.

5.4 Summary

JET is an important clinical problem because of the associated morbidity. Since the mechanisms of its induction are unknown, current treatment tends to be non-specific

(e.g. core temperature cooling and/or Mg^{2+} administration) and often lacks efficacy. In this study, we examined the effects of dopamine on the pre- and post-ischemic neonatal myocardium, and the data indicate that dopamine has a positive chronotropic effect but not a positive inotropic effect under these conditions. The data also show that dopamine has an arrhythmogenic effect on the ischemia/reperfusion stunned neonatal myocardium. HOE642 has significant effect on the reduction of I/R myocardial injury, but does not appear to play a robust antiarrhythmic effect in this animal model.

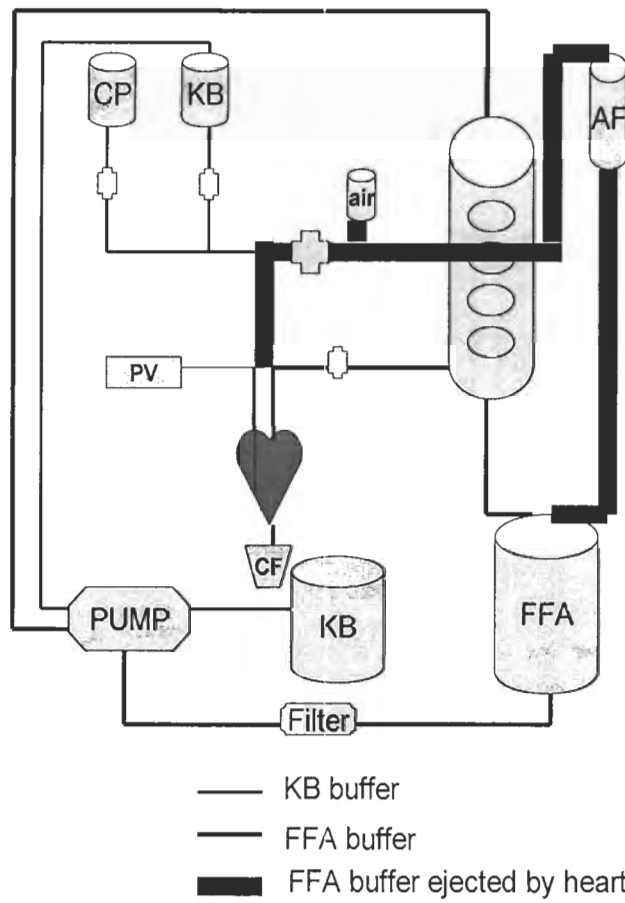


Figure 1 Isolated Langendorff /working heart apparatus.
 (Adapted from Panagiotis Galanopoulos²⁰⁰¹ with permission)

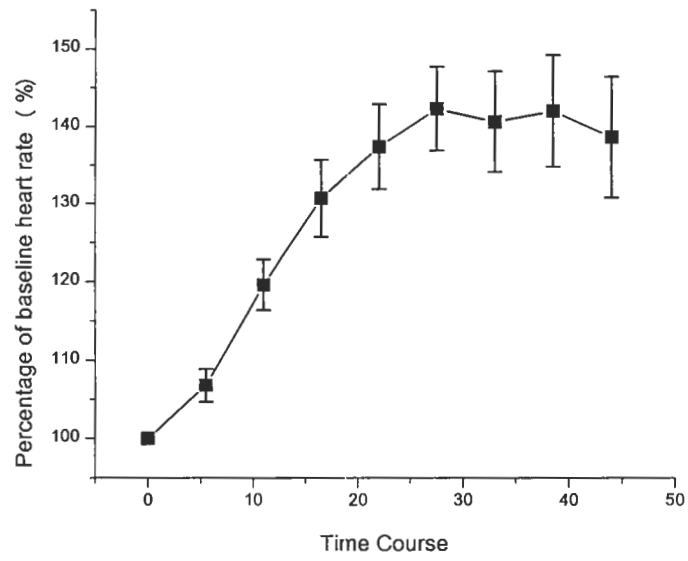


Figure 2 Pre-ischemia 2.5 μ M dopamine applied every 5'30 (N=10)

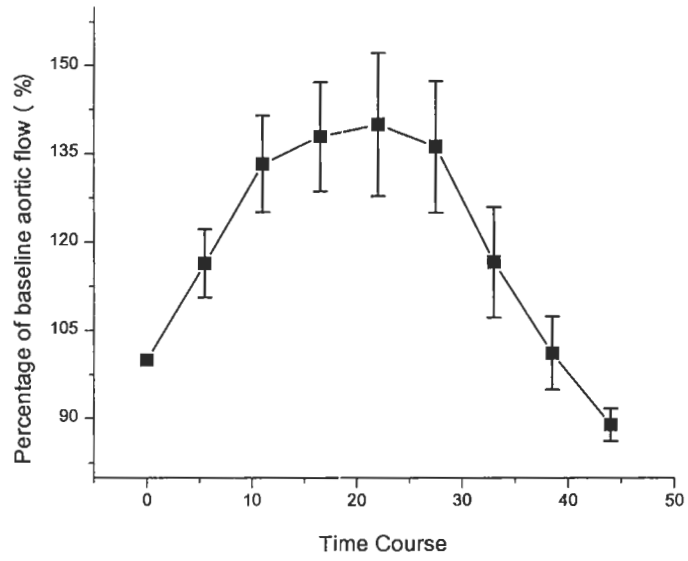


Figure 3 Pre-ischemia 2.5 μ M dopamine applied every 5'30 (N=10)

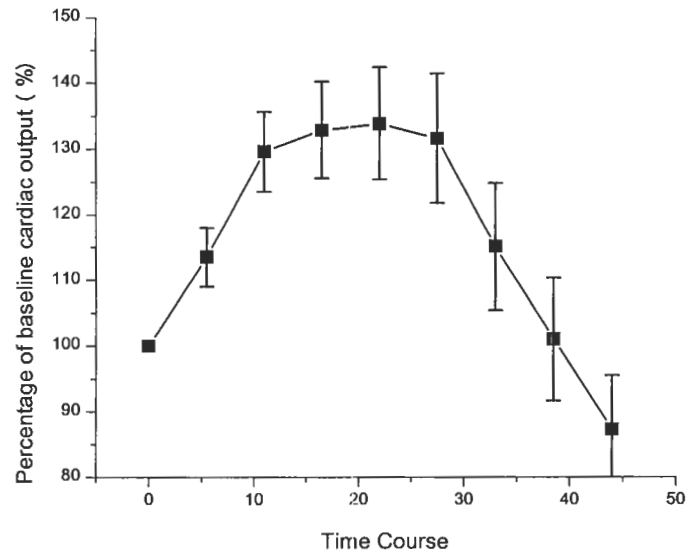


Figure 4 Pre-ischemia 2.5 μ M dopamine applied every 5'30 (N=10)

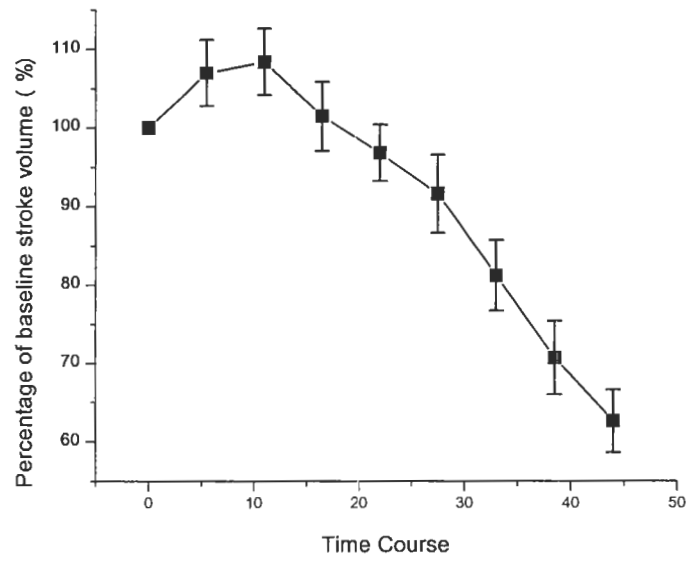


Figure 5 Pre-ischemia 2.5 μ M dopamine applied every 5'30 (N=10)

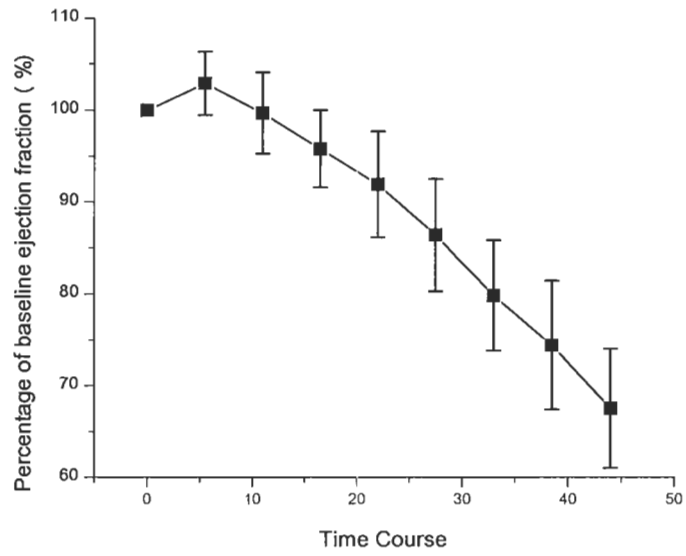


Figure 6 Pre-ischemia 2.5 μ M dopamine applied every 5'30 (N=10)

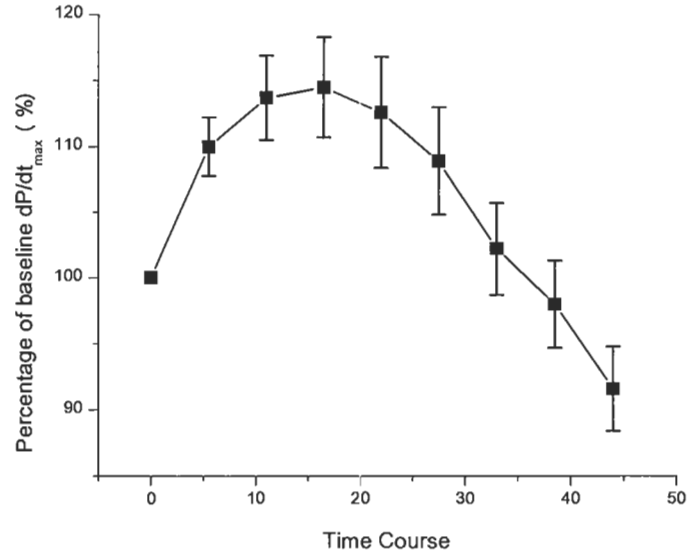


Figure 7 Pre-ischemia 2.5 μ M dopamine applied every 5'30 (N=10)

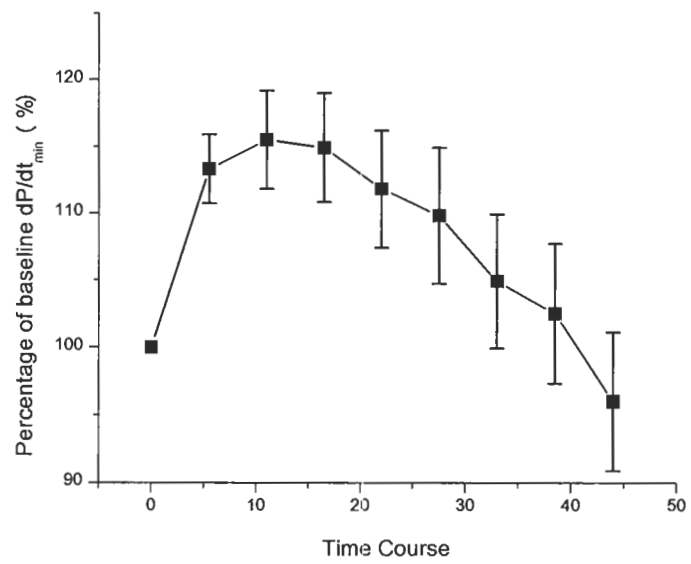


Figure 8 Pre-ischemia 2.5 μ M dopamine applied every 5'30 (N=10)

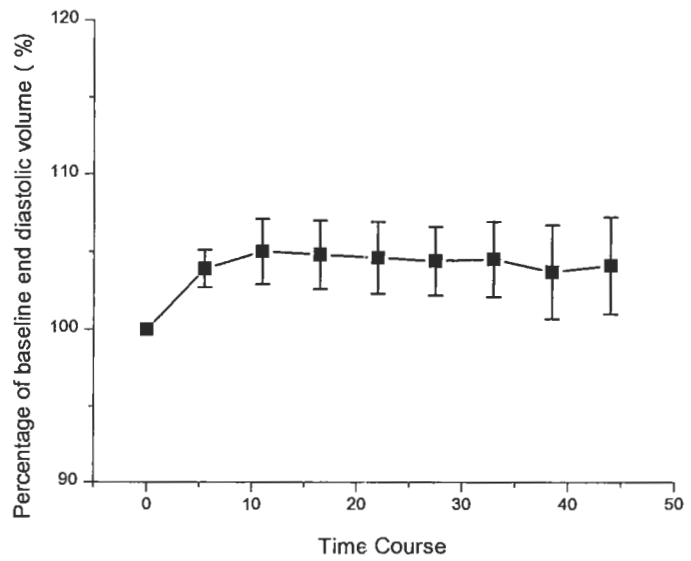


Figure 9 Pre-ischemia 2.5 μ M dopamine applied every 5'30 (N=10)

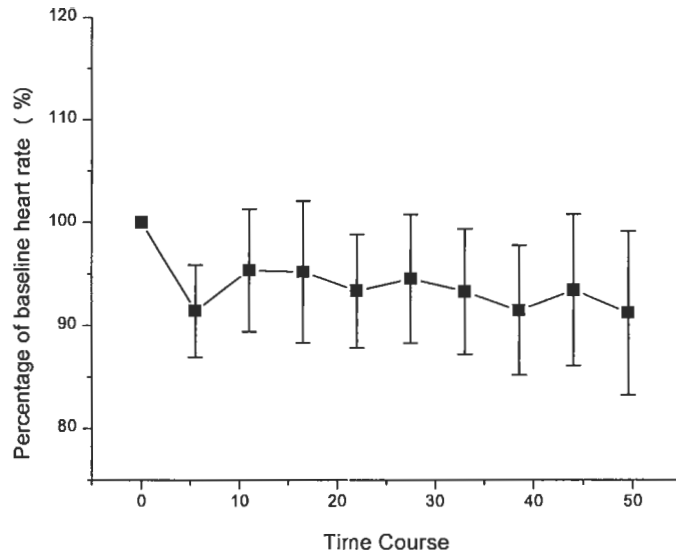


Figure 10 Pre-ischemia 10 μ M esmolol followed by 2.5 μ M dopamine (N=8)

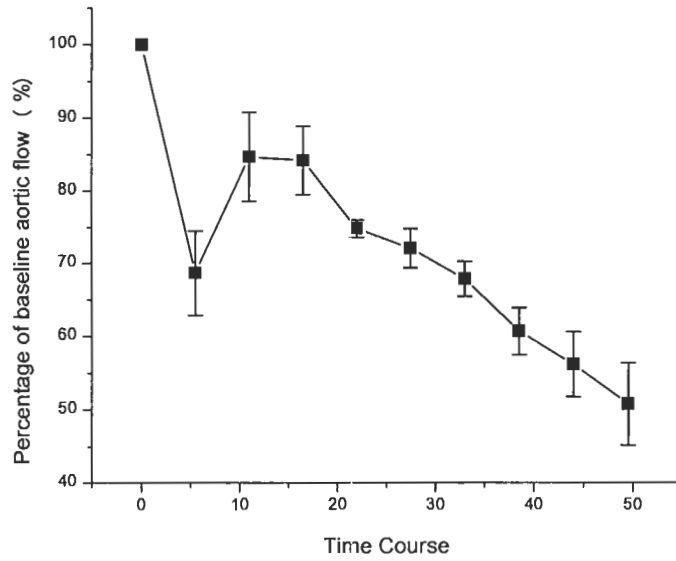


Figure 11 Pre-ischemia 10 μ M esmolol followed by 2.5 μ M dopamine (N=8)

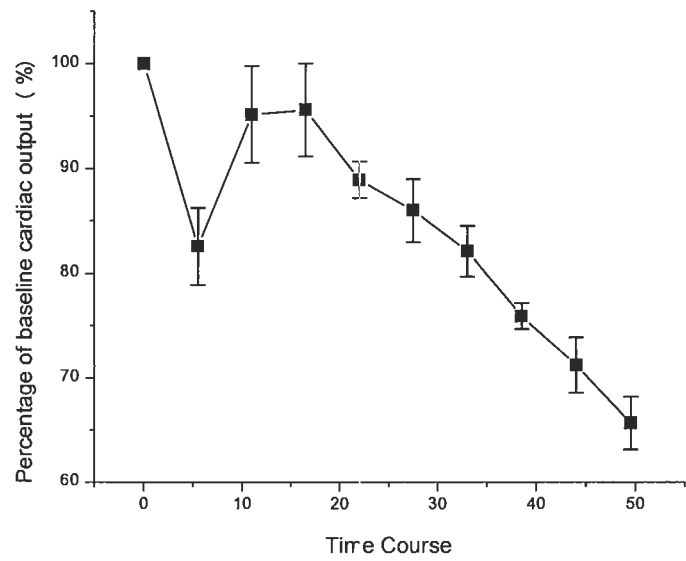


Figure 12 Pre-ischemia 10 μ M esmolol followed by 2.5 μ M dopamine (N=8)

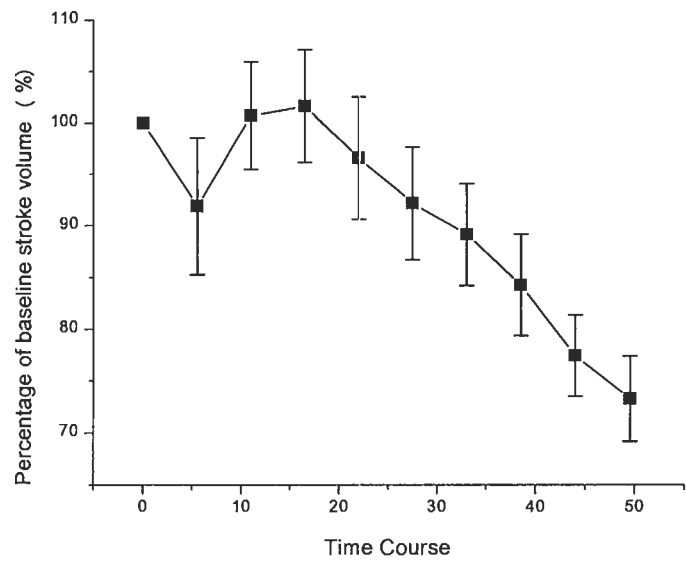


Figure 13 Pre-ischemia 10 μ M esmolol followed by 2.5 μ M dopamine (N=8)

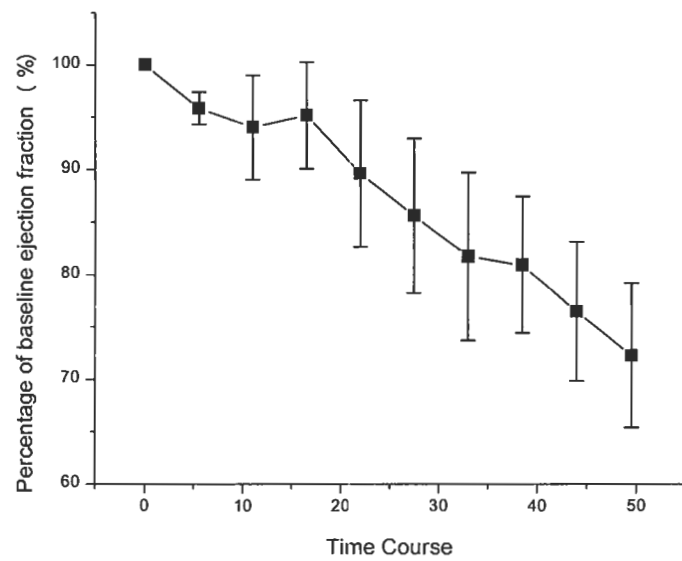


Figure 14 Pre-ischemia 10 μ M esmolol followed by 2.5 μ M dopamine (N=8)

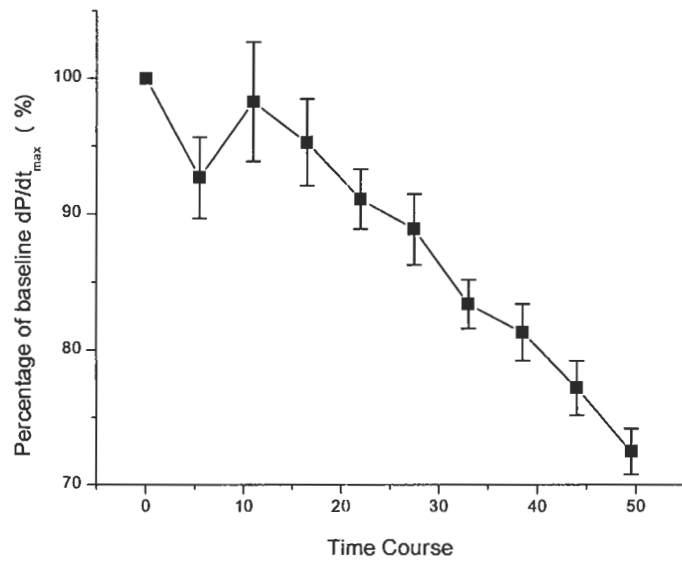


Figure 15 Pre-ischemia 10 μ M esmolol followed by 2.5 μ M dopamine (N=8)

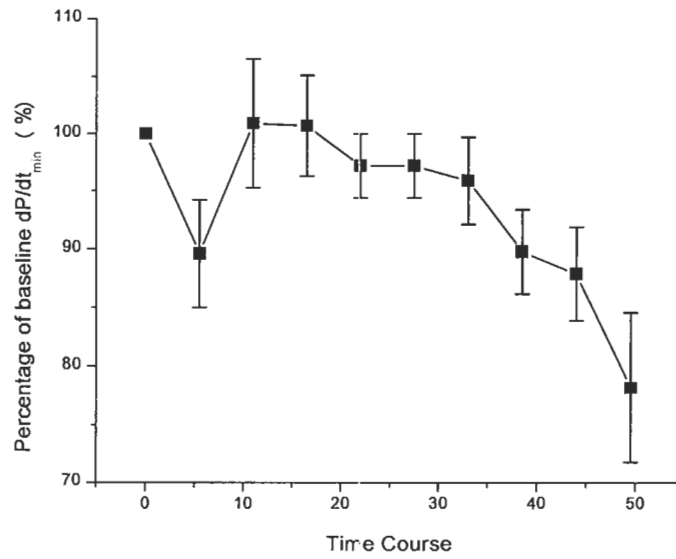


Figure 16 Pre-ischemia 10 μ M esmolol followed by 2.5 μ M dopamine (N=8)

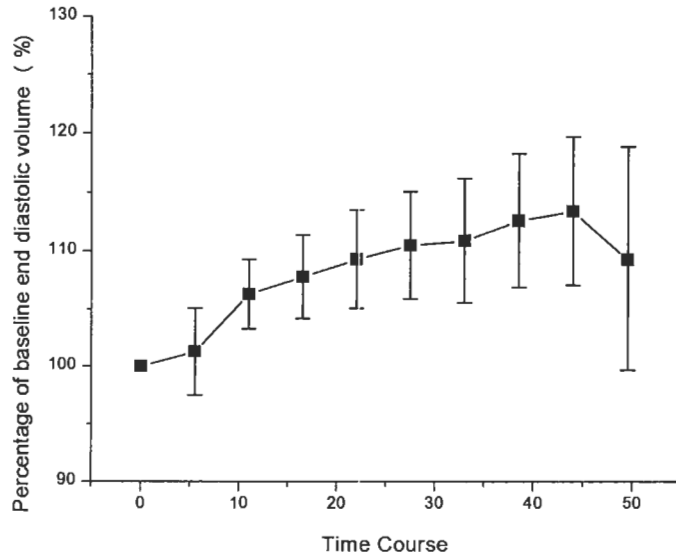


Figure 17 Pre-ischemia 10 μ M esmolol followed by 2.5 μ M dopamine (N=8)

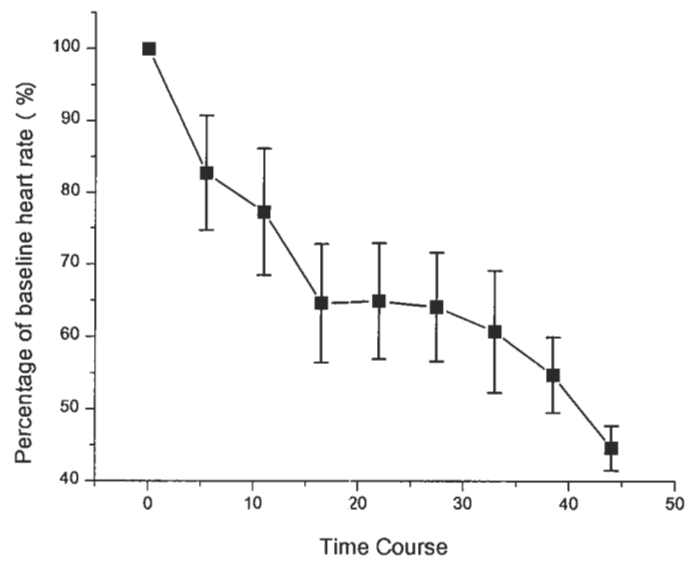


Figure 18 Pre-ischemia 10 μ M propranolol followed by 20 μ M dopamine (N=8)

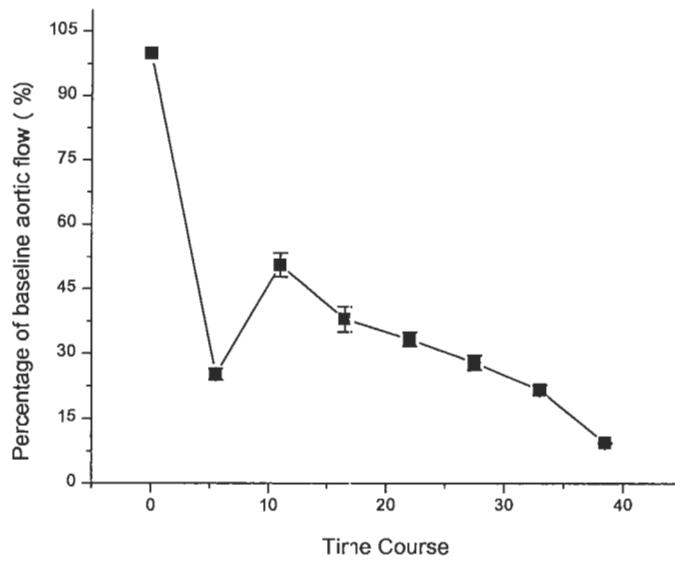


Figure 19 Pre-ischemia 10 μ M propranolol followed by 20 μ M dopamine (N=8)

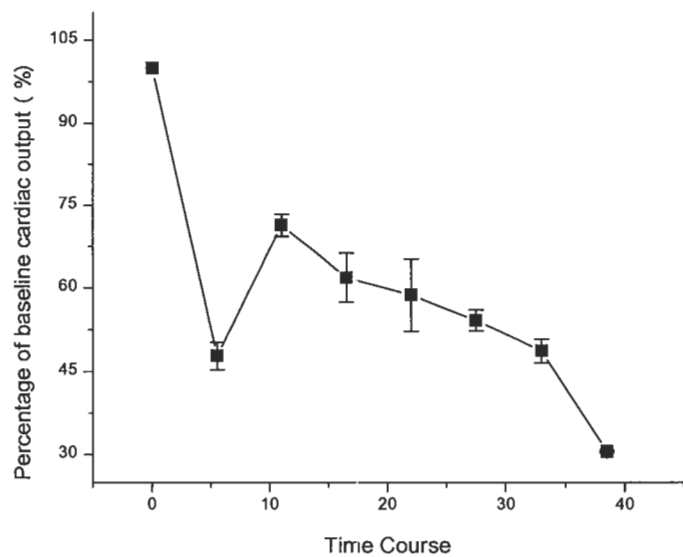


Figure 20 Pre-ischemia 10 μ M propranolol followed by 20 μ M dopamine (N=8)

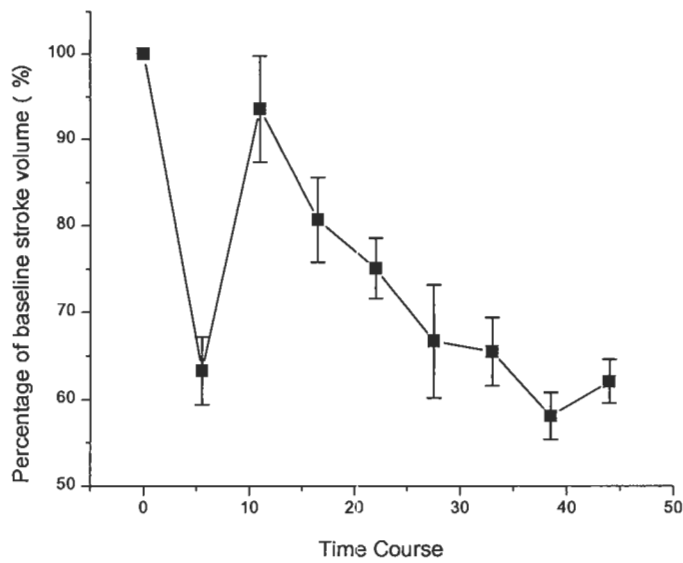


Figure 21 Pre-ischemia 10 μ M propranolol followed by 20 μ M dopamine (N=8)

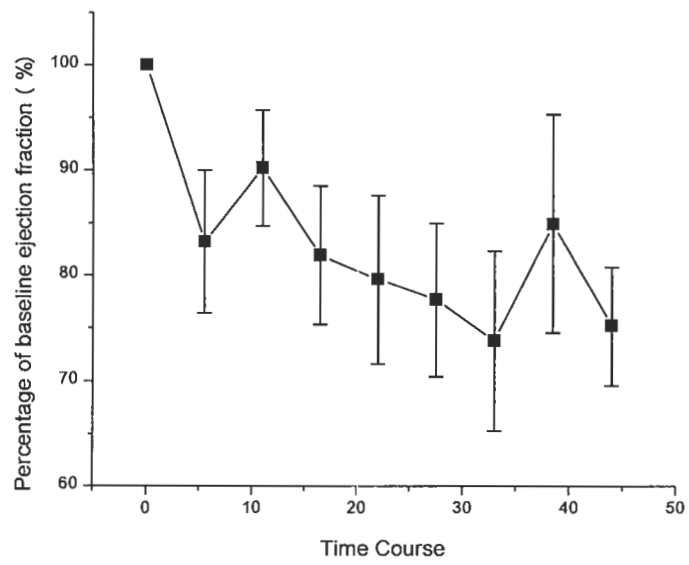


Figure 22 Pre-ischemia 10 μ M propranolol followed by 20 μ M dopamine (N=8)

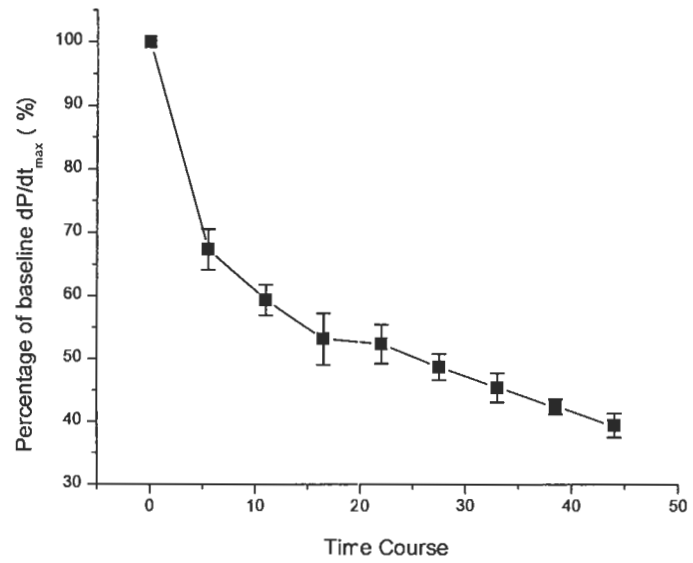


Figure 23 Pre-ischemia 10 μ M propranolol followed by 20 μ M dopamine (N=8)

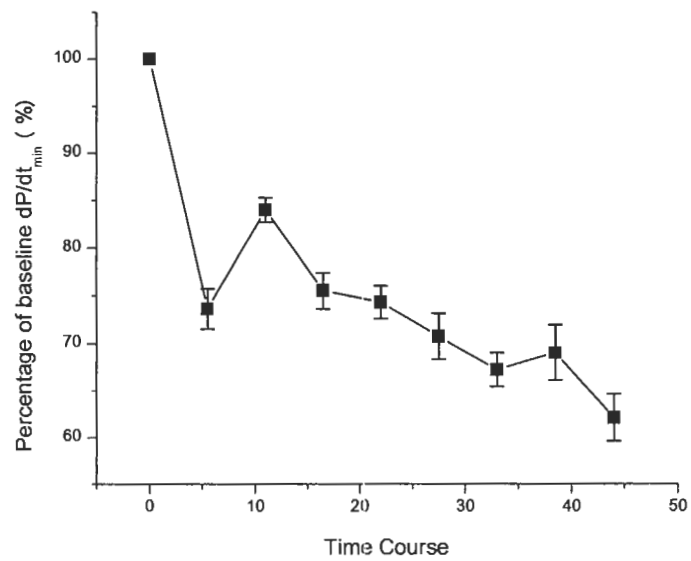


Figure 24 Pre-ischemia 10 μ M propranolol followed by 20 μ M dopamine (N=8)

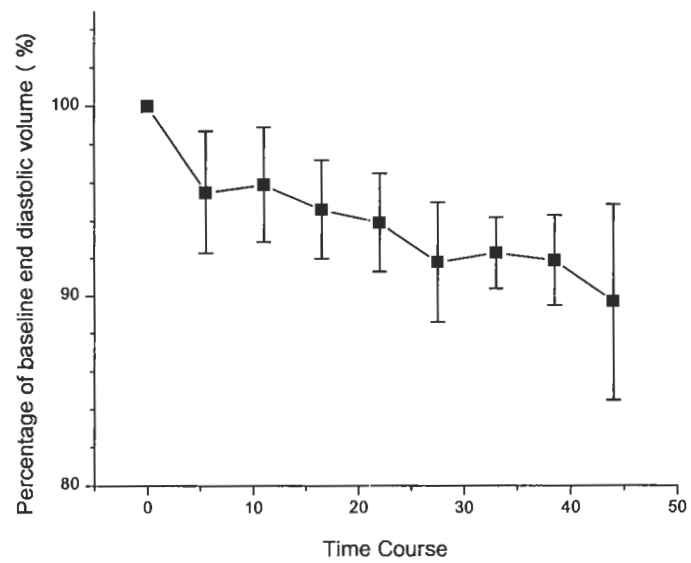


Figure 25 Pre-ischemia 10 μ M propranolol followed by 20 μ M dopamine (N=8)

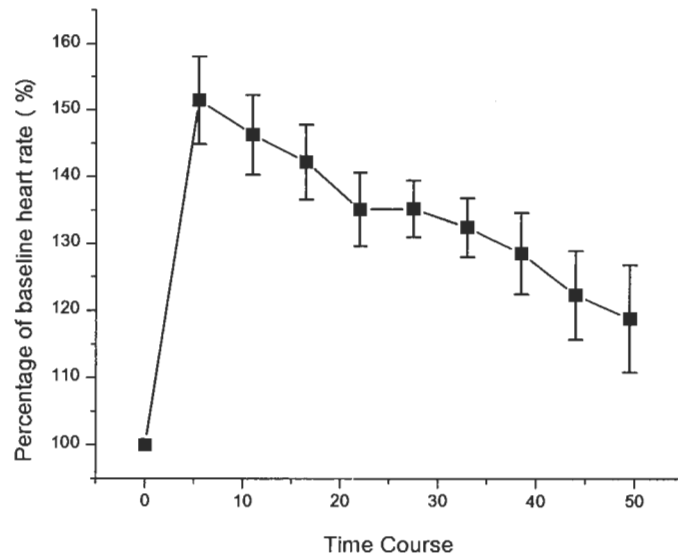


Figure 26 Pre-ischemia single dose of 40 nM isoproterenol (N=8)

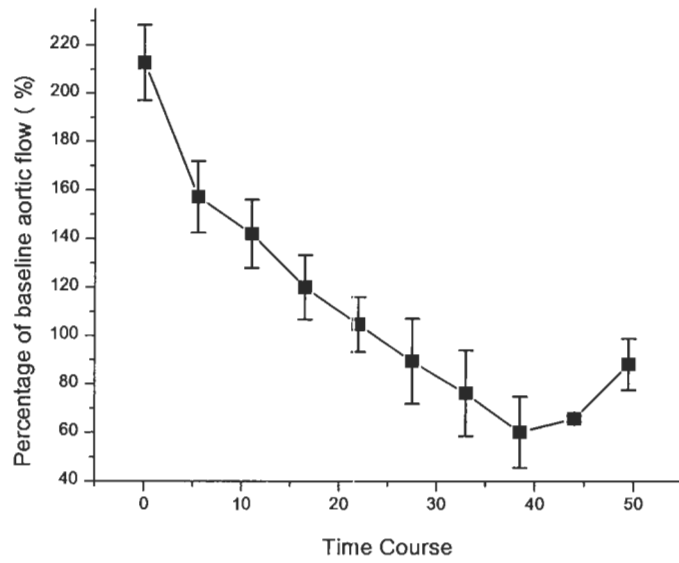


Figure 27 Pre-ischemia single dose of 40 nM isoproterenol (N=8)

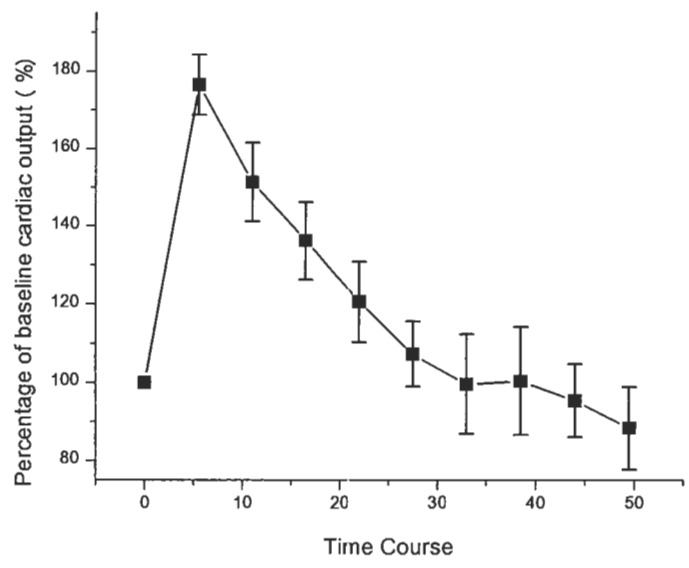


Figure 28 Pre-ischemia single dose of 40 nM isoproterenol (N=8)

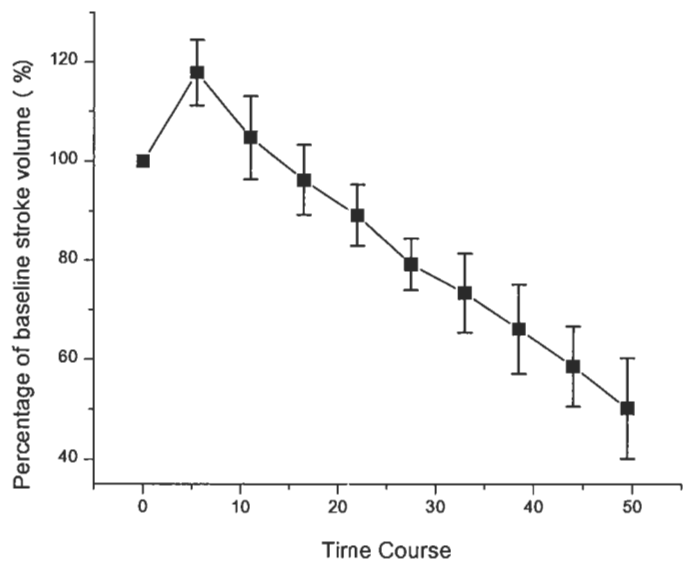


Figure 29 Pre-ischemia single dose of 40 nM isoproterenol (N=8)

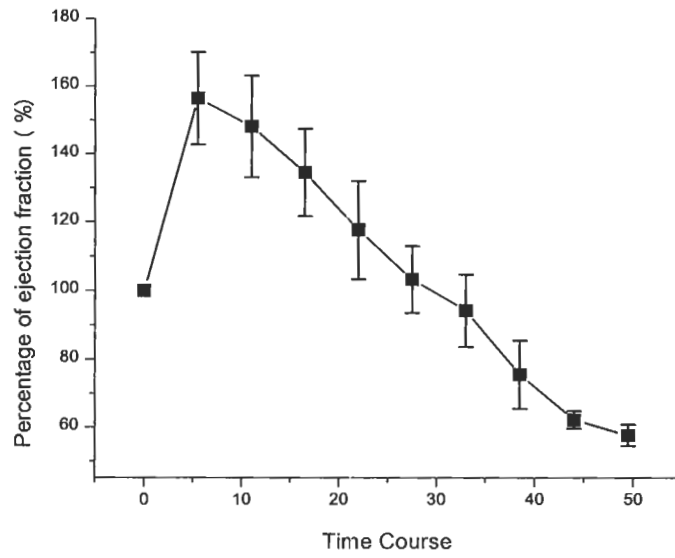


Figure 30 Pre-ischemia single dose of 40 nM isoproterenol (N=8)

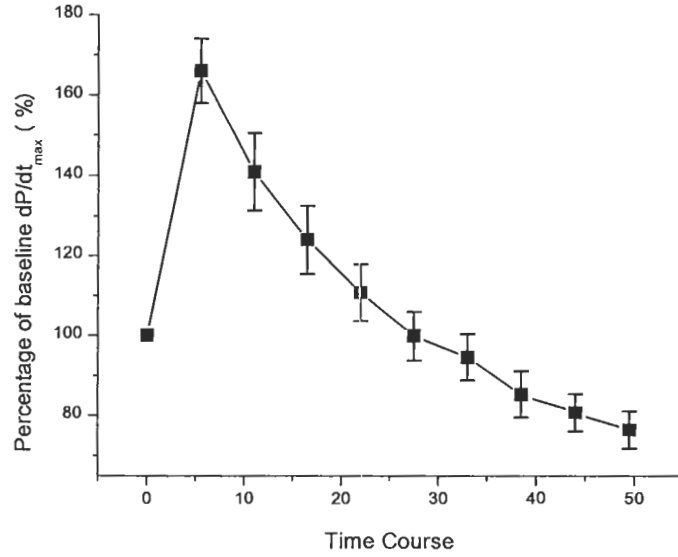


Figure 31 Pre-ischemia single dose of 40 nM isoproterenol (N=8)

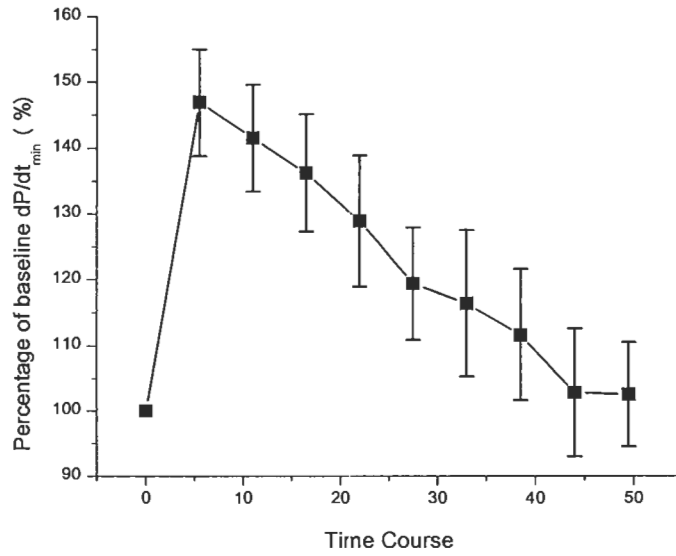


Figure 32 Pre-ischemia single dose of 40 nM isoproterenol (N=8)

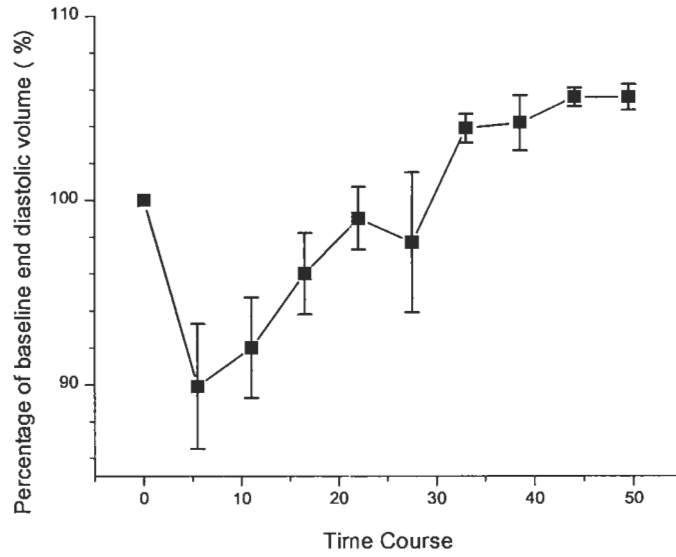


Figure 33 Pre-ischemia single dose of 40 nM isoproterenol (N=8)

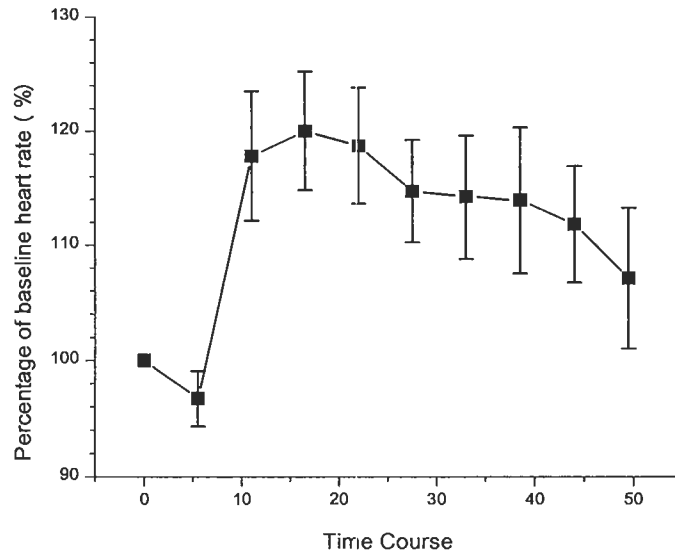


Figure 34 Pre-ischemia 10 μ M esmolol followed by 40 nM isoproterenol (N=8)

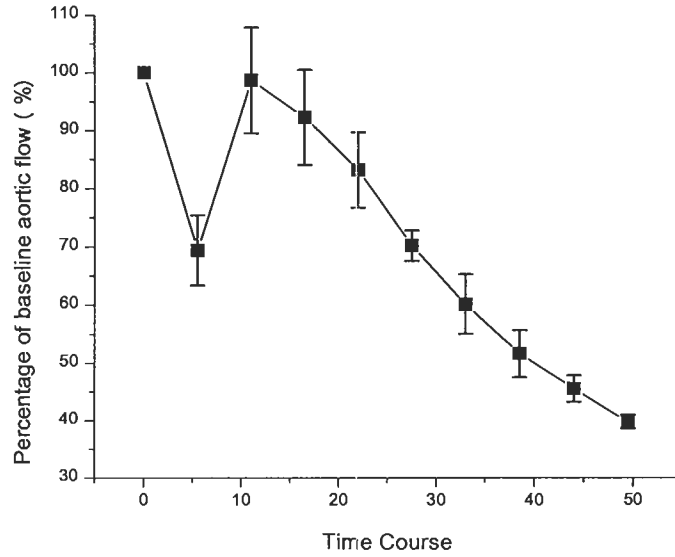


Figure 35 Pre-ischemia 10 μ M esmolol followed by 40 nM isoproterenol (N=8)

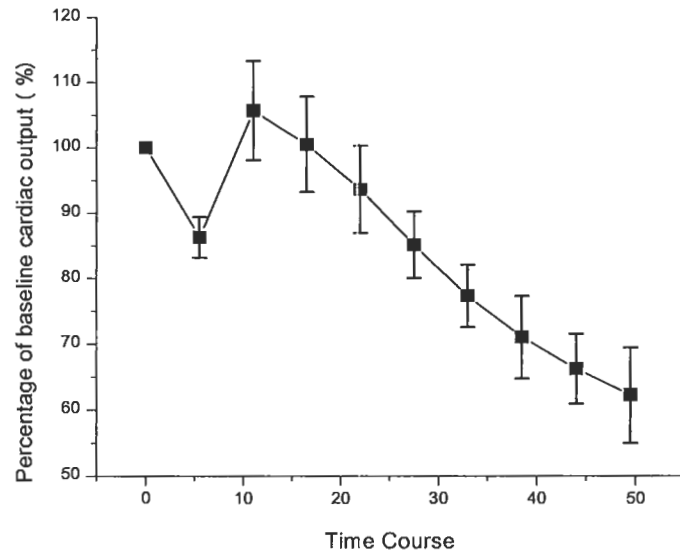


Figure 36 Pre-ischemia 10 μ M esmolol followed by 40 nM isoproterenol (N=8)

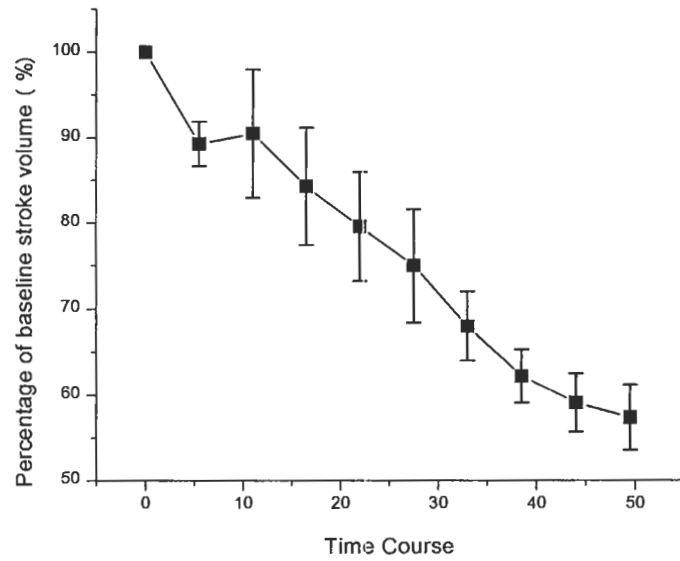


Figure 37 Pre-ischemia 10 μ M esmolol followed by 40 nM isoproterenol (N=8)

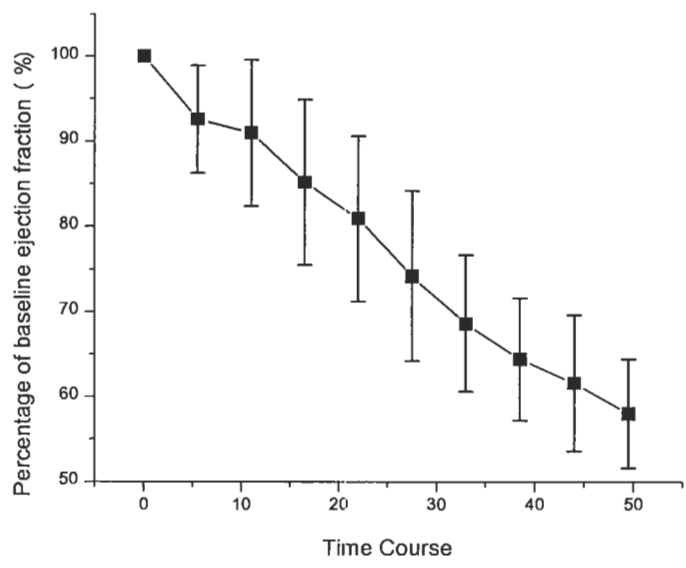


Figure 38 Pre-ischemia 10 μ M esmolol followed by 40 nM isoproterenol (N=8)

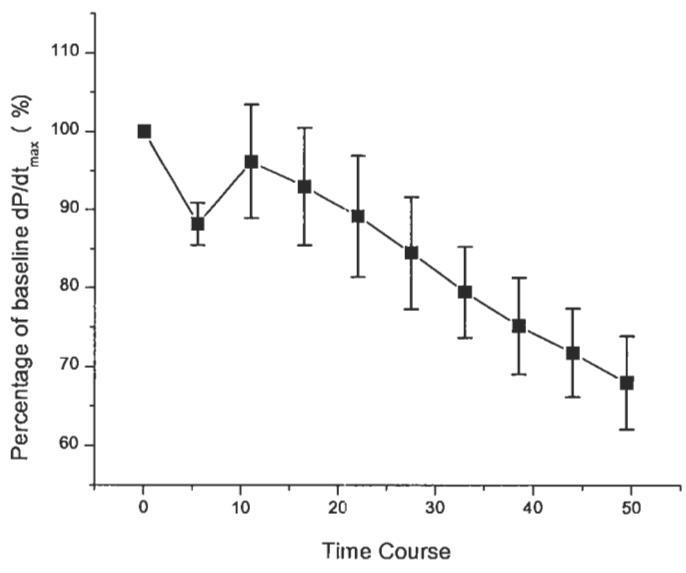


Figure 39 Pre-ischemia 10 μ M esmolol followed by 40 nM isoproterenol (N=8)

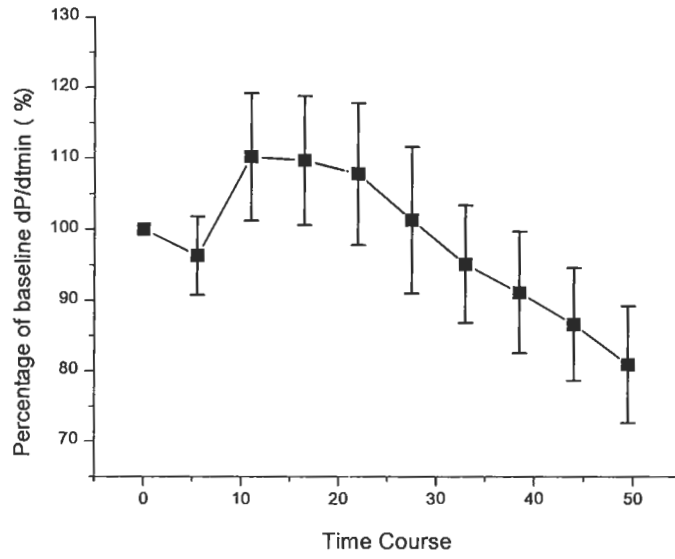


Figure 40 Pre-ischemia 10 μ M esmolol followed by 40 nM isoproterenol (N=8)

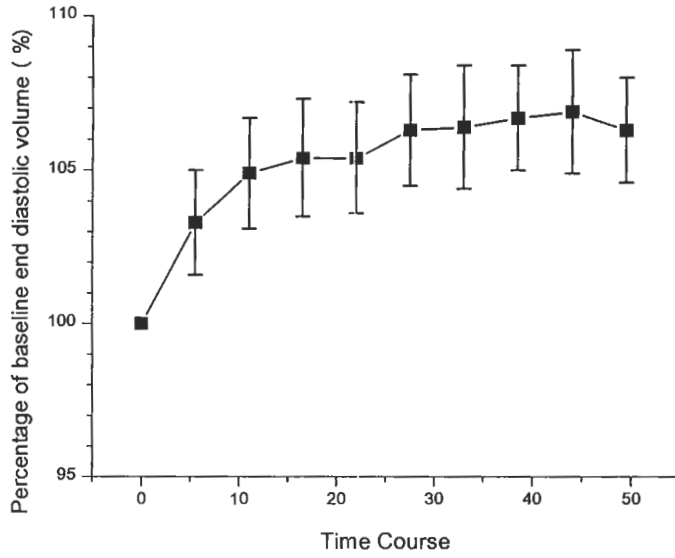


Figure 41 Pre-ischemia 10 μ M esmolol followed by 40 nM isoproterenol (N=8)

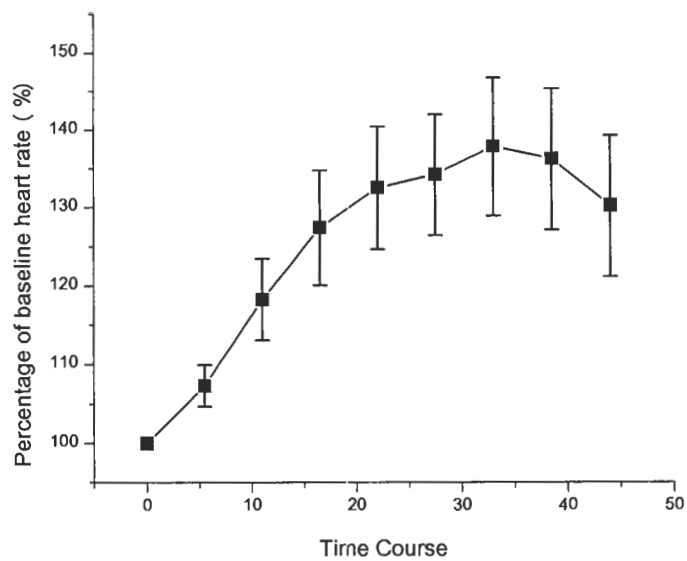


Figure 42 Post-ischemia 2.5 μ M dopamine applied every 5'30 (N=10)

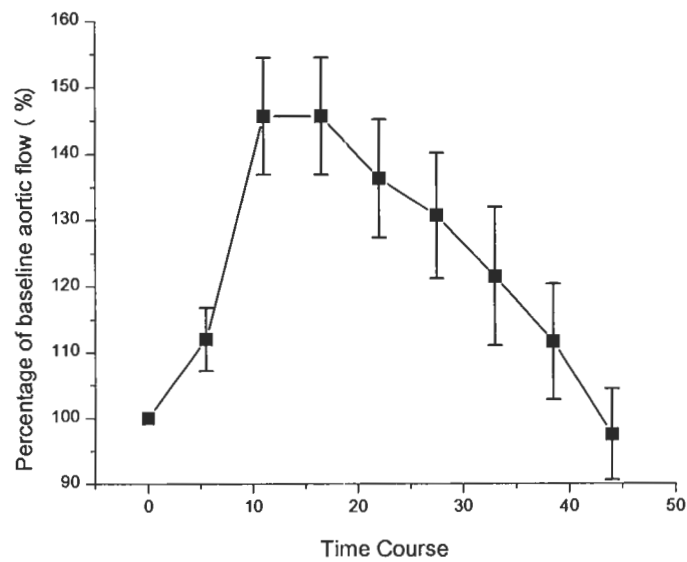


Figure 43 Post-ischemia 2.5 μ M dopamine applied every 5'30 (N=10)

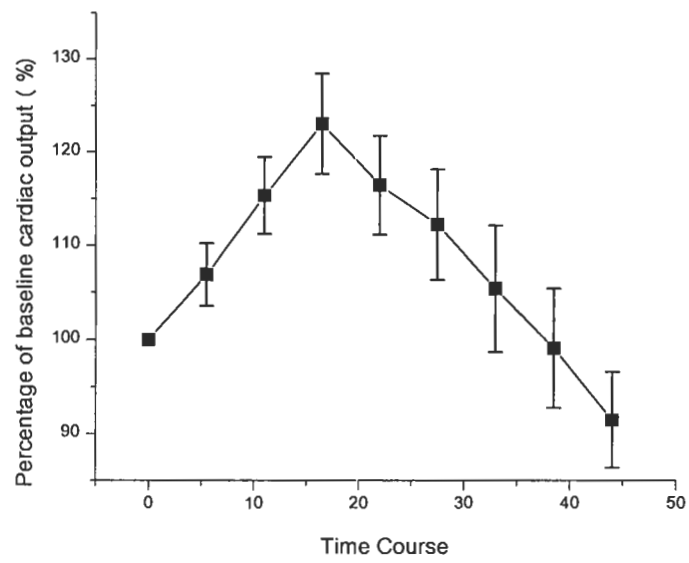


Figure 44 Post-ischemia 2.5 μ M dopamine applied every 5'30 (N=10)

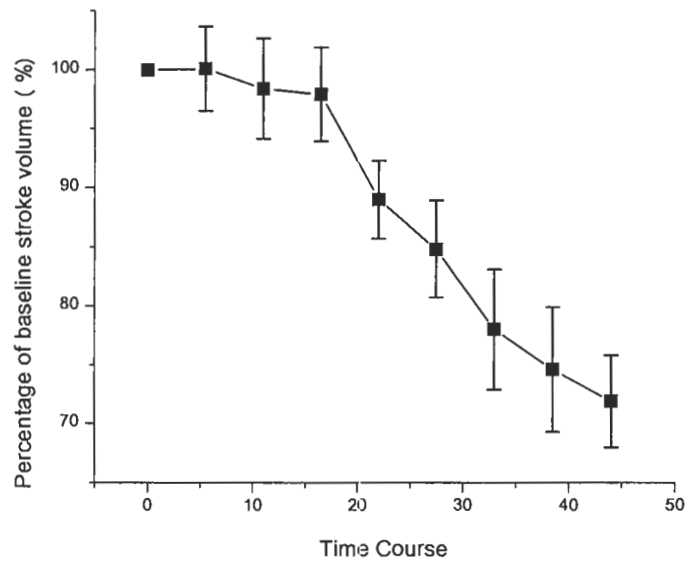


Figure 45 Post-ischemia 2.5 μ M dopamine applied every 5'30 (N=10)

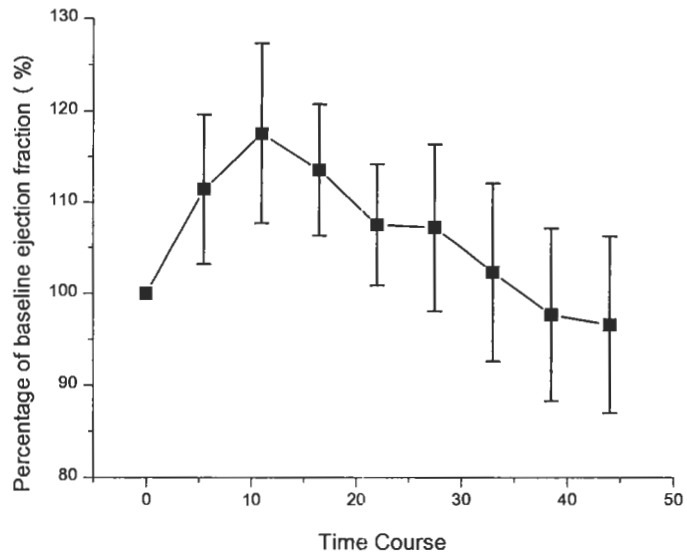


Figure 46 Post-ischemia 2.5 μ M dopamine applied every 5'30 (N=10)

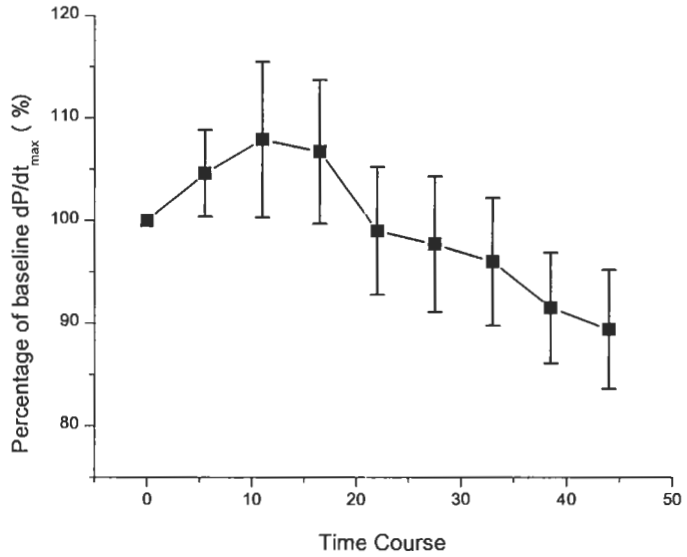


Figure 47 Post-ischemia 2.5 μ M dopamine applied every 5'30 (N=10)

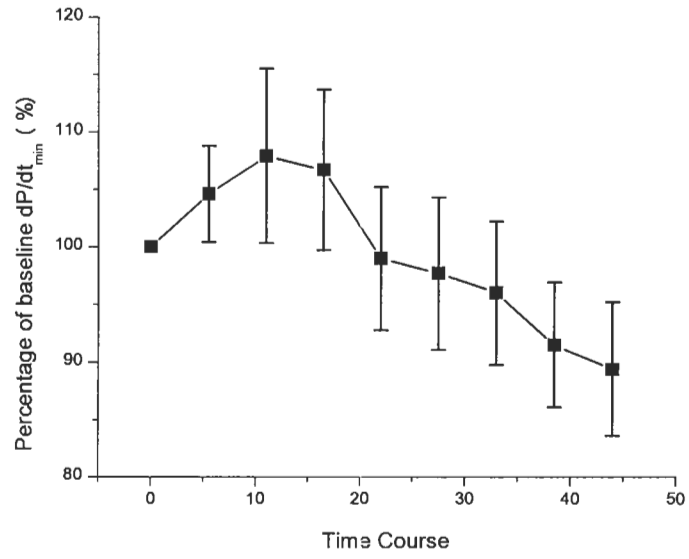


Figure 48 Post-ischemia 2.5 μ M dopamine applied every 5'30 (N=10)

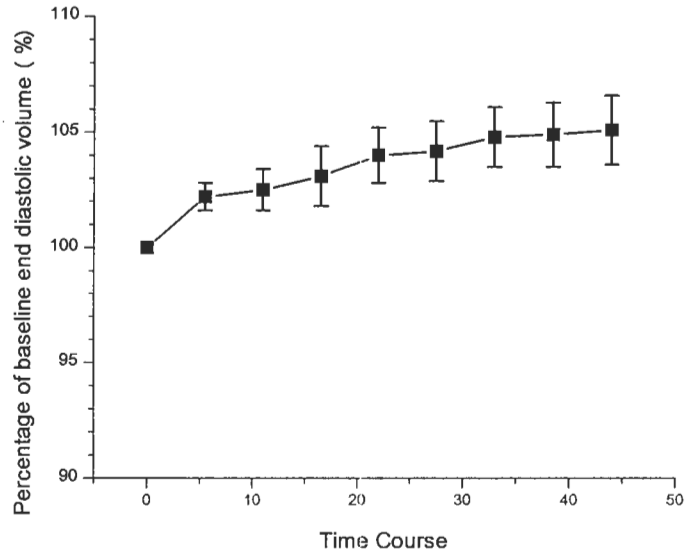


Figure 49 Post-ischemia 2.5 μ M dopamine applied every 5'30 (N=10)

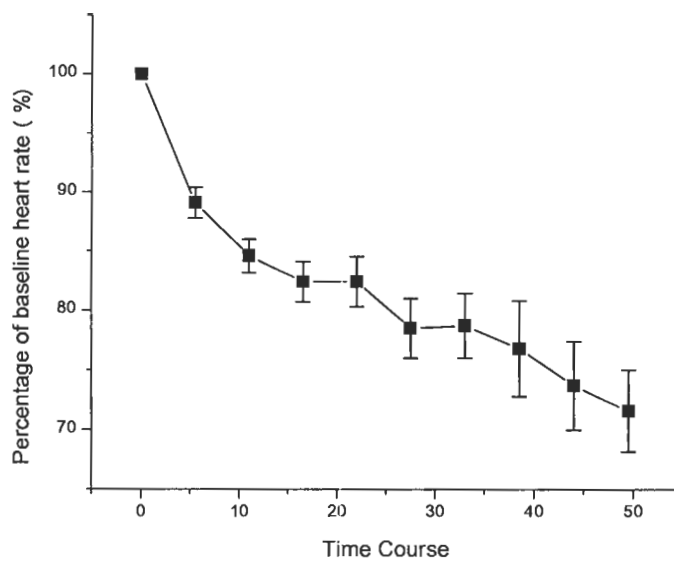


Figure 50 Pre-ischemia single dose of 5 μ M ZD7288 (N=8)

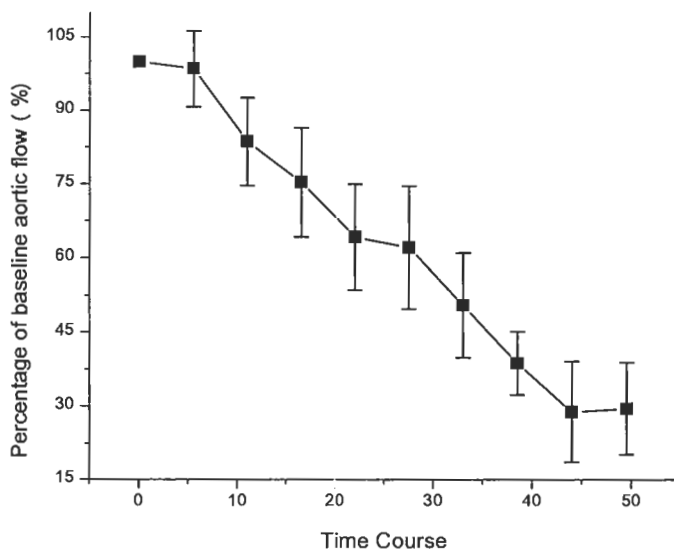


Figure 51 Pre-ischemia single dose of 5 μ M ZD7288 (N=8)

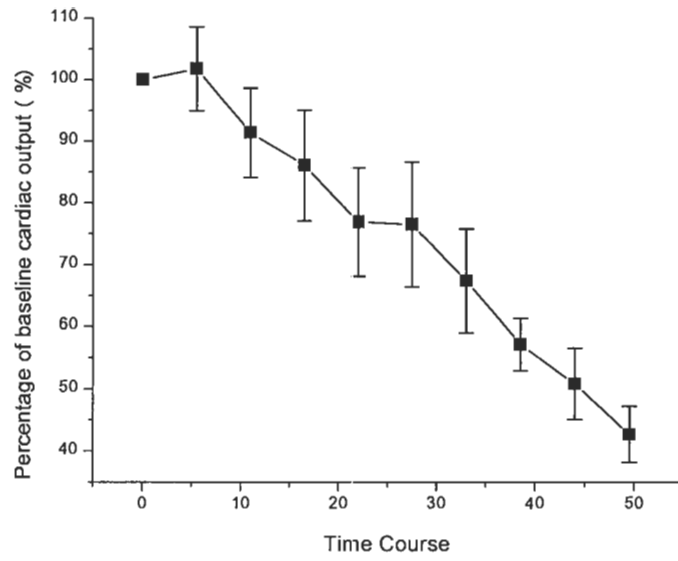


Figure 52 Pre-ischemia single dose of 5 μ M ZD7288 (N=8)

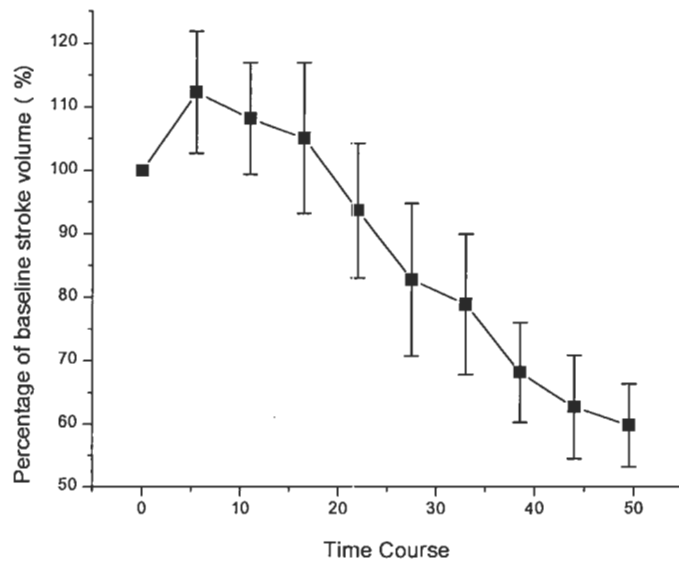


Figure 53 Pre-ischemia single dose of 5 μ M ZD7288 (N=8)

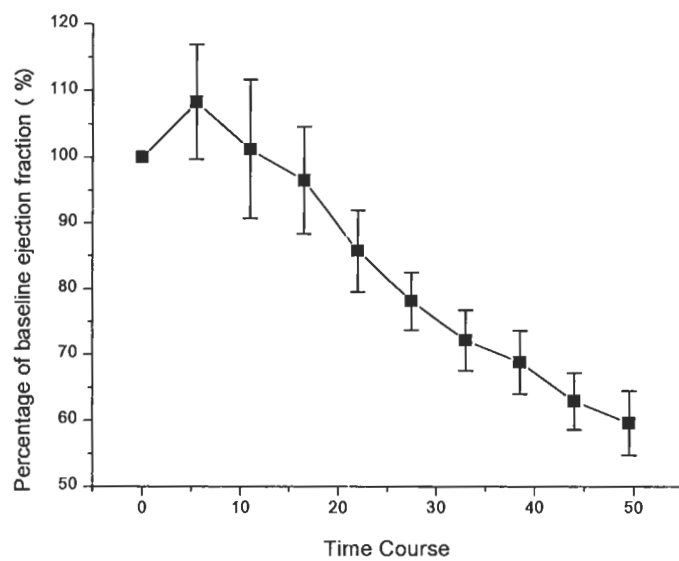


Figure 54 Pre-ischemia single dose of 5 μ M ZD7288 (N=8)

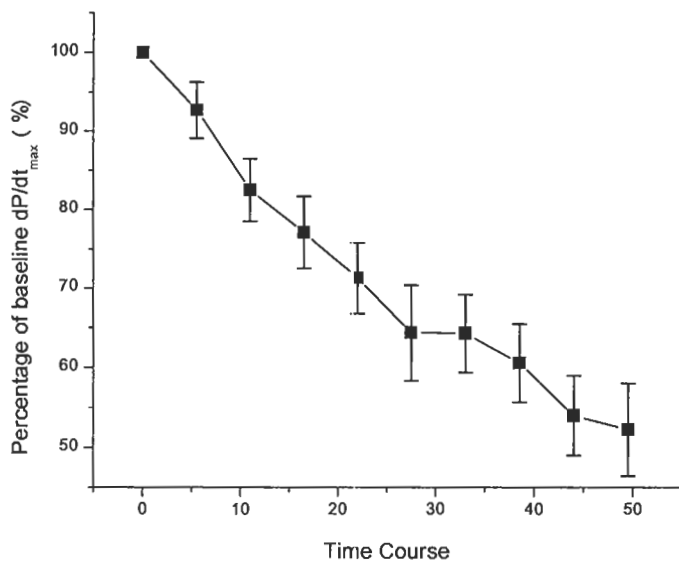


Figure 55 Pre-ischemia single dose of 5 μ M ZD7288 (N=8)

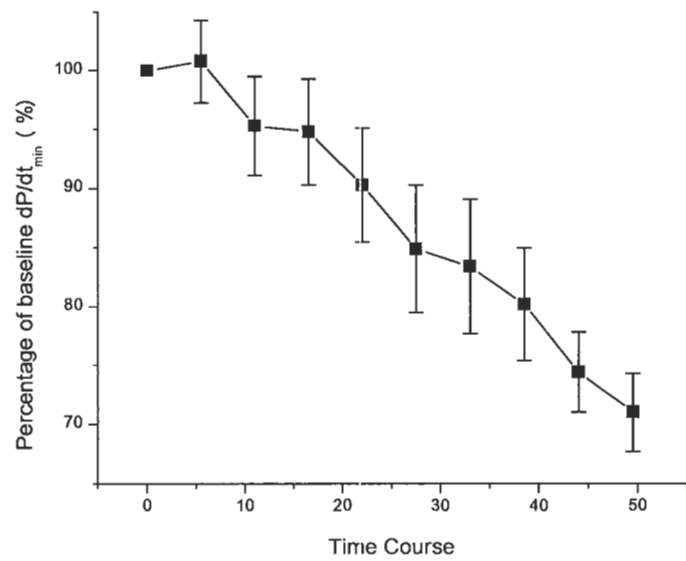


Figure 56 Pre-ischemia single dose of 5 μ M ZD7288 (N=8)

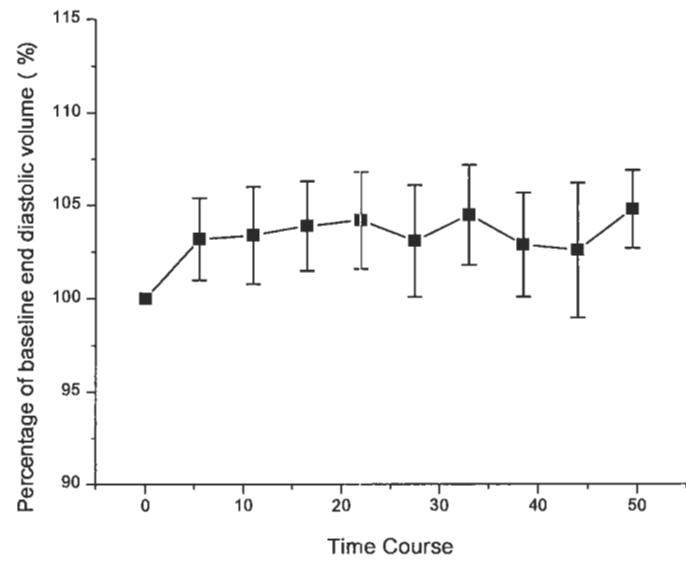


Figure 57 Pre-ischemia single dose of 5 μ M ZD7288 (N=8)

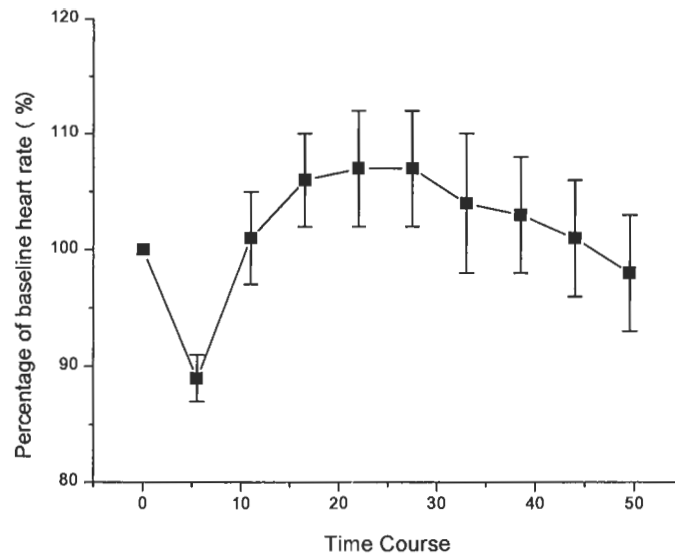


Figure 58 Pre-ischemia 5 μ M ZD7288 followed by 20 μ M dopamine (N=8)

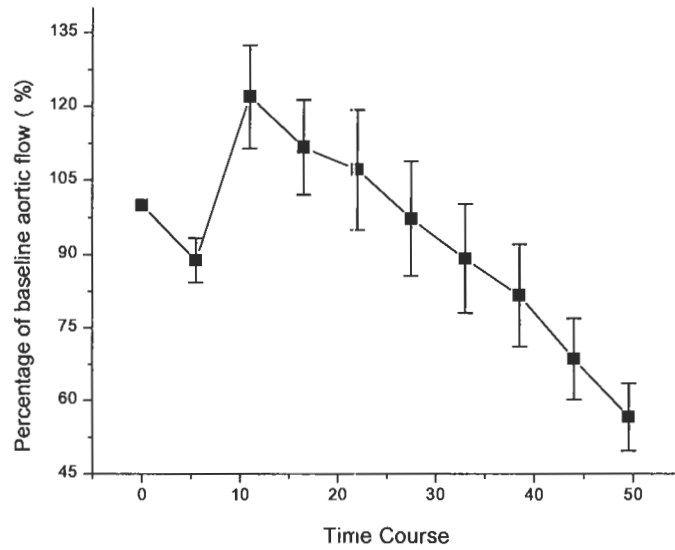


Figure 59 Pre-ischemia 5 μ M ZD7288 followed by 20 μ M dopamine (N=8)

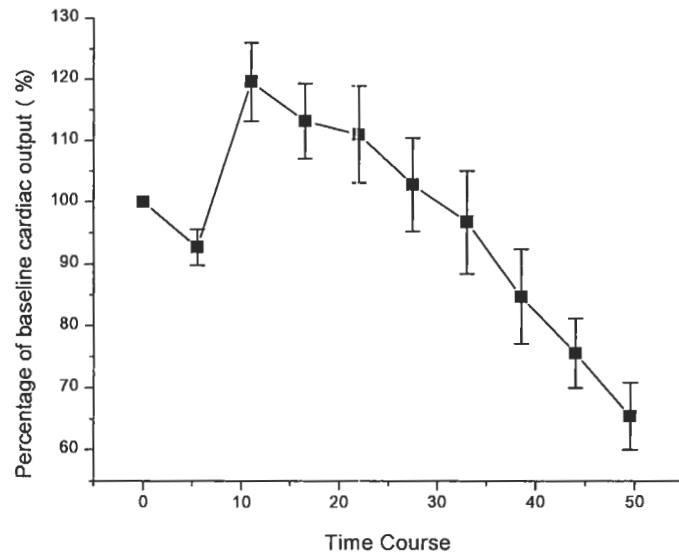


Figure 60 Pre-ischemia 5 μ M ZD7288 followed by 20 μ M dopamine (N=8)

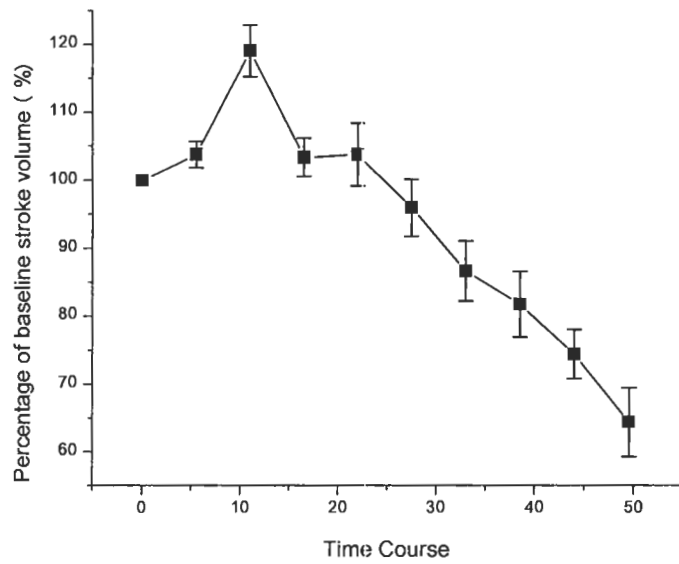


Figure 61 Pre-ischemia 5 μ M ZD7288 followed by 20 μ M dopamine (N=8)

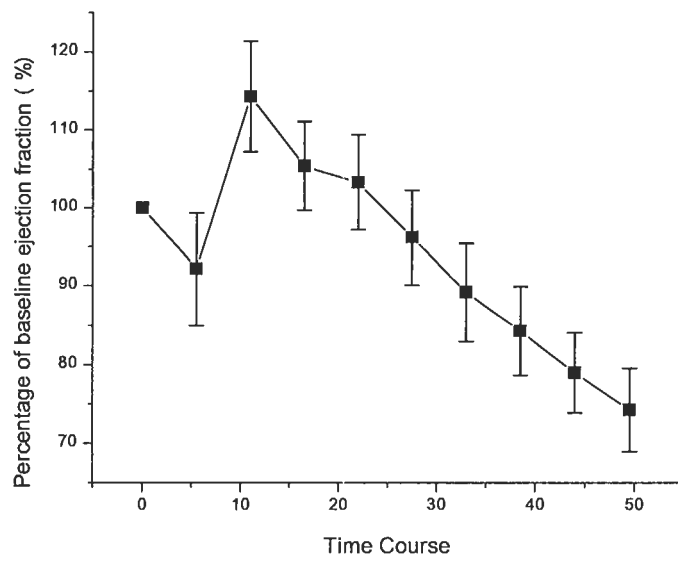


Figure 62 Pre-ischemia 5 μ M ZD7288 followed by 20 μ M dopamine (N=8)

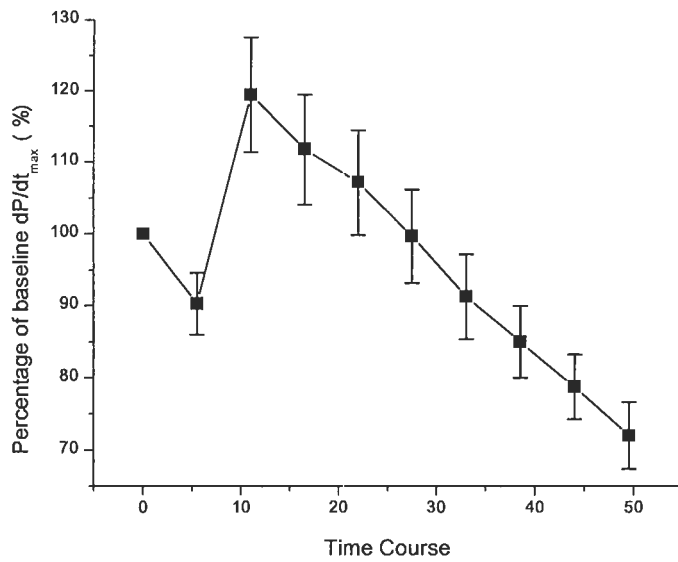


Figure 63 Pre-ischemia 5 μ M ZD7288 followed by 20 μ M dopamine (N=8)

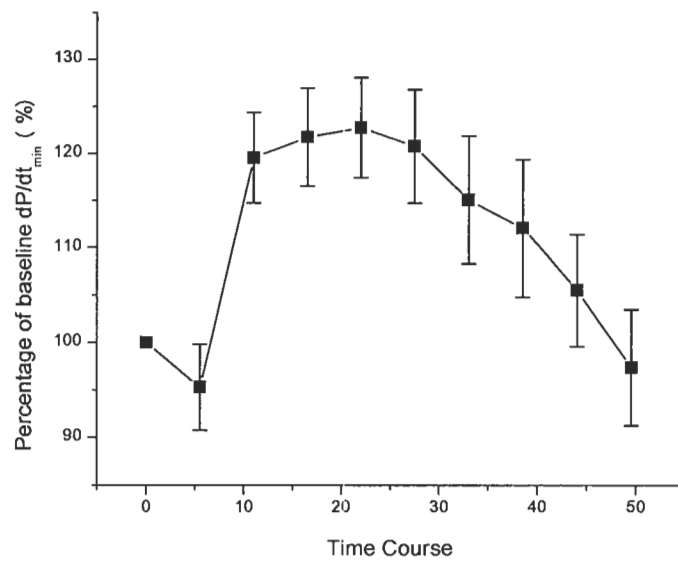


Figure 64 Pre-ischemia 5 μ M ZD7288 followed by 20 μ M dopamine (N=8)

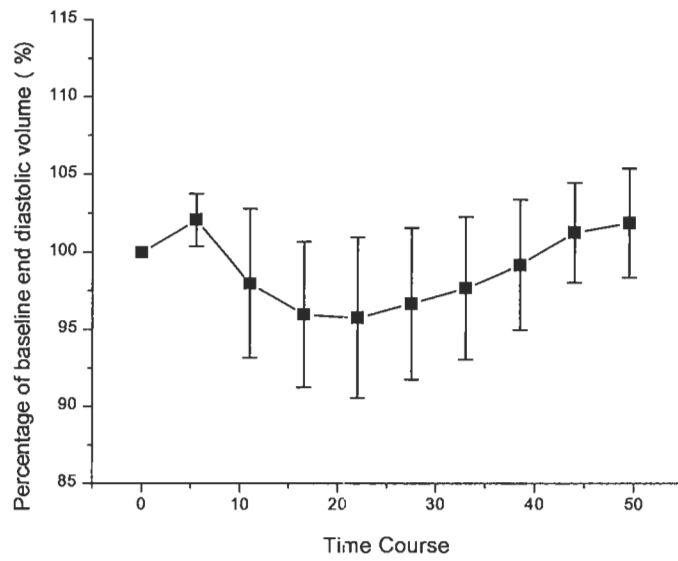


Figure 65 Pre-ischemia 5 μ M ZD7288 followed by 20 μ M dopamine (N=8)

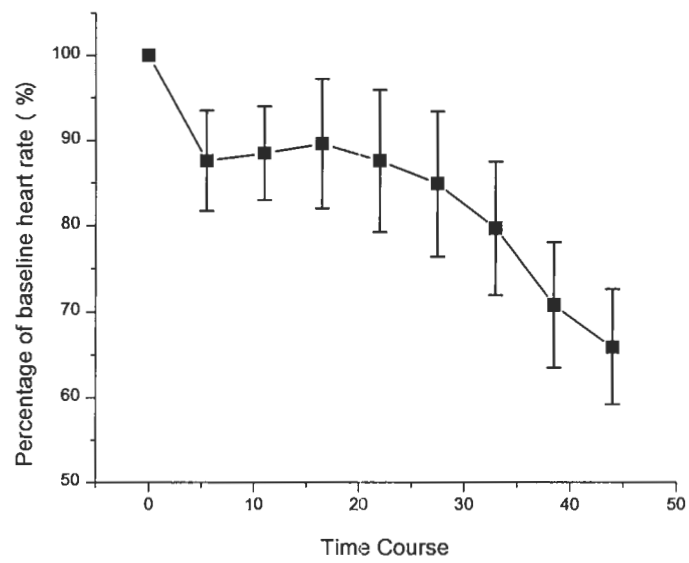


Figure 66 Pre-ischemia single dose of 30 μM atropine (N=8)

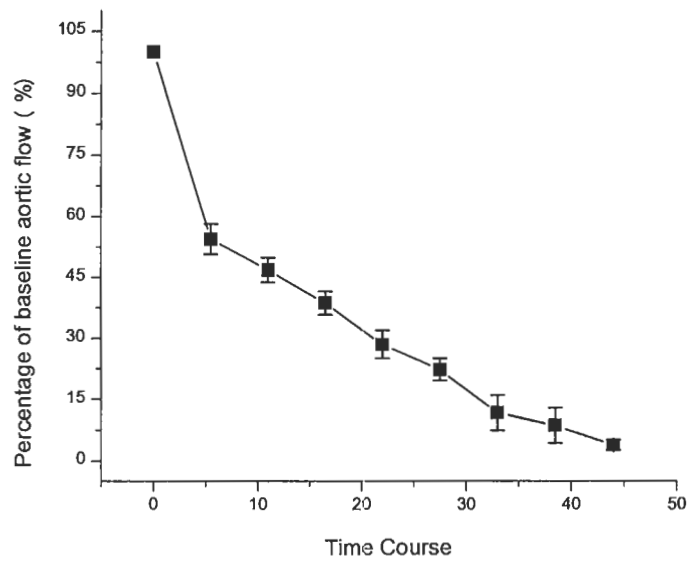


Figure 67 Pre-ischemia single dose of 30 μM atropine (N=8)

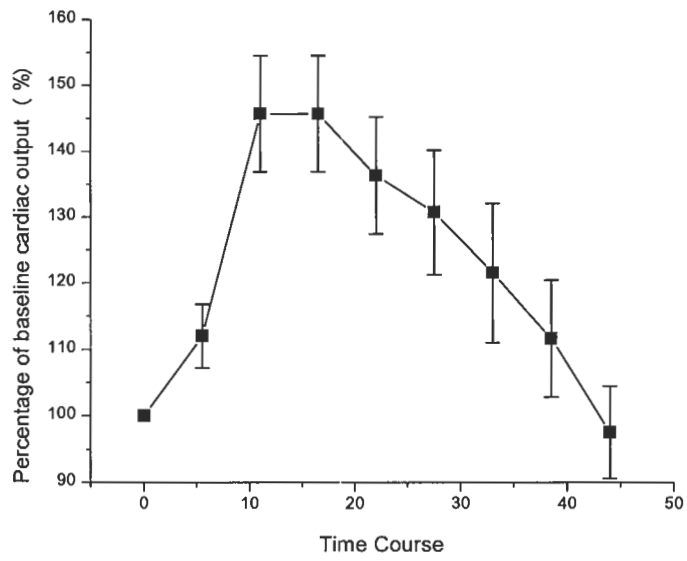


Figure 68 Pre-ischemia single dose of 30 μ M atropine (N=8)

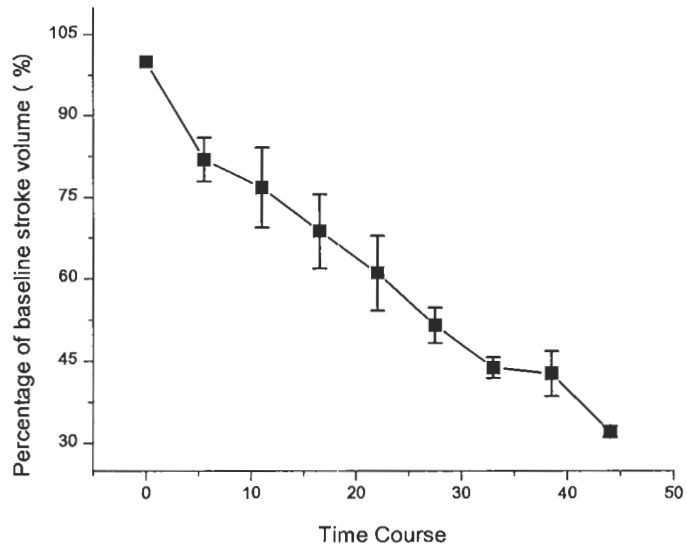


Figure 69 Pre-ischemia single dose of 30 μ M atropine (N=8)

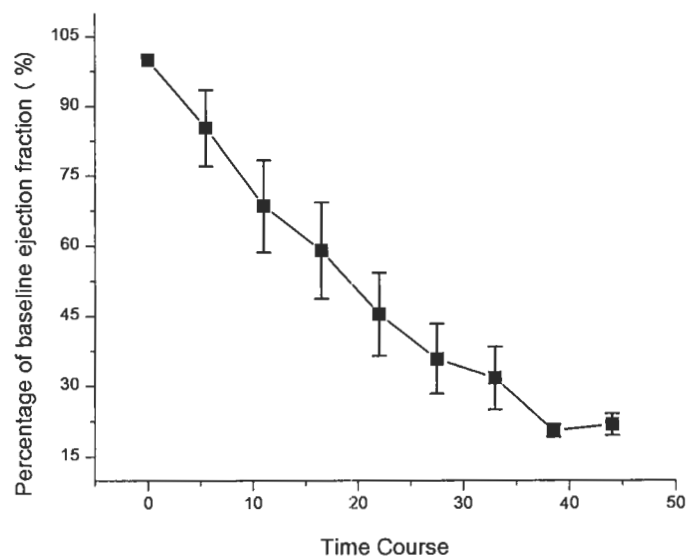


Figure 70 Pre-ischemia single dose of 30 μ M atropine (N=8)

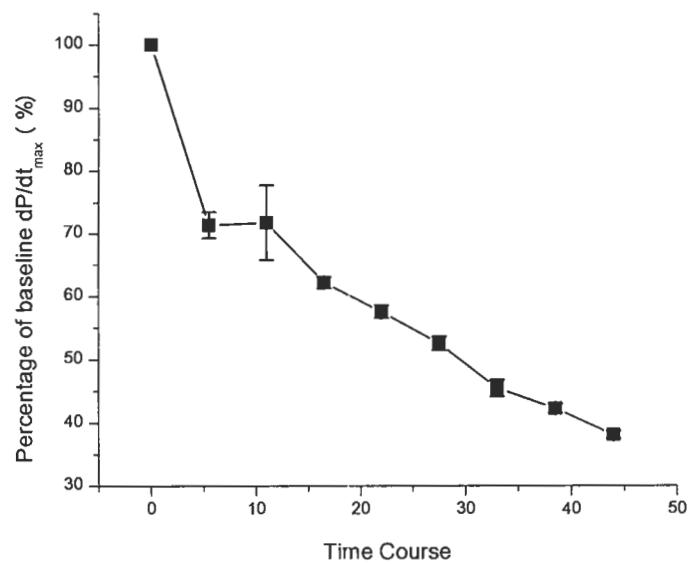


Figure 71 Pre-ischemia single dose of 30 μ M atropine (N=8)

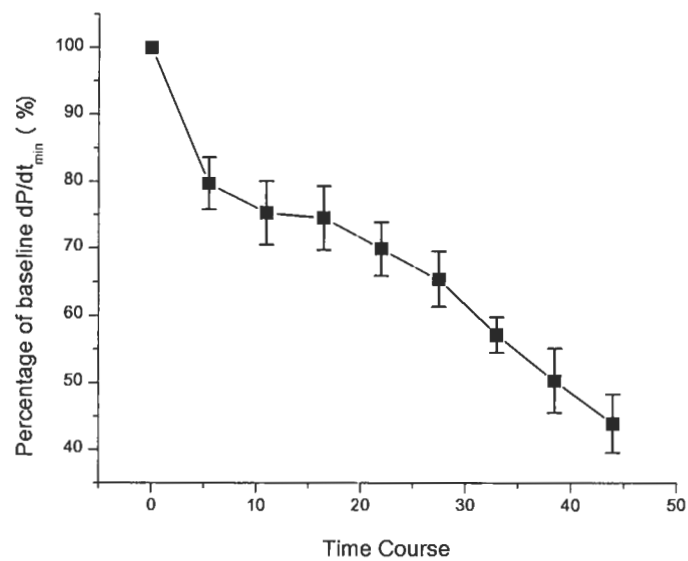


Figure 72 Pre-ischemia single dose of 30 μ M atropine (N=8)

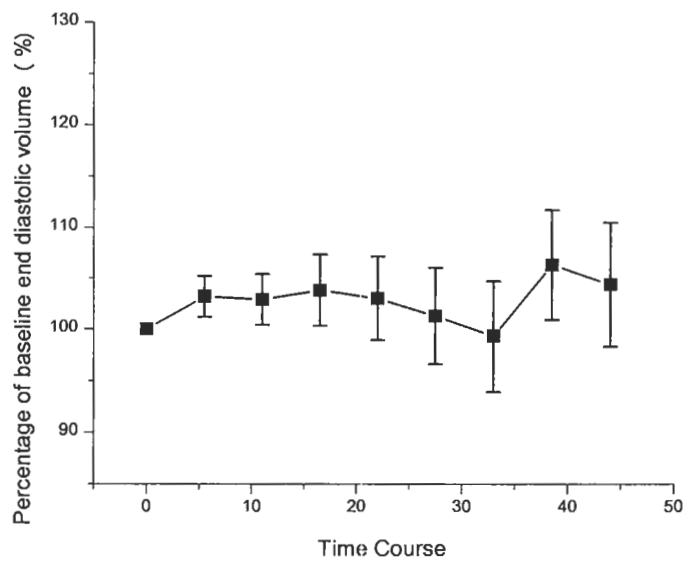


Figure 73 Pre-ischemia single dose of 30 μ M atropine (N=8)

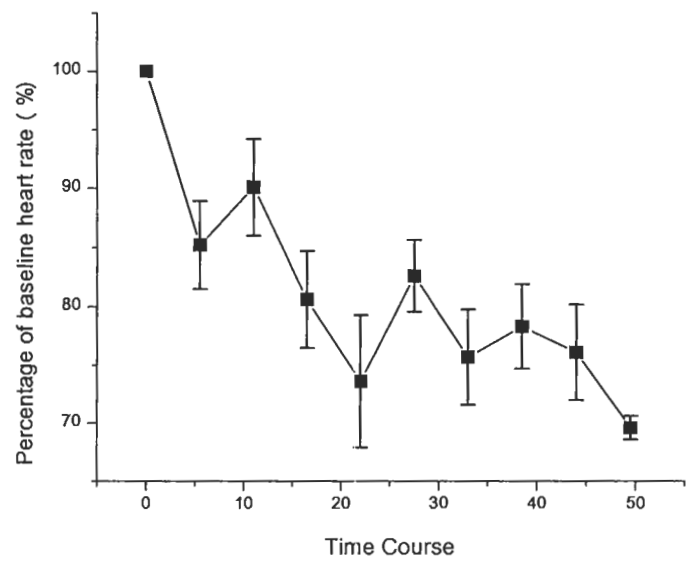


Figure 74 Pre-ischemia 5 μ M ACh followed by 30 μ M atropine (N=8)

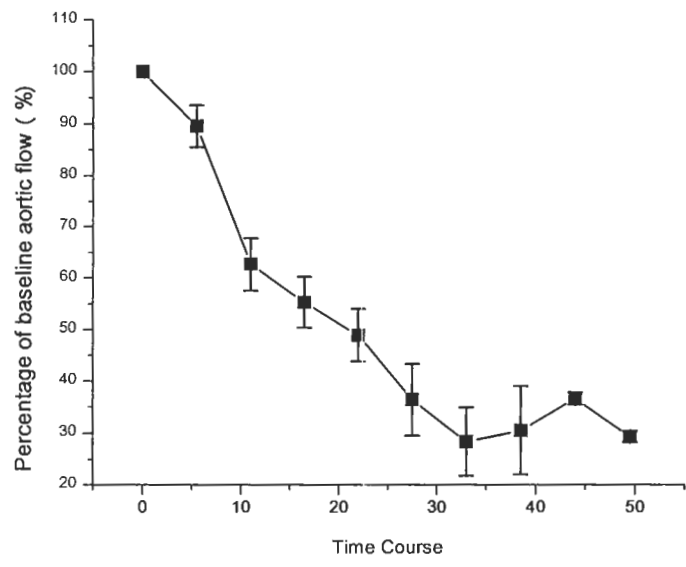


Figure 75 Pre-ischemia 5 μ M ACh followed by 30 μ M atropine (N=8)

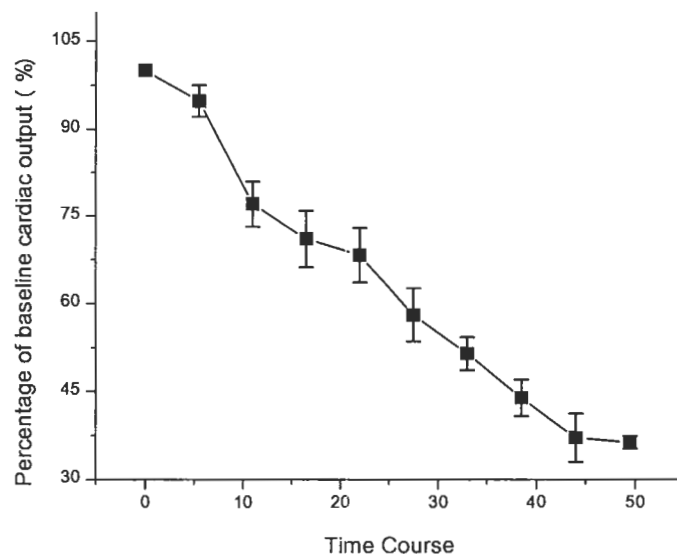


Figure 76 Pre-ischemia 5 μ M ACh followed by 30 μ M atropine (N=8)

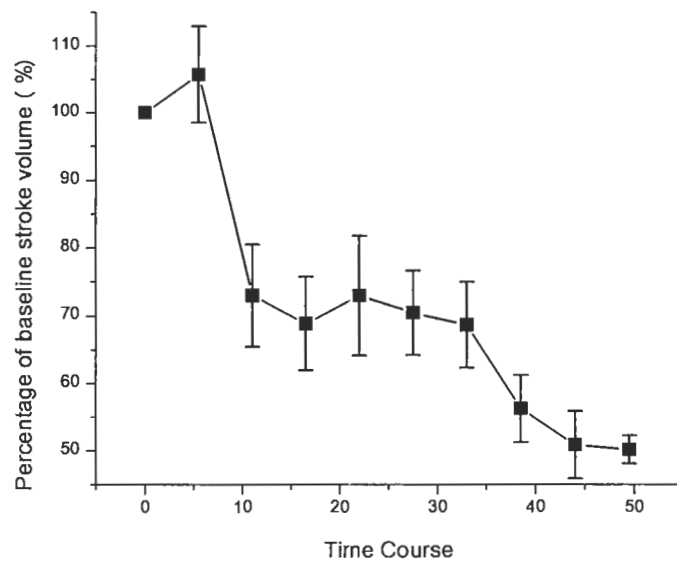


Figure 77 Pre-ischemia 5 μ M ACh followed by 30 μ M atropine (N=8)

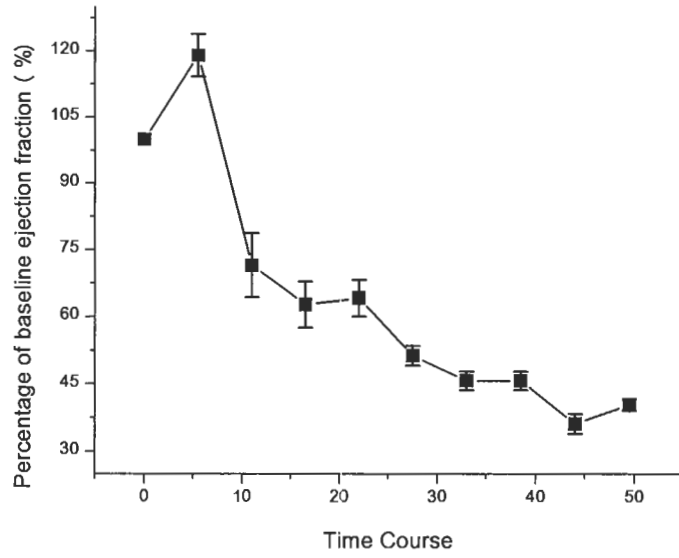


Figure 78 Pre-ischemia 5 μ M ACh followed by 30 μ M atropine (N=8)

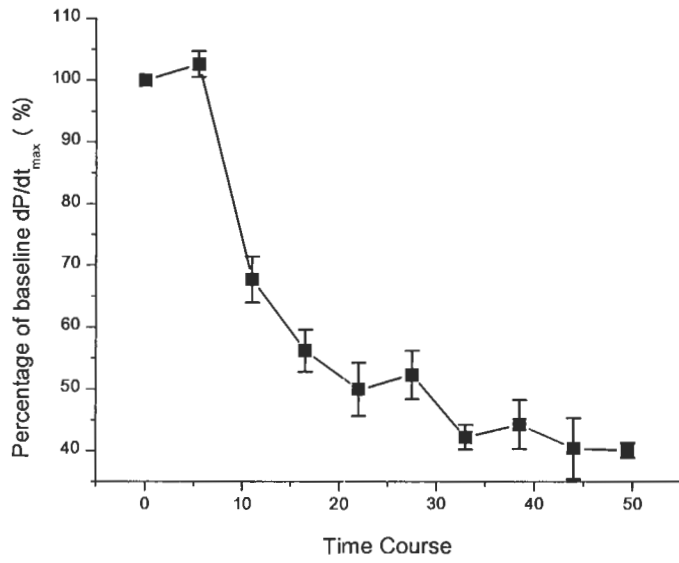


Figure 79 Pre-ischemia 5 μ M ACh followed by 30 μ M atropine (N=8)

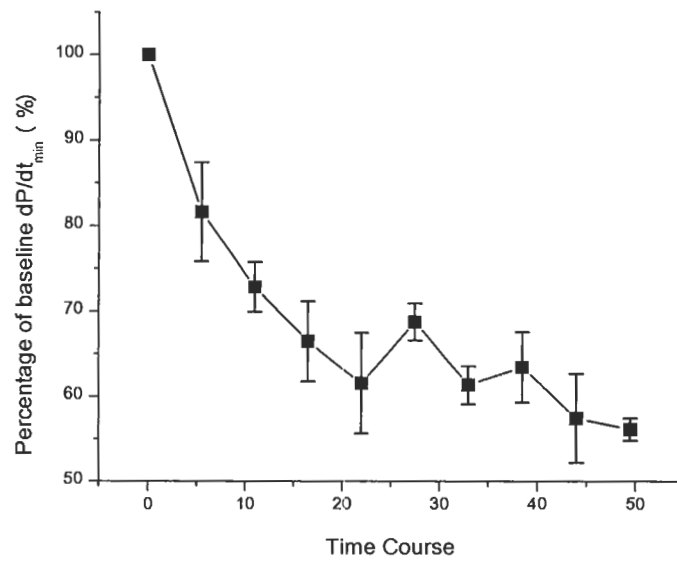


Figure 80 Pre-ischemia 5 μ M ACh followed by 30 μ M atropine (N=8)

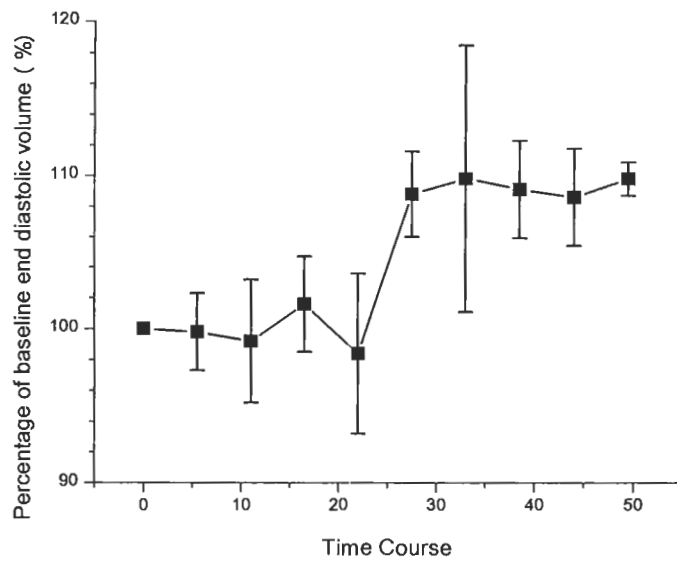


Figure 81 Pre-ischemia 5 μ M ACh followed by 30 μ M atropine (N=8)

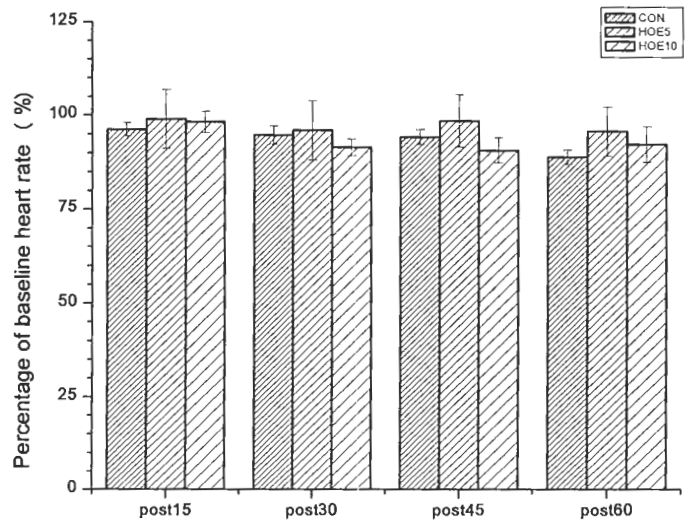
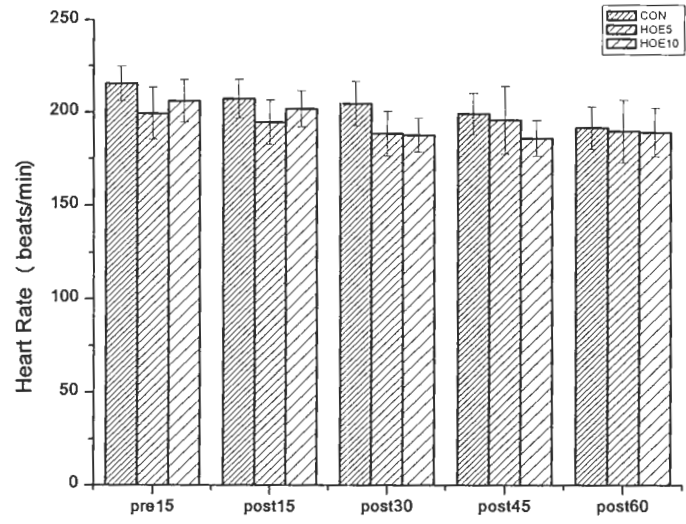


Figure 82 Post-ischemia heart rate recovery (N=6)

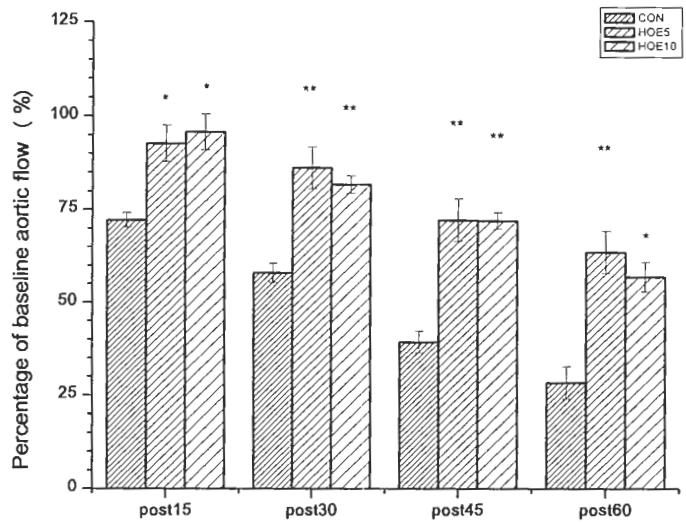
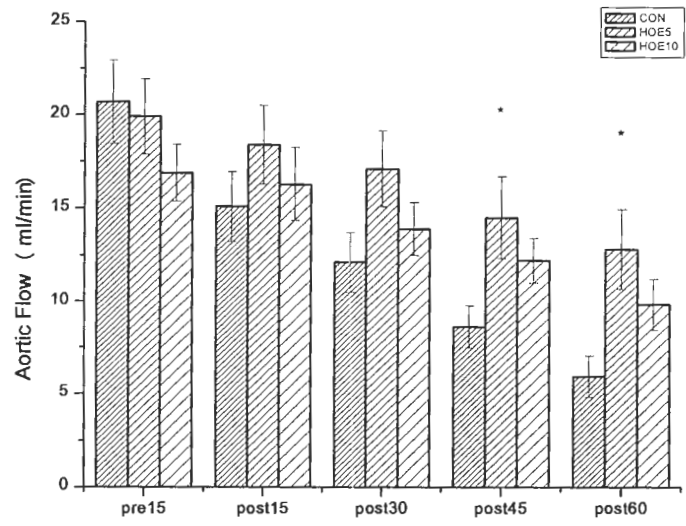


Figure 83 Post-ischemia aortic flow recovery (N=6) * P<0.05 ** P<0.01

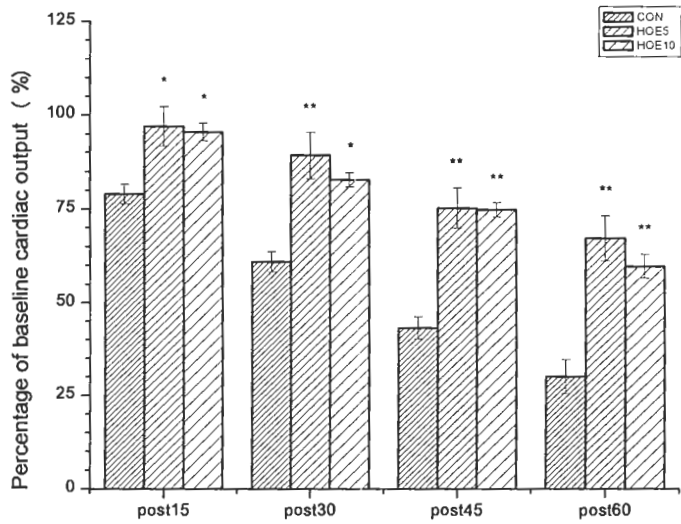
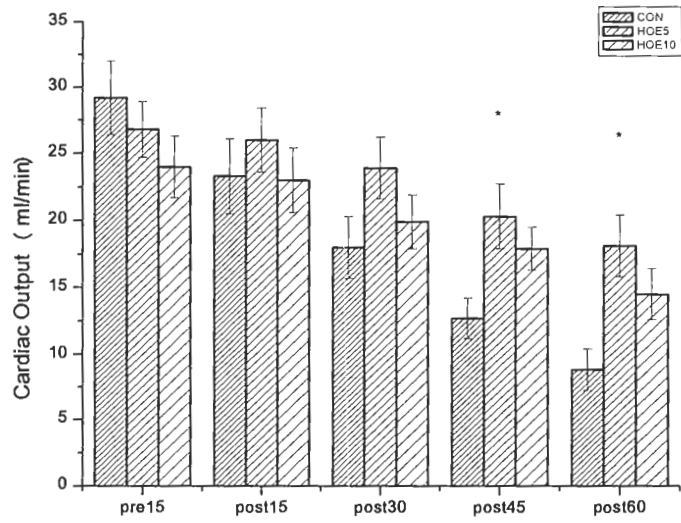


Figure 84 Post-ischemia cardiac output recovery (N=6) * P<0.05 ** P<0.01

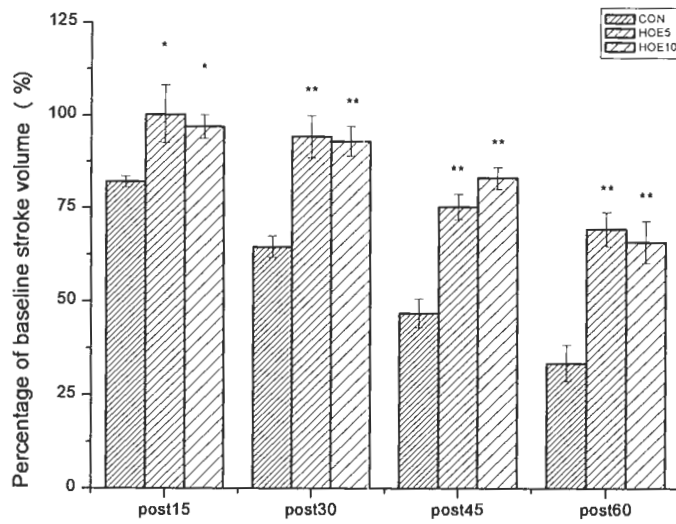
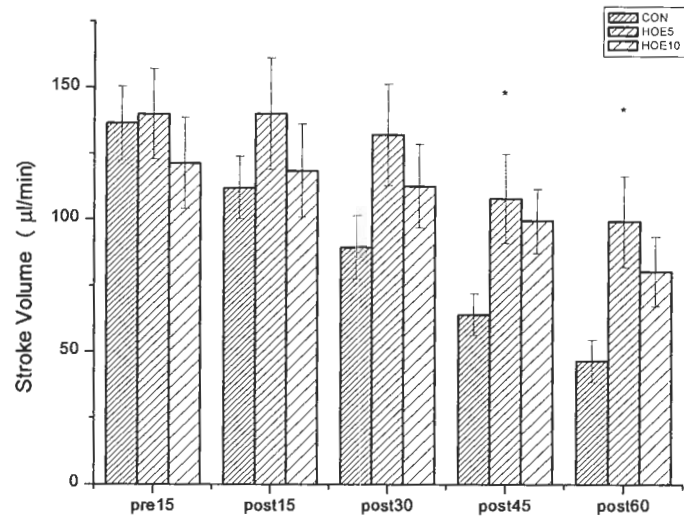


Figure 85 Post-ischemia stroke volume recovery (N=6) * P<0.05 **P<0.01

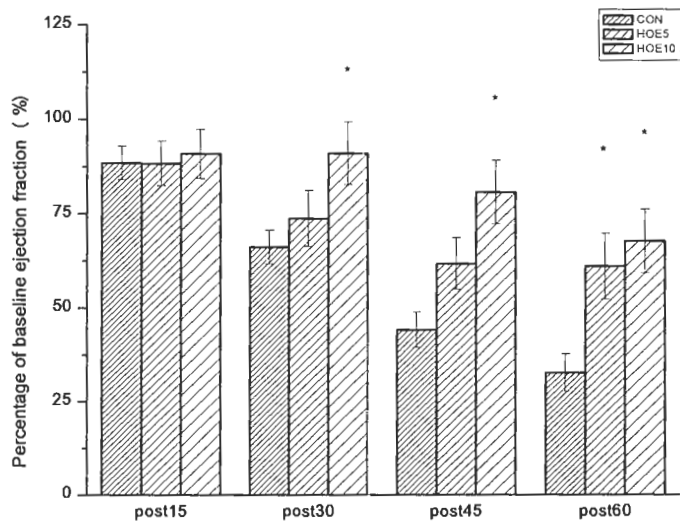
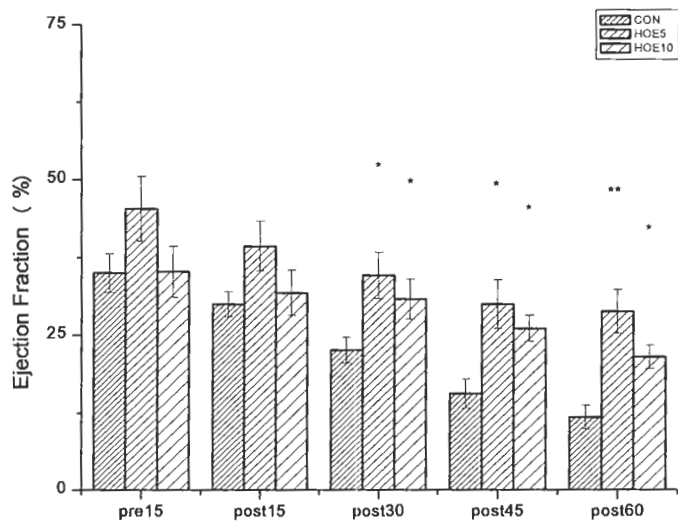


Figure 86 Post-ischemia ejection fraction recovery (N=6) * P<0.05 **P<0.01

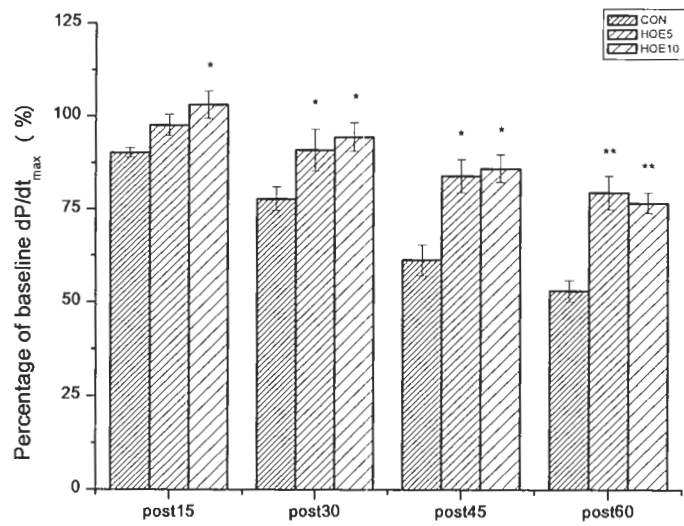
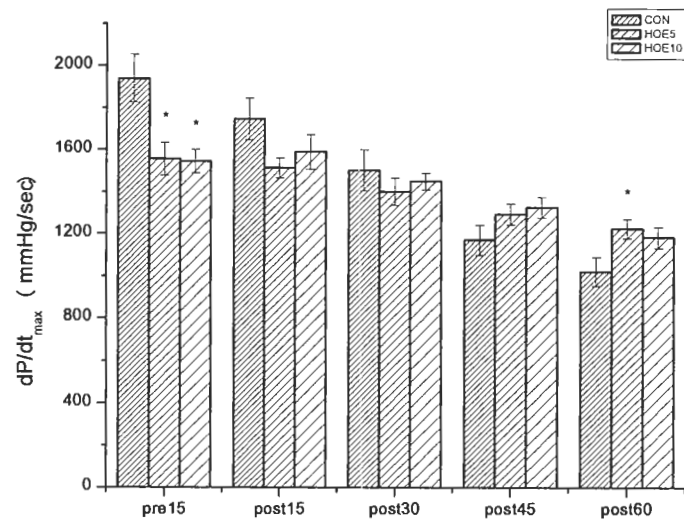


Figure 87 Post-ischemia dP/dt_{max} recovery (N=6) * P<0.05 **P<0.01

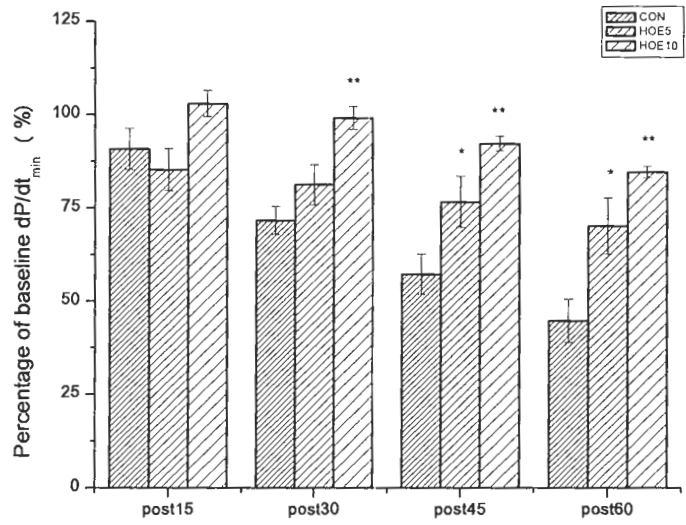
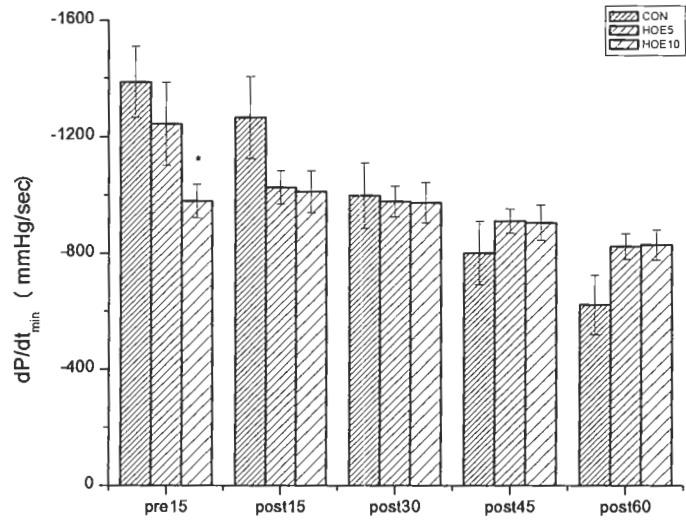


Figure 88 Post-ischemia dP/dt_{min} recovery (N=6) * P<0.05 ** P<0.01

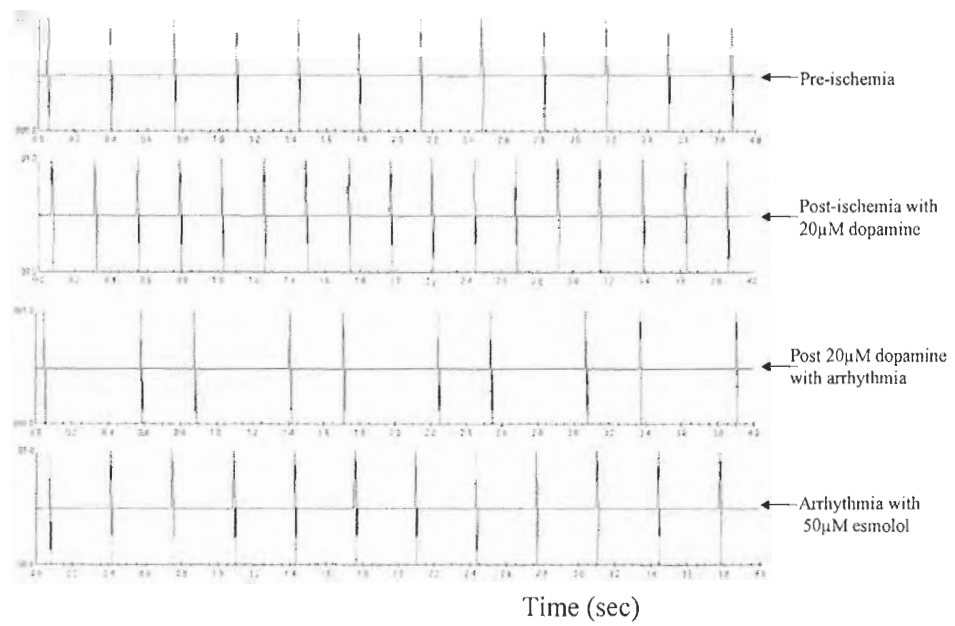


Figure 89 Dopamine-induced arrhythmogenesis in the reperfusion phase

Table 1 Arrhythmogenesis induced by 20 μ M dopamine

Group	2h ischemia			3h ischemia +dopamine
	No dopamine	+dopamine	+dopamine + HOE	
Arrhythmia Incidence	1/10	5/11	3/11	4/9

BIBLIOGRAPHY

1. Mitchell, S.C., S.B. Korones, and H.W. Berendes, *Congenital heart disease in 56,109 births. Incidence and natural history*. *Circulation*, 1971. **43**(3): p. 323-32.
2. Hoffman, J.I., *Incidence of congenital heart disease: I. Postnatal incidence*. *Pediatr Cardiol*, 1995. **16**(3): p. 103-13.
3. Hoffman, J.I., *Incidence of congenital heart disease: II. Prenatal incidence*. *Pediatr Cardiol*, 1995. **16**(4): p. 155-65.
4. Samanek, M., *Congenital heart malformations: prevalence, severity, survival, and quality of life*. *Cardiol Young*, 2000. **10**(3): p. 179-85.
5. Hoffman, J.I. and S. Kaplan, *The incidence of congenital heart disease*. *J Am Coll Cardiol*, 2002. **39**(12): p. 1890-900.
6. Lan, Y.T., J.C. Lee, and G. Wetzel, *Postoperative arrhythmia*. *Curr Opin Cardiol*, 2003. **18**(2): p. 73-8.
7. Bronzetti, G., et al., *Intravenous flecainide for the treatment of junctional ectopic tachycardia after surgery for congenital heart disease*. *Ann Thorac Surg*, 2003. **76**(1): p. 148-51; discussion 151.
8. Hoffman, T.M., et al., *Postoperative junctional ectopic tachycardia in children: incidence, risk factors, and treatment*. *Ann Thorac Surg*, 2002. **74**(5): p. 1607-11.
9. Valsangiacomo, E., et al., *Early postoperative arrhythmias after cardiac operation in children*. *Ann Thorac Surg*, 2002. **74**(3): p. 792-6.
10. Dodge-Khatami, A., et al., *Impact of junctional ectopic tachycardia on postoperative morbidity following repair of congenital heart defects*. *Eur J Cardiothorac Surg*, 2002. **21**(2): p. 255-9.
11. Till, J.A., S.Y. Ho, and E. Rowland, *Histopathological findings in three children with His bundle tachycardia occurring subsequent to cardiac surgery*. *Eur Heart J*, 1992. **13**(5): p. 709-12.
12. Gillette, P.C., *Diagnosis and management of postoperative junctional ectopic tachycardia*. *Am Heart J*, 1989. **118**(1): p. 192-4.
13. Sheikh, F., et al., *Diagnosis and management of junctional ectopic tachycardia*. *J Cardiothorac Vasc Anesth*, 1997. **11**(2): p. 203-5.
14. Rossi, A.F., et al., *Use of adenosine in the management of perioperative arrhythmias in the pediatric cardiac intensive care unit*. *Crit Care Med*, 1992. **20**(8): p. 1107-11.
15. Overholt, E.D., et al., *Usefulness of adenosine for arrhythmias in infants and children*. *Am J Cardiol*, 1988. **61**(4): p. 336-40.

16. Cabrera Duro, A., et al., [*The treatment of postoperative junctional ectopic tachycardia*]. *An Esp Pediatr*, 2002. **56**(6): p. 505-9.
17. Guccione, P., et al., [*Hypothermia treatment of junctional ectopic tachycardia after surgical repair of congenital heart defects*]. *G Ital Cardiol*, 1990. **20**(5): p. 415-8.
18. Pfammatter, J.P., et al., *Successful management of junctional tachycardia by hypothermia after cardiac operations in infants*. *Ann Thorac Surg*, 1995. **60**(3): p. 556-60.
19. Luedtke, S.A., R.J. Kuhn, and F.M. McCaffrey, *Pharmacologic management of supraventricular tachycardias in children. Part 2: Atrial flutter, atrial fibrillation, and junctional and atrial ectopic tachycardia*. *Ann Pharmacother*, 1997. **31**(11): p. 1347-59.
20. Shah, M.J. and L.A. Rhodes, *Management of postoperative arrhythmias and junctional ectopic tachycardia*. *Semin Thorac Cardiovasc Surg Pediatr Card Surg Annu*, 1998. **1**: p. 91-102.
21. Braunstein, P.W., Jr., R.M. Sade, and P.C. Gillette, *Life-threatening postoperative junctional ectopic tachycardia*. *Ann Thorac Surg*, 1992. **53**(4): p. 726-8.
22. Carmeliet, E., *Cardiac ionic currents and acute ischemia: from channels to arrhythmias*. *Physiol Rev*, 1999. **79**(3): p. 917-1017.
23. Ward, C.A. and W.R. Giles, *Ionic mechanism of the effects of hydrogen peroxide in rat ventricular myocytes*. *J Physiol*, 1997. **500** (Pt 3): p. 631-42.
24. Kukreja, R.C. and M.L. Hess, *The oxygen free radical system: from equations through membrane-protein interactions to cardiovascular injury and protection*. *Cardiovasc Res*, 1992. **26**(7): p. 641-55.
25. O'Neill, C.A., et al., *Hydroxyl radical production during myocardial ischemia and reperfusion in cats*. *Am J Physiol*, 1996. **271**(2 Pt 2): p. H660-7.
26. Goldhaber, J.I. and E. Liu, *Excitation-contraction coupling in single guinea-pig ventricular myocytes exposed to hydrogen peroxide*. *J Physiol*, 1994. **477** (Pt 1): p. 135-47.
27. Cerbai, E., et al., *Cellular electrophysiological basis for oxygen radical-induced arrhythmias. A patch-clamp study in guinea pig ventricular myocytes*. *Circulation*, 1991. **84**(4): p. 1773-82.
28. Jabr, R.I. and W.C. Cole, *Alterations in electrical activity and membrane currents induced by intracellular oxygen-derived free radical stress in guinea pig ventricular myocytes*. *Circ Res*, 1993. **72**(6): p. 1229-44.
29. Shattock, M.J. and H. Matsuura, *Measurement of Na⁺-K⁺ pump current in isolated rabbit ventricular myocytes using the whole-cell voltage-clamp technique. Inhibition of the pump by oxidant stress*. *Circ Res*, 1993. **72**(1): p. 91-101.

30. Crompton, M. and L. Andreeva, *On the involvement of a mitochondrial pore in reperfusion injury*. Basic Res Cardiol, 1993. **88**(5): p. 513-23.
31. Hu, K., et al., *Protein kinase C activates ATP-sensitive K^+ current in human and rabbit ventricular myocytes*. Circ Res, 1996. **78**(3): p. 492-8.
32. Kurachi, Y., et al., *Arachidonic acid metabolites as intracellular modulators of the G protein-gated cardiac K^+ channel*. Nature, 1989. **337**(6207): p. 555-7.
33. Williamson, A.P., et al., *Alpha 1b-adrenoceptor-mediated stimulation of Na-K pump current in adult rat ventricular myocytes*. Am J Physiol, 1993. **264**(4 Pt 2): p. H1315-8.
34. Sato, R. and S. Koumi, *Modulation of the inwardly rectifying K^+ channel in isolated human atrial myocytes by alpha 1-adrenergic stimulation*. J Membr Biol, 1995. **148**(2): p. 185-91.
35. Walker, *intracellular inorganic ions in cardiac tissue*, in *The heart and cardiovascular system*. 1986. p. 561-572.
36. Friedrich, M., et al., *Effects of anoxia on K and Ca currents in isolated guinea pig cardiocytes*. Pflugers Arch, 1990. **416**(1-2): p. 207-9.
37. DiFrancesco, D., P. Ducouret, and R.B. Robinson, *Muscarinic modulation of cardiac rate at low acetylcholine concentrations*. Science, 1989. **243**(4891): p. 669-71.
38. Philipson, K.D., M.M. Bersohn, and A.Y. Nishimoto, *Effects of pH on Na^+ - Ca^{2+} exchange in canine cardiac sarcolemmal vesicles*. Circ Res, 1982. **50**(2): p. 287-93.
39. Malloy, C.R., et al., *Influence of global ischemia on intracellular sodium in the perfused rat heart*. Magn Reson Med, 1990. **15**(1): p. 33-44.
40. van Echteld, C.J., et al., *Intracellular sodium during ischemia and calcium-free perfusion: a ^{23}Na NMR study*. J Mol Cell Cardiol, 1991. **23**(3): p. 297-307.
41. Bassani, R.A., J.W. Bassani, and D.M. Bers, *Mitochondrial and sarcolemmal Ca^{2+} transport reduce $[Ca^{2+}]_i$ during caffeine contractures in rabbit cardiac myocytes*. J Physiol, 1992. **453**: p. 591-608.
42. Bassani, J.W., R.A. Bassani, and D.M. Bers, *Relaxation in rabbit and rat cardiac cells: species-dependent differences in cellular mechanisms*. J Physiol, 1994. **476**(2): p. 279-93.
43. Levitsky, D.O. and D.S. Benevolensky, *Effects of changing Ca^{2+} -to- H^+ ratio on Ca^{2+} uptake by cardiac sarcoplasmic reticulum*. Am J Physiol, 1986. **250**(3 Pt 2): p. H360-5.
44. Ming, Z., C. Nordin, and R.S. Aronson, *Role of L-type calcium channel window current in generating current-induced early afterdepolarizations*. J Cardiovasc Electrophysiol, 1994. **5**(4): p. 323-34.

45. Priori, S.G. and P.B. Corr, *Mechanisms underlying early and delayed afterdepolarizations induced by catecholamines*. Am J Physiol, 1990. **258**(6 Pt 2): p. H1796-805.
46. Han, X. and G.R. Ferrier, *Contribution of Na⁺-Ca²⁺ exchange to stimulation of transient inward current by isoproterenol in rabbit cardiac Purkinje fibers*. Circ Res, 1995. **76**(4): p. 664-74.
47. Hagiwara, N. and H. Irisawa, *Modulation by intracellular Ca²⁺ of the hyperpolarization-activated inward current in rabbit single sino-atrial node cells*. J Physiol, 1989. **409**: p. 121-41.
48. Duchen, M.R., et al., *On the involvement of a cyclosporin A sensitive mitochondrial pore in myocardial reperfusion injury*. Cardiovasc Res, 1993. **27**(10): p. 1790-4.
49. Kirkels, J.H., C.J. van Echteld, and T.J. Ruigrok, *Intracellular magnesium during myocardial ischemia and reperfusion: possible consequences for postischemic recovery*. J Mol Cell Cardiol, 1989. **21**(11): p. 1209-18.
50. Schreur, J.H., et al., *Post-ischemic contractile dysfunction does not correlate with an elevated intracellular free [Mg²⁺]: a 31P-NMR study on isolated rat and rabbit hearts*. J Mol Cell Cardiol, 1993. **25**(9): p. 1015-24.
51. Murphy, E., et al., *Cytosolic free magnesium levels in ischemic rat heart*. J Biol Chem, 1989. **264**(10): p. 5622-7.
52. Malloy, C.R., et al., *In vivo phosphorus-31 nuclear magnetic resonance study of the regional metabolic response to cardiac ischemia*. Adv Myocardiol, 1985. **6**: p. 461-4.
53. Boyett, M.R., G. Hart, and A.J. Levi, *Factors affecting intracellular sodium during repetitive activity in isolated sheep Purkinje fibres*. J Physiol, 1987. **384**: p. 405-29.
54. Irisawa, H., H.F. Brown, and W. Giles, *Cardiac pacemaking in the sinoatrial node*. Physiol Rev, 1993. **73**(1): p. 197-227.
55. DiFrancesco, D., *The pacemaker current (I_p) plays an important role in regulating SA node pacemaker activity*. Cardiovasc Res, 1995. **30**(2): p. 307-8.
56. Bers, D.M., *Excitation-Contraction Coupling and Cardiac Contractile Force*. Second Edition ed. 2001: KLUWER ACADEMIC PUBLISHERS.
57. Huser, J., L.A. Blatter, and S.L. Lipsius, *Intracellular Ca²⁺ release contributes to automaticity in cat atrial pacemaker cells*. J Physiol, 2000. **524 Pt 2**: p. 415-22.
58. Hagiwara, N., H. Irisawa, and M. Kameyama, *Contribution of two types of calcium currents to the pacemaker potentials of rabbit sino-atrial node cells*. J Physiol, 1988. **395**: p. 233-53.
59. Muramatsu, H., et al., *Characterization of a TTX-sensitive Na⁺ current in pacemaker cells isolated from rabbit sinoatrial node*. Am J Physiol, 1996. **270**(6 Pt 2): p. H2108-19.

60. Accili, E.A., et al., *From funny current to HCN channels: 20 years of excitement*. News Physiol Sci, 2002. **17**: p. 32-7.
61. Pape, H.C., *Queer current and pacemaker: the hyperpolarization-activated cation current in neurons*. Annu Rev Physiol, 1996. **58**: p. 299-327.
62. DiFrancesco, D., *Pacemaker mechanisms in cardiac tissue*. Annu Rev Physiol, 1993. **55**: p. 455-72.
63. Denyer, J.C. and H.F. Brown, *Pacemaking in rabbit isolated sino-atrial node cells during Cs⁺ block of the hyperpolarization-activated current I_f*. J Physiol, 1990. **429**: p. 401-9.
64. DiFrancesco, D. and P. Tortora, *Direct activation of cardiac pacemaker channels by intracellular cyclic AMP*. Nature, 1991. **351**(6322): p. 145-7.
65. Ludwig, A., et al., *Absence epilepsy and sinus dysrhythmia in mice lacking the pacemaker channel HCN2*. Embo J, 2003. **22**(2): p. 216-24.
66. Vassalle, M., *The pacemaker current (I_f) does not play an important role in regulating SA node pacemaker activity*. Cardiovasc Res, 1995. **30**(2): p. 309-10.
67. Lakatta, E.G., et al., *Cyclic variation of intracellular calcium: a critical factor for cardiac pacemaker cell dominance*. Circ Res, 2003. **92**(3): p. e45-50.
68. Bogdanov, K.Y., T.M. Vinogradova, and E.G. Lakatta, *Sinoatrial nodal cell ryanodine receptor and Na⁺-Ca²⁺ exchanger: molecular partners in pacemaker regulation*. Circ Res, 2001. **88**(12): p. 1254-8.
69. Vinogradova, T.M., K.Y. Bogdanov, and E.G. Lakatta, *beta-Adrenergic stimulation modulates ryanodine receptor Ca²⁺ release during diastolic depolarization to accelerate pacemaker activity in rabbit sinoatrial nodal cells*. Circ Res, 2002. **90**(1): p. 73-9.
70. Boyett, M.R., et al., *Ionic basis of the chronotropic effect of acetylcholine on the rabbit sinoatrial node*. Cardiovasc Res, 1995. **29**(6): p. 867-78.
71. Ates, S. and Z. Kaygisiz, *Positive inotropic, negative chronotropic, and coronary vasoconstrictor effects of acetylcholine in isolated rat hearts: role of muscarinic receptors, prostaglandins, protein kinase C, influx of extracellular Ca²⁺, intracellular Ca²⁺ release, and endothelium*. Jpn J Physiol, 1998. **48**(6): p. 483-91.
72. Tanaka, H., et al., *Acetylcholine-induced positive inotropy mediated by prostaglandin released from endocardial endothelium in mouse left atrium*. Naunyn Schmiedebergs Arch Pharmacol, 2001. **363**(5): p. 577-82.
73. Korth, M. and V. Kuhlkamp, *Muscarinic receptor-mediated increase of intracellular Na⁺-ion activity and force of contraction*. Pflugers Arch, 1985. **403**(3): p. 266-72.
74. Tsuji, Y., et al., *Positive inotropic effects of acetylcholine and BAY K 8644 in embryonic chick ventricle*. Am J Physiol, 1987. **252**(4 Pt 2): p. H807-15.

75. Du, X.Y., et al., *Characterization of the positive and negative inotropic effects of acetylcholine in the human myocardium*. Eur J Pharmacol, 1995. **284**(1-2): p. 119-27.
76. Wang, Y.G. and S.L. Lipsius, *Acetylcholine elicits a rebound stimulation of Ca^{2+} current mediated by pertussis toxin-sensitive G protein and cAMP-dependent protein kinase A in atrial myocytes*. Circ Res, 1995. **76**(4): p. 634-44.
77. Sperelakis, N., et al., *Regulation of slow calcium channels of myocardial cells and vascular smooth muscle cells by cyclic nucleotides and phosphorylation*. Mol Cell Biochem, 1994. **140**(2): p. 103-17.
78. Lindemann, J.P., et al., *beta-Adrenergic stimulation of phospholamban phosphorylation and Ca^{2+} -ATPase activity in guinea pig ventricles*. J Biol Chem, 1983. **258**(1): p. 464-71.
79. Mundina de Weilenmann, C., et al., *Dissociation between contraction and relaxation: the possible role of phospholamban phosphorylation*. Basic Res Cardiol, 1987. **82**(6): p. 507-16.
80. Yoshida, A., et al., *Phosphorylation of ryanodine receptors in rat myocytes during beta-adrenergic stimulation*. J Biochem (Tokyo), 1992. **111**(2): p. 186-90.
81. Hain, J., et al., *Phosphorylation modulates the function of the calcium release channel of sarcoplasmic reticulum from cardiac muscle*. J Biol Chem, 1995. **270**(5): p. 2074-81.
82. Lokuta, A.J., et al., *Modulation of cardiac ryanodine receptors of swine and rabbit by a phosphorylation-dephosphorylation mechanism*. J Physiol, 1995. **487** (Pt 3): p. 609-22.
83. Ray, K.P. and P.J. England, *Phosphorylation of the inhibitory subunit of troponin and its effect on the calcium dependence of cardiac myofibril adenosine triphosphatase*. FEBS Lett, 1976. **70**(1): p. 11-6.
84. Solaro, R.J., A.J. Moir, and S.V. Perry, *Phosphorylation of troponin I and the inotropic effect of adrenaline in the perfused rabbit heart*. Nature, 1976. **262**(5569): p. 615-7.
85. DiFrancesco, D., *Characterization of single pacemaker channels in cardiac sino-atrial node cells*. Nature, 1986. **324**(6096): p. 470-3.
86. DiFrancesco, D., et al., *Properties of the hyperpolarizing-activated current (I_f) in cells isolated from the rabbit sino-atrial node*. J Physiol, 1986. **377**: p. 61-88.
87. Bennett, P., et al., *Adrenergic modulation of the delayed rectifier potassium channel in calf cardiac Purkinje fibers*. Biophys J, 1986. **49**(4): p. 839-48.
88. Noma, A., *Ionic mechanisms of the cardiac pacemaker potential*. Jpn Heart J, 1996. **37**(5): p. 673-82.
89. Garson, A., *The ECG in Infant and Children: a systematic approach*. 1983.

90. Huynh, T.V., et al., *Developmental changes in membrane Ca^{2+} and K^+ currents in fetal, neonatal, and adult rabbit ventricular myocytes*. *Circ Res*, 1992. **70**(3): p. 508-15.
91. Osaka, T. and R.W. Joyner, *Developmental changes in calcium currents of rabbit ventricular cells*. *Circ Res*, 1991. **68**(3): p. 788-96.
92. Brillantes, A.M., S. Bezprozvannaya, and A.R. Marks, *Developmental and tissue-specific regulation of rabbit skeletal and cardiac muscle calcium channels involved in excitation-contraction coupling*. *Circ Res*, 1994. **75**(3): p. 503-10.
93. Wetzel, G.T., F. Chen, and T.S. Klitzner, *L- and T-type calcium channels in acutely isolated neonatal and adult cardiac myocytes*. *Pediatr Res*, 1991. **30**(1): p. 89-94.
94. Fisher, D.J., C.A. Tate, and S. Phillips, *Developmental regulation of the sarcoplasmic reticulum calcium pump in the rabbit heart*. *Pediatr Res*, 1992. **31**(5): p. 474-9.
95. Huang, J., L. Hove-Madsen, and G. Tibbit, *SR Ca uptake rates during development in rabbit ventricular myocytes*. *Biophysical J*, 2005. **88**: p. 483a.
96. Artman, M., *Sarcolemmal Na^+ - Ca^{2+} exchange activity and exchanger immunoreactivity in developing rabbit hearts*. *Am J Physiol*, 1992. **263**(5 Pt 2): p. H1506-13.
97. Artman, M., et al., *Na^+ / Ca^{2+} exchange current density in cardiac myocytes from rabbits and guinea pigs during postnatal development*. *Am J Physiol*, 1995. **268**(4 Pt 2): p. H1714-22.
98. Chen, F., et al., *Distribution of the Na^+ / Ca^{2+} exchange protein in developing rabbit myocytes*. *Am J Physiol*, 1995. **268**(5 Pt 1): p. C1126-32.
99. Papka, R.E., *Development of innervation to the ventricular myocardium of the rabbit*. *J Mol Cell Cardiol*, 1981. **13**(2): p. 217-28.
100. Pappano, A.J., *Ontogenetic development of autonomic neuroeffector transmission and transmitter reactivity in embryonic and fetal hearts*. *Pharmacol Rev*, 1977. **29**(1): p. 3-33.
101. Hageman, G.R., B.H. Neely, and F. Urthaler, *Cardiac autonomic efferent activity during baroreflex in puppies and adult dogs*. *Am J Physiol*, 1986. **251**(2 Pt 2): p. H443-7.
102. Neely, J.R., et al., *Effect of pressure development on oxygen consumption by isolated rat heart*. *Am J Physiol*, 1967. **212**(4): p. 804-14.
103. Lopaschuk, G.D., et al., *Plasma fatty acid levels in infants and adults after myocardial ischemia*. *Am Heart J*, 1994. **128**(1): p. 61-7.
104. Lopaschuk, G.D. and M.A. Spafford, *Energy substrate utilization by isolated working hearts from newborn rabbits*. *Am J Physiol*, 1990. **258**(5 Pt 2): p. H1274-80.

105. Erdfelder, E., Faul, F., & Buchner, A, *GPOWER: A general power analysis program*. Behavior Research Methods, Instruments, & Computers, 1996. **28**: p. 1-11.
106. Endoh, M., *Effects of dopamine on sinus rate and ventricular contractile force of the dog heart in vitro and in vivo*. Br J Pharmacol, 1975. **55**(4): p. 475-86.
107. Benfield, P. and E.M. Sorkin, *Esmolol. A preliminary review of its pharmacodynamic and pharmacokinetic properties, and therapeutic efficacy*. Drugs, 1987. **33**(4): p. 392-412.
108. Bory, M., et al., [*Therapeutic applications of an adrenergic beta-receptor-blocking agent, propranolol, in cardiology*]. Coeur Med Interne, 1969. **8**(2): p. 273-83.
109. Hinds, J.E. and E.W. Hawthorne, *Comparative cardiac dynamic effects of dobutamine and isoproterenol in conscious instrumented dogs*. Am J Cardiol, 1975. **36**(7): p. 894-901.
110. BoSmith, R.E., I. Briggs, and N.C. Sturgess, *Inhibitory actions of ZENECA ZD7288 on whole-cell hyperpolarization activated inward current (I_f) in guinea-pig dissociated sinoatrial node cells*. Br J Pharmacol, 1993. **110**(1): p. 343-9.
111. Woods, W.T., F. Urthaler, and T.N. James, *Progressive postnatal changes in sinus node response to atropine and propranolol*. Am J Physiol, 1978. **234**(4): p. H412-5.
112. Durandy, Y., et al., [*Postoperative inotropic treatment in cardiac surgery of the newborn infant and infant*]. Ann Fr Anesth Reanim, 1988. **7**(2): p. 105-9.
113. Kollar, A., V. Kekesi, and A. Juhasz-Nagy, *Dopamine-induced aggravation of myocardial ischaemia in the paced heart: cardiosurgical perspectives*. Acta Chir Hung, 1991. **32**(3): p. 237-44.
114. Dugger, B., *Peripheral dopamine infusions: are they worth the risk of infiltration?* J Intraven Nurs, 1997. **20**(2): p. 95-9.
115. Gray, R.J., et al., *Esmolol: a new ultrashort-acting beta-adrenergic blocking agent for rapid control of heart rate in postoperative supraventricular tachyarrhythmias*. J Am Coll Cardiol, 1985. **5**(6): p. 1451-6.
116. Mooss, A.N., et al., *Esmolol versus diltiazem in the treatment of postoperative atrial fibrillation/atrial flutter after open heart surgery*. Am Heart J, 2000. **140**(1): p. 176-80.
117. Greenslade, F.C. and K.L. Newquist, *In vitro measurement of the beta-adrenergic blocking properties of ORF 12592, the 5-hydroxy analog of propranolol*. Arch Int Pharmacodyn Ther, 1978. **233**(2): p. 270-80.
118. Holloway, E.L., et al., *Action of drugs in patients early after cardiac surgery. I. Comparison of isoproterenol and dopamine*. Am J Cardiol, 1975. **35**(5): p. 656-9.

119. Sakata, Y., et al., [*Effects of dobutamine and isoproterenol on systemic hemodynamics and myocardial metabolism in children after open heart surgery*]. Kokyu To Junkan, 1992. **40**(1): p. 65-70.
120. Schlack, W., et al., *Effect of heart rate reduction by 4-(N-ethyl-N-phenyl-amino)-1,2-dimethyl-6-(methylamino)pyrimidinium chloride on infarct size in dog*. Arzneimittelforschung, 1998. **48**(1): p. 26-33.
121. Kottmeier, C.A. and J.S. Gravenstein, *The parasympathomimetic activity of atropine and atropine methylbromide*. Anesthesiology, 1968. **29**(6): p. 1125-33.
122. Gumina, R.J., et al., *Na⁺/H⁺ exchange inhibition prevents endothelial dysfunction after I/R injury*. Am J Physiol Heart Circ Physiol, 2001. **281**(3): p. H1260-6.
123. Knight, D.R., et al., *A novel sodium-hydrogen exchanger isoform-1 inhibitor, zoniporide, reduces ischemic myocardial injury in vitro and in vivo*. J Pharmacol Exp Ther, 2001. **297**(1): p. 254-9.
124. Sett, S.S., et al., *Na⁺/H⁺ exchange inhibition with HOE 642 improves recovery of the injured neonatal rabbit heart*. Can J Cardiol, 2003. **19**(13): p. 1515-9.
125. Furukawa, S., et al., *Effects of dopamine infusion on cardiac and renal blood flows in dogs*. J Vet Med Sci, 2002. **64**(1): p. 41-4.
126. Tani, M. and J.R. Neely, *Role of intracellular Na⁺ in Ca²⁺ overload and depressed recovery of ventricular function of reperfused ischemic rat hearts. Possible involvement of H⁺-Na⁺ and Na⁺-Ca²⁺ exchange*. Circ Res, 1989. **65**(4): p. 1045-56.
127. Dyck, J.R., et al., *Induction of expression of the sodium-hydrogen exchanger in rat myocardium*. Cardiovasc Res, 1995. **29**(2): p. 203-8.
128. Aye, N.N., Y.X. Xue, and K. Hashimoto, *Antiarrhythmic effects of cariporide, a novel Na⁺-H⁺ exchange inhibitor, on reperfusion ventricular arrhythmias in rat hearts*. Eur J Pharmacol, 1997. **339**(2-3): p. 121-7.